On the role of the cell end marker protein TeaC in the filamentous fungus *Aspergillus nidulans*

DISSERTATION

**zur Erlangung des akademischen Grades eines
DOKTORS DER NATURWISSENSCHAFTEN
(Dr. rer. nat.)
der Fakultät für Chemie und Biowissenschaften der
Universität Karlsruhe (TH)**

**vorgelegt
von**

**Dipl. Biol. Yuhei Higashitsuji
aus NARA (JAPAN)**

Die Untersuchungen zur vorliegenden Arbeit wurden von Juli 2006 bis September 2009 im Institut für Angewandte Biowissenschaften, Abteilung Mikrobiologie unter der Betreuung von Prof. Dr. Reinhard Fischer durchgeführt.

Im Zusammenhang mit der Thematik der vorliegenden Dissertation wurden folgende Publikationen erstellt:

1: **Higashitsuji Y.,** Herrero S., Takeshita N. and Fischer R. (2009) The cell end marker protein TeaC is involved in both growth directionality and septation in *Aspergillus nidulans*. Eukaryot. Cell. 8(7): 957-967.

2: Takeshita N., **Higashitsuji Y.**, Konzack S., Fischer R. (2008) Apical sterol-rich membranes are essential for localizing cell end markers that determine growth directionality in the filamentous fungus *Aspergillus nidulans*. Mol. Biol. Cell. 19(1): 339-351.

Content

Abbreviations

DAPI	4',6-Diamidino-2-phenylindole
GFP	Green Fluorescent Protein
HA	Hemagglutinin epitope
MM	Minimal medium
mRFP	monomeric red fluorescent protein
TAE	Tris-Acetate-EDTA
TBS-T	Tris-buffered saline-Tween 20
TE	Tris-EDTA

I. Summary

One kind of the most extremely polarized cells in nature are the indefinitely growing hyphae of filamentous fungi. Polarized growth in filamentous fungi depends on the correct spatial organization of the microtubule (MT) and the actin cytoskeleton. In *Schizosaccharomyces pombe* it was shown that the MT cytoskeleton is required for the delivery of so called cell end marker proteins e.g. Tea1 and Tea4, to the cell poles. Subsequently, they recruit several proteins required for polarized growth, e.g. a formin, which catalyzes actin cable formation. At the beginning of this work it was not clear whether this machinery was also conserved in filamentous fungi. Meanwhile several of the components known from *S. pombe,* among them TeaC of this work, have been identified in *Aspergillus nidulans*. They were already used to isolate novel proteins to further understand polarized growth in filamentous fungi.

Here, we have characterized TeaC, a putative homologue of *S. pombe* Tea4. Sequence identity between TeaC and Tea4 is only 12.5 %, but they both share a SH3 domain in the N-terminal region. Deletion of *teaC* affected polarized growth and hyphal directionality. Whereas wild-type hyphae grow straight, hyphae of the mutant grew in a zig-zag way, similar to hyphae of *teaA*-deletion (*tea1* in *S. pombe*) strains. Furthermore, deletion of *teaC* showed on increased number of septa and some small compartments. Likewise, TeaC localized to hyphal tips and to forming septa. The TeaC localization depended on the MT and the actin cytoskeleton. TeaC accumulated at MT plus ends, with which it was delivered to the apical cortex. The motor protein KipA was required for correct positioning at the hyphal apex, but unlike to the situation in *S. pombe*, not for the transportation to the MT plus end. Overexpression of *teaC* showed rarely branching of hyphae and caused lysis at the hyphal tips, moreover it repressed septation and caused abnormal swelling of germinating conidia. Overexpression of *teaC* together with the formin *sepA,* did not recover the repression of septum formation as observed after *teaC* overexpression alone. In addition, overexpression of both proteins caused very large hyphal tips.

In agreement with the two roles in polarized growth and in septation, TeaC interacted with the cell end marker protein TeaA at hyphal tips and with the formin SepA at hyphal tips and at septa.

Zusammenfassung

Das Auftreten extrem polarer Zellen in der Natur ist in unbegrenzt wachsenden Hyphen filamentöser Pilze möglich. Das polare Wachstum dieser Organismen ist abhängig von der genauen räumlichen Organisation des Mikrotubuli- (MT) und des Aktin-Cytoskeletts. In *Schizosaccharomyces pombe* konnte dargestellt werden, dass das MT-Cytoskelett notwendig ist, um so genannte Zellenmarker-Proteine, z.B. Tea1 und Tea4, an die Zellpole zu transportieren. Anschließend werden weitere Proteine, die für das polare Wachstum der Zelle benötigt werden, z.B. Formin, rekrutiert, welche die Bildung von Aktinfilamenten katalysieren. Zu Beginn dieser Arbeit war nicht bekannt, ob dieses System auch in filamentösen Pilzen konserviert ist. Inzwischen konnten mehrere in *S. pombe* bekannte Komponenten, darunter TeaC aus dieser Arbeit, in *Aspergillus nidulans* identifiziert werden.

Hier wurde TeaC charakterisiert, ein putatives Homolog zu Tea4 aus *S. pombe*. Die Übereinstimmung der Sequenz zwischen TeaC und Tea4 beträgt nur 12,5%, aber beide Proteine besitzen eine SH3-Domäne innerhalb der N-terminalen Region. Die Deletion des *teaC* beeinträchtigt das polare Wachstum und die Direktion der Hyphen. Während das Wachstum der Hyphen im Wildtyp geradlinig verläuft, konnte in Mutanten ein Zick-Zack-Verlauf beobachtet werden, was dem Hyphenwachstum in teaA-Deletionsstämmen (*tea1* in *S. pombe*) entspricht. Zudem führt die Deletion des *teaC* zu einer vermehrten Anzahl an Septen und kleineren Kompartimenten. TeaC lokalisiert ebenfalls an Hyphenspitzen und gebildeten Septierungen, was von dem MT- und Aktin-Cytoskelett abhängig ist. TeaC akkumuliert am Plusende des MT und wird damit an den apikalen Kortex gebracht. Das Motorprotein KipA wird für die genaue Positionierung an der Hyphenspitze, aber anders als in *S. pombe*, nicht für den Transport an das MT-Plusende, benötigt. Überexpression des teaC führt zu geringfügig verzweigten Hyphen und bewirkt die Lyse an der Hyphenspitze. Außerdem hemmt es die Septierung und führt zu abnormalem Anschwellen gekeimter Sporen. Durch die Überexpression des *teaC* zusammen mit dem Formin *sepA* wird die Repression der Septierung nicht aufgehoben. Zusätzlich führt die Überexpression beider Proteine zu sehr großen Hyphenspitzen.

In Übereinstimmung beider Rollen in polarem Wachstum und Septierung interagiert TeaC mit dem Zellendmarker TeaA an den Hyphenspitzen und mit dem Formin SepA an Hyphenspitzen und Septen.

II. Introduction

1. Filamentous fungi

Filamentous fungi are widely distributed in nature and have a great impact on human life. They have been used for food and feed production or processing since many hundret years. Another important aspect is that filamentous fungi are widely used in biotechnology. Their high extracellular secretion ability is used to produce many useful enzymes, for example amylases, proteases or lipases. Heterologously produced hydrolytic enzymes are secreted through the same machinery as the enzymes required for polarized growth (Seiler *et al.*, 1997; Pel *et al.*, 2007). On the other hand, filamentous fungi such as *Magnaporthe grisea* and *Aspergillus fumigatus* cause severe problems as pathogens of plants and animals. To find antifungal drug against those fungi is thus very important. Many laboratories are currently trying to get a detailed understanding of the functioning of fungal cells, because the molecular analysis of filamentous fungus may lead to the identification of targets for new antifungal drugs but also new biotechnological products.

Aspergillus nidulans is one of many species of filamentous fungi in the *phylum Ascomycota*. The formal name is *Emericella nidulans* although the name for the asexual form, *A. nidulans*, is much more common. It has been an important research organism for studying eukaryotic cell biology for over 50 years, being used to study a wide range of subjects including recombination, DNA repair, mutation, cell cycle control, polarity, and metabolism (Morris and Enos, 1989: Osmani *et al.*, 2004: Nierman *et al.*, 2005). It is one of the few species in its genus able to form sexual spores through meiosis, allowing crossing of strains in the laboratory. *A. nidulans* is a homothallic fungus, meaning it is able to self-fertilize and form fruiting bodies in the absence of a mating partner. The genome of *A. nidulans* has been sequenced at the Broad Institute (Galagan JE *et al.,* 2005). It is 30 million base pairs in size and is predicted to contain around 9,500 protein-coding genes on eight chromosomes.

2. Polarized growth

Polarized growth of fungi has been studied by genetic, molecular biological, and cell biological methods. Especially many breakthroughs come from the fission yeast *Schizosaccharomyces pombe,* the budding yeast *Saccharomyces cerevisiae* and filamentous fungi. The yeasts polarized growth is restricted to exact times during the cell cycles, whereas filamentous fungal cell growth takes place at the tip of the extremely elongated hyphae. Hyphal extension requires the continuous expansion of the membrane and the cell wall and is driven by continuous fusion of secretion vesicles at the tip (Fischer, R *et al.*, 2008; Harris, *et al.* 2005) For this reason, filamentous fungi represent good model organisms to study the establishment and maintenance of cell polarity. Phase contrast microscopy revealed already early on a dark spot at the growing tip. It was called "Spitzenkörper". This structrue is thought to act as vesicle supply center (VSC) for the growing tip **(Fig. II. 1)**. Besides the Spitzenkörper, MTs and the actin cytoskeleton play important roles. MTs distribute along the long axis and actin accumulates at the hyphal tip region **(Fig. II. 2)**. According to a model, vesicles are transported MT-dependently from the hyphal body to the Spitzenkörper and from there in an actin-dependent manner to the cell cortex. From ultra structural studies with *Fusarium acruminatum,* vesicles were observed closely associated with Microtubules (MTs). Furthermore after treatment of hyphae with the anti-MT agent benomyl intracellular vesicle movement was inhibited (Howard and Aist, 1980; Howard, 1981). More evidence for long distance transportation of vesicles along MTs came from MT-dependent kinesin studies. For instance, in a mutant of conventional kinesin (kinesin-1) of *A. nidulans* and *Neurospora crassa*, hyphal growth was delayed. Especially the kinesin-1 mutation in *Neurospora crassa* affected Spitzenkörper stability and protein secretion. Moreover, stronger evidence for the importance of secretion for polarized growth came recently from a study on exocytosis (Taheri-halech *et al*., 2008). In this research, GFP-tagged markers for exocytotic vesicles localization pattern was observed in living cell, which showed that exocytotic vesicles accumulate in the Spitzenkörper, and are transported from there to the membrane. Hence exocytosis is involved in vesicle movement and is required for tip growth. MT-dependent vesicle

secretion is not necessary for growth in all fungi, for instance in *Candida albicans*, that is able to switch from filamentous growth to budding growth and in *Ashbya gossypii* that grows constitutively filamentously (Alberti-Segui *et al*., 2001; Rida *et al*., 2006). However actin-dependent vesicle secretion is necessary for growth in all fungi, which was shown by experiments using actin destabilizing drugs.

Fig. II. 1 The Spitzenkörper in *A. nidulans*. vesicle supply center (VSC) for the growing tip. The picture was provided by B. Richardson (Athens, GA).
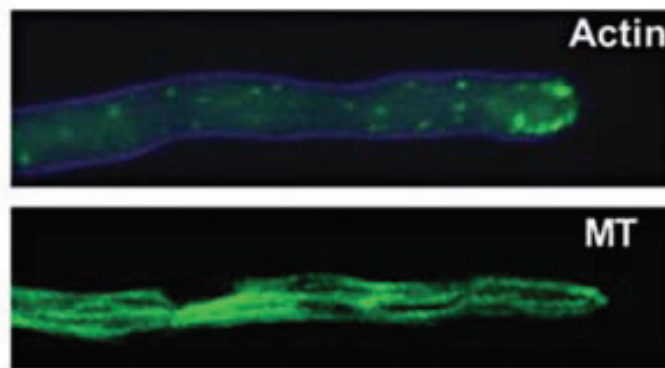

Fig. II. 2: Distribution of the MT and actin cytoskeleton in *A. nidulans*.
Actin and MTs visualized in a hyphal tip as GFP fusion proteins. MTs distribute along the long axis and actin accumulates at the hyphal tip region (Araujo-Bazan *et al.*, 2008;Taheri-Talesh *et al.*, 2008).

3. Distribution of microtubules in *S. cerevisiae, S.pomb*e and *A. nidulans*

Microtubules (MTs) are required for vesicle transportation, morphological maintenance of cell shape and polarized growth. MTs are nucleated from a perinuclear centrosome or MT-organizing centre (MTOC) with their plus ends facing to the cell periphery (Keating and Borisy, 1999). In *S. cerevisiae*, the MTOC is localized in the nuclear envelope and named spindle pole body (SPB) (Jaspersen and Winey, 2004). Only few MTs are found in interphase cells and they are disassembled as the mitotic spindle is formed. *S. pombe* has both the SPB and perinuclear MTOCs (Sawin and Tran, 2006) and, in the filamentous fungus *A. nidulans* SPBs, cytoplasmic MTOCs and MTOCs associated with septa are responsible for the formation and maintenance of the MT array (Veith *et al*., 2005). MTs are oriented along the long axis in the cigar shaped cells of *S. pombe* as well as in the extremely elongated compartments of *A. nidulans* (Höög *et al*., 2007). Understanding the regulation of MT formation and their dynamics is one of the main foci of recent research. Moreover, how MT plus ends reach and interact with the cell cortex is also an interesting point. In *S. cerevisiae*, MT plus end interactions with the cell cortex play crucial roles in positioning of the mitotic spindle; in *S. pombe*, MTs signal polarity information to the cell cortex; and in *A. nidulans*, MTs are involved in both nuclear migration and polarity determination.

4. Cell-end markers and polarity determination

In *S. cerevisiae*, the decision to initiate a new polarized growth site depends on intrinsic factors and is determined by the last budding site. In *S. pombe*, cell growth occurs first at the previous cell division site, and interphase MTs are used to establish the polarity site. In both yeasts, mutation analysis revealed some proteins that act as cortical landmarks. Once the polarity site is marked at the cell cortex, the landmarks regulate localization and activation of cascades of small GTPases (Cdc42 and other Rho type GTPase) (Chang and Peter, 2003). In *S. cerevisiae*, activated Cdc42 regulates multiple downstream effectors and establishes cell polarity, organizes the

actin cytoskeleton and the septin ring, and directs membrane traffic and the formation of membrane compartments (Pruyne and Bretscher, 2000; Park and Bi, 2007).

S. cerevisiae

In general, polarity site selection is not essential for polarized growth, but the polarity-establishing machinery is essential for cell polarity. Interestingly, the initiation of polarized growth in *S. cerevisiae* depends on the genotype at the mating-type (MAT) locus. MAT a or α cells exhibit axial budding, which means that a new daughter bud emerges next to the previous one. On the other hand, diploid MAT a/α cells exhibit a bipolar budding pattern, where a new bud emerges from the opposite pole of the previous daughter (Kron and Gow, 1995). Bud3, Bud4 and Axl2/Bud10 are landmark proteins for the axial budding pattern, and Bud8, Bud9 and Rax2 for the bipolar budding pattern (Madden and Snyder, 1998). In the case of axial budding, the landmark proteins localize to a septin ring. Septins are GTPases, which assemble into a ring structure (septin ring) at the previous bud neck at the end of the cell cycle, and guide new bud formation next to the septin ring. In contrast, the mechanism of landmark protein localization for bipolar budding is not fully understood. Genetic analyses revealed that several other processes besides the septin ring and the timing of BUD8 and BUD9 gene expression are involved in the mechanism (Ni and Snyder, 2001; Schenkman *et al*., 2002). In both cases, the landmarks recruit and activate the polarity-establishing machinery, the Cdc42 cascade, at the cell surface. The mediator Rsr1-Bud1 (Ras small GTPase) regulates the link between the landmarks and Cdc42. The landmarks activate Rsr1-Bud1 through the recruitment of its guanine nucleotide exchange factor (GEF) Bud5 (Bender, 1993). Activated Rsr1-Bud1 regulates Cdc42 activity through the recruitment of its GEF Cdc24. Once Cdc42 is activated at the proper site, multiple effectors, such as formins (Bni1, Bnr1), p21-activated kinases (Ste20 and Cla4) and GTPase activating protein (GAP) for the Rab-type GTPase Sec4 (Msb3 and Msb4), lead to the local assembly and orientation of the actin cytoskeleton and vesicle delivery for bud growth. The local Cdc42 activity is amplified in a self-sustaining positive feedback loop (Butty *et al*., 2002; Wedlich-Söldner and Li, 2003).

S. pombe

In *S. pombe*, some of the bud site landmark proteins from *S. cerevisiae* are not conserved Reference required, some review about the genome for instance. However, other genes were identified by polarity mutant screening (T-shaped or bent cells). Among these were the above mentioned *tea1* and *tea2* genes, and the novel landmark encoding *mod5* gene (morphology defective). Mutants of these genes exhibit T-shaped or bent cells as a result of the mislocalization of the polarity site away from the centre of the cell end. Mod5 plays a very important role, because it anchors Tea1 at the cell pole. Mod5 harbours a CAAX (cysteine, two aliphatic amino acids followed by any amino acid) prenylation motif at the C terminus. The cysteine is covalently prenylated, which anchors the protein in the membrane (Snaith and Sawin, 2003). Tea1 and Mod5, also named cell-end markers, accumulate interdependently at the growing cell ends and contribute to the spatial distribution of actin cables. At the cell ends, Tea1 interacts with a number of additional components, and a large protein complex is formed that includes the formin For3, which nucleates the actin cable assembly, and Bud6, an actin-binding protein (Feierbach *et al*., 2004; Martin *et al*., 2005). Bud6 in *S. cerevisiae* stimulates formin activity and Bud6 in *S. pombe* is required for proper For3 localization (Feierbach *et al*., 2004; Moseley and Goode, 2005). After cell division, Tea1 is delivered to the new end by MTs, and For3 and Bud6 localize there after Tea1 is anchored. Therefore, Tea1 contributes to cell polarity and actin cable organization through the interaction with For3 and Bud6. Their interactions link the MT with the actin cytoskeleton in fission yeast. Transition from monopolar to bipolar growth(NETO) depends on the localization of For3 to the new end and, thus, *tea1* and *bud6* mutants display defects in NETO. Besides these components, Tea4, which links Tea1 and For3, and Tea3, a Tea1-related, Kelch repeat containing protein, are also necessary for NETO (Arellano *et al*., 2002; Martin *et al*., 2005). Tea3 binds independently to Tea1 and Mod5, and is required for Tea1 anchorage specifically at non-growing cell ends (Snaith *et al*., 2005). Although the contribution of Cdc42 on For3 localization in *S. pombe* is not well understood, relief of autoinhibition of For3 by Cdc42 and/or Bud6 is necessary for For3 localization (Martin *et al*., 2007). Bud6 is also directly or indirectly recruited to the new end by Tea1 and Tea4 (Feierbach *et al*., 2004). Whereas MTs and

Tea1 play central roles in the decision of the growth site, they are not required for polarity establishment. This led to models that local self-activation and lateral inhibition are responsible for polarized growth (Castagnetti *et al*., 2007).

5. Cell end marker of *S. pombe*

S. pombe forms a rod shaped structure to extend both cell ends and divide at the center of the cell. The process generates two daughter cells of the same size. Cell growth in *S. pombe* is exactly regulated by the cell cycle. In the G1 phase, a new daughter cell grows at the previous cell end in a monopolar manner. Consequently in G2 phase, the daughter cell initiates growth at the previous cell division site in a bipolar manner. This phenomenon is named NETO (new end take-off) and requires the MT and the actin cytoskeleton (Mitchison and Nurse, 1985). Recently, some important proteins were identified to act in the maintenance of the actin and MT cytoskeleton from temperature sensitive morphology screening. From the screening, some genes were isolated and named tea (tip elongation aberrant) because the mutants show T shaped or bend shaped cells. From such screenings, the cell end marker protein Tea1 and anchor protein Mod5 were identified (Verde, F. *et al.,* 1995). Another component, the kinesin-7 motor protein, Tea2, was isolated by PCR with primers derived from conserved kinesin regions (Browning *et al.*, 2000). Further cell end maker proteins and interacting proteins, such as Tea4, were identified by tandem mass spectrometry, (Martin, G. *et al.*, 2005). The formin For3p was identified on the basis of its amino acid similarity (Feierbach and Chang, 2001).

Cell end marker protein Tea1

Tea1 has six Kelch domains, in the N-terminal region and a coild-coil domain in the C-terminal region. Kelch repeats are involved in mating projection formation in *S. cerevisiae* (Phelips and Herskowitz, 1998). Δ*tea1* strains cells display a T shape and only one end of a daughter cell grows. Tea1 localized at MT plus ends in interphase and is transported together with the extending MTs to both cell ends. After TBZ treatment, which is a MT depolymerizing drug, Tea1 did not localize to both cell ends.

These results suggest that MTs deliver Tea1 to both cell ends and that Tea1 acts as a marker to determine the polarity of growth.

Anchor protein Mod5

Mod5 (morphology defective) act as anchoring protein for Tea1 at the cell ends membrane. Mod5 comprises a CaaX motif (cysteine, two aliphatic amino acids followed by any amino acid), which is prenylation motif, at the C-terminus. The cysteine is covalently prenylated, which anchors the protein in the membrane (Snaith and Sawin, 2003). It is required for the localization of Mod5 at the membrane and Tea1 at both cell ends (Snaith and Sawin, 2003). In Δ*mod5*, Tea1 localized to MT plus ends but did not localize to both cell ends. In Δ*teaA*, Mod5 was no longer restricted to the cell tips but instead spread out along the entire plasma membrane (Snaith and Sawin, 2003). Those results suggest Tea1 and Mod5 are interdependent. A positive feedback model was proposed. However, direct interaction between Tea1 and Mod5 was not found. Instead, Tea3 was identified as a linker of Tea1 and Mod5 (Arellano *et al*. 2002: Snaith *et al.*, 2003).

Cell end marker protein Tea3

Homology searches of the fission yeast genome revealed a gene encoding a protein annotated with significant homology to Tea1. It has been called Tea3. Tea1 and Tea3 share 21% identity (45% similarity) and have similar domain structures, which is four Kelch-repeat domains. Tea3 localizes to cell ends, and its localization depends on microtubules and Tea1 (Arellano *et al.*, 2002). Yeast two hybrid experiments suggested that Tea3 connects Tea1 and Mod5 (Arellano *et al*. 2002: Snaith *et al.*, 2003).

Tea2 (kinesin-7) motor protein

Tea2 is a kinesin motor of the kinesin-7 family required for polarized growth. I thought Tea2 was isolated with degenerated primers against kinesin motor domains. Please check. Ts mutants is for sure wrong, because they are not temperature sensitive. (Browning *et al.*, 2003). Tea2 accumulated at MT plus ends and quickly moved along

the MTs to the cell end (Browning *et al*., 2003). Δ*tea2* mutants showed also a T shape or bent type phenotype and MTs were shorter than wild type. In a Δ*tea2* mutant, Tea1 did not localize at MT plus ends. Those results suggest that Tea2 transports Tea1 to the MT plus ends.

Cell end marker Tea4

Tea4 was identified by tandem mass spectrometry as Tea1 interacting protein (Martin *et al*., 2005). This protein is an ortholog of Bud14, which is involved in bipolar bud site selection in *S. cerevisiae*. Tea4 has a SH3 domain, which is conserved in Bud14 (*S. cerevisiae*). Δ*tea4* cells show monopolar growth and T shape phenotype similar to Δ*tea1* cells. Tea4 is transported through the interaction with Tea1 and colocalized at MT plus ends and both cell ends (Martin *et al*., 2005). In Δ*tea1*, Tea4 appeared diffuse in the cytoplasm. In Δ*tea4*, another interacting partner For3 localized at new growing ends but Tea1 localized at old ends which not growing ends. These results suggest that Tea4 is required to construct Tea1-For3 complex.

Formin For3

Formin regulates the assembly of actin filaments and is widely conserved in eukaryotes. In *S.pombe*, three kinds of formin (Cdc12p, Fus1p and For3p) are conserved, especially For3p is required for actin cable formation at cell ends in interphase. The formin For3p was identified on the basis of its amino acid similarity to other formins for3p is most similar to Bin1 in *S. cerevisiae* (Feierbach and Chang, 2001: Kohno *et al*., 1996). For3 is including formin homology domains FH1, FH2, and FH3 and rho binding sites. In fact, Δ*for3* mutants lacked functional actin cable and often showed egg shape structure. Besides, For3 localized to the cell tips and cytokinesis ring.

6. *A. nidulans* cell end marker proteins

S. cerevisiae-type landmarks are poorly or not conserved in *A. nidulans* and other filamentous fungi, leading to speculations hat novel mechanisms could be at work (Harris and Momany, 2004). However, the *S. pombe* cell end marker homologous proteins of Tea1, Tea2 and mod5 were identified in *A. nidulans* (Fischer *et al*., 2008). The first component identified was the Tea2 homologue, KipA, a kinesin-7 motor protein (Konzack *et al*., 2005). Deletion of the gene did not affect hyphal tip extension but polarity determination. Instead of growing straight, hyphae grew in curves. KipA moves along MTs and accumulates at the MT plus end. The identification of Tea1 and a Mod5 homologue was more difficult, because the primary structure of these cell end marker proteins is not well conserved in filamentous fungi. A Tea1 homologue, TeaA, only displayed 27% sequence identity. However, the presence of Kelch repeats in both proteins suggested conserved functions (Takeshita *et al*., 2008). A Mod5 homologue was identified by a conserved CAAX prenylation motif at the C terminus. Systematic analyses of proteins with such a motif in the *A. nidulans* genome led to the identification of TeaR. Like Tea1 and Mod5, TeaA and TeaR localize at or close to the hyphal membrane at the growing cell end (Takeshita *et al*., 2008). However, correct localization of TeaR requires TeaA. In addition, sterol rich membrane domains define the place of TeaR attachment to the hyphal tip. In contrast to *S. pombe*, TeaA and TeaR are still transported to the hyphal tip in the absence of the motor protein KipA, but their localization is disturbed in comparison to wild type. This suggests that other proteins are necessary for exact TeaA positioning, whose localization depends on KipA. Here exhibit detail of each cell end marker protein and relationship of those proteins.

In this PhD work, I characterized a homologue of the *S. pombe* cell end marker protein, Tea4, and found that the protein is required for the maintenance of straight polar growth but that it also appears to be involved in septation.

Tea1 homologues protein TeaA

A $\Delta teaA$ mutation caused a rather zigzag growth phenotype, affected bipolar second germ tube initiation and also affected TeaR localization. that signal localized at the membrane of the apex and others dispersed along the membrane away from the tip not understandable **(Fig. II. 3)**. TeaA localized at the hyphal apex and co-localized with TeaR. TeaA-TeaR interaction was shown with a BiFC and Yeast two hybrid analysis. Furthermore, TeaA is important for MT accumulation at hyphal apex. In $\Delta teaA$ mutants, MTs reached the tip cortex, but sometimes did not converge to one point, but attached to several points (Takeshita *et al*., 2008). This experiment shows that TeaA is required for MT convergence in one point at the apex. After MT destabilization with the drug benomyl, the TeaA point at the tips was sometimes divided into several points and disappeared. This result indicated that TeaA localization at the center of the apex depends on MT (Takeshita *et al.*, 2008).

Tea2 homologues protein KipA

The Tea2 homologue, KipA, a kinesin-7 motor protein was identified in *A. nidulans* by sequence comparisons **(Fig. II. 3)**. A $\Delta kipA$ mutant showed meandering instead of straight growing hyphae and an aberrant position of the Spitzenkörper (Konzack *et al.,* 2005). KipA localized along MTs and accumulated at the MT plus end. In a KipA rigor mutant, which harbor a mutation in the ATP binding site and thus cannot be released from MTs, KipA localized along MTs but did not move (Konzack *et al.,* 2005).

Mod5 homologues protein TeaR

Despite the central role of Mod5 for polarized growth in *S. pombe*, a sequence homologue was not identified in *S. cerevisiae* or any filamentous fungus. In recent work, a protein that could act as a membrane anchor for TeaA was discovered in *A. nidulans* and named TeaR (Takeshita *et al.,* 2008) **(Fig. II. 3)**. TeaR was identified by screening for proteins that harbour a C-terminal prenylation motif. TeaR shows low identity to Mod5 (15.4%) and is conserved in all filamentous fungi whose genomes have been analyzed. Deletion of *teaR* produces meandering instead of straight hyphae. Both TeaA and TeaR localize to one point at the tip and along the tip membrane. TeaR

was shown to interact with TeaA by split YFP and yeast two-hybrid technology. In a *ΔteaR* mutant, TeaA was not observed at the tip. The localization of both proteins is interdependent, as it is in *S. pombe*.

Formin SepA

Temperature sensitive mutations in the s*epA, sepD, sepG* and *sepH* genes block septum formation at restrictive temperatures (Harris *et al*., 1997). Molecular characterization of *sepA* revealed that it encodes a member of the conserved formin homology (FH) domain family of proteins **(Fig. II. 3)** (Harris *et al*., 1997). In *ΔsepA* mutants hyphal width is 1.5-2.5 fold that of wild type and hyphal tips sometimes divide and grow into two directions (Harris *et al.,* 1997: Sharpless *et al.,* 2002). Actin was observed only at hyphal tips and in cortical spots but no actin rings were observed in *ΔsepA* mutants (Sharpless *et al.,* 2001). SepA localized faintly to the cytoplasm and brightly to the tips of hyphae and at septation sites and co-localized with actin rings. Those results suggest that SepA is involved in the maintenance of polarity at hyphal tips and in septum formation throught actin cytoskeleton regulation.

A

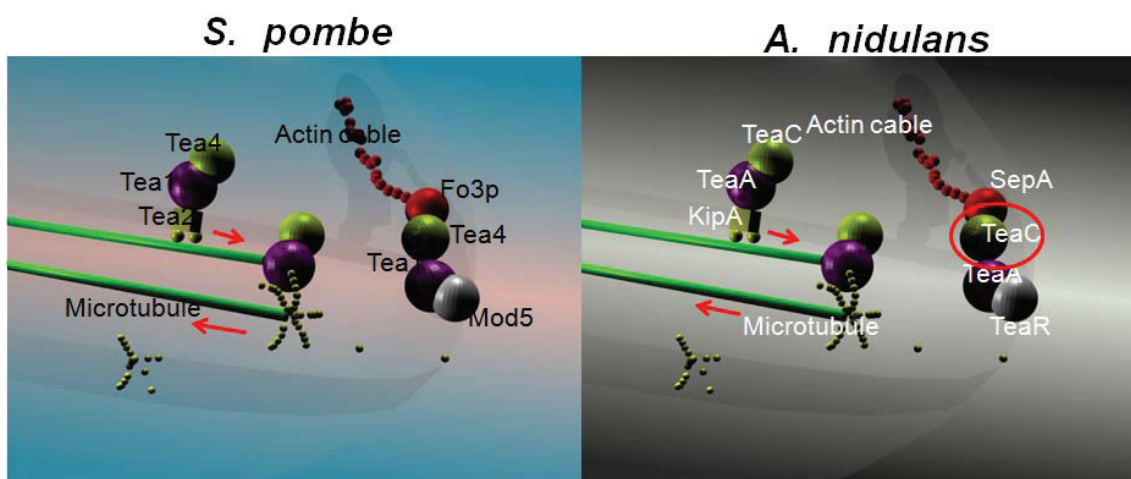| Family/Class		function
S. pombe	*A. nidulans*	
Tea1p	TeaA	Cell end marker
Mod5	TeaR	Anker protein
For3p	SepA	Actin forming protein
Tea4p	TeaC	Cell end marker
Tea2p	KipA	Motor protein

B

Fig. II. 3: Scheme of the transport of cell-end markers in *S. pombe* and *A. nidulans*.

(A) Corresponding proteins in *S. pombe* and *A. nidulans*. (B) Localizations and interaction pattern of cell end markers in *S. pombe* and *A. nidulans.*

7. Septum formation in *A. nidulans*

In *A. nidulans*, septum formation requires the assembly of a septal band following the completion of mitosis. Recent observations show that this band is a dynamic structure composed of actin, a septin and a formin. *A. nidulans* is a complement to the model yeasts for understanding the basic process of cytokinesis. In particular, *A. nidulans* has been shown that the formation of the first septum does not occur until hyphae reach a certain cell size (Wolkow *et al*., 1996). Unlike yeast cells, multiple rounds of nuclear division occur in the absence of cytokinesis. Once the size threshold is attained, septum formation is triggered by the completion of the next round of mitosis.

Actin

An early cytological study detected a contracting septal band in filamentous fungi that were undergoing septum formation (Girbardt. *et al*., 1979). More recent studies have characterized the temporal and spatial requirements for actin ring formation at septation sites in *A. nidulans* (Momany *at al*., 1997). The actin ring forms before the appearance of the septum, and subsequently contracts coincident with the deposition of septal wall material. Combined with the observation that the septation site is specified by the nuclear position in *A. nidulans* (Wolkow *at al*., 1996), these results are consistent with a model in which signals emanating from mitotic spindles organize both the assembly and the dynamics of the septal band.

Septin

The septins are a conserved family of eukaryotic proteins that appear to function as morphogenetic scaffolds at sites of cell division and polarized growth. The use of PCR-based cloning and genomics has revealed that *A. nidulans* possesses five members of the septin family (aspA–E). Mutation and localization experiments suggest an important role for the septin AspB (Momany and Hamer 1997). Coincident with the contraction of the actin ring and deposition of septal wall material, AspB splits into two rings that flank the new septum. Subsequently, the AspB ring located on the apical side of septum persists, whereas the basal ring is lost. By specifically marking the

apical side of the completed septum (or the basal end of the new hyphal cell), AspB may help propagate the intrinsic polarity of *A. nidulans* hyphae.

Relationship between Formin, Septin and Actin cytoskeleton during septation

SepA, which is the only conserved formin in *A. nidulans*. Here shows SepA play role septum formation though ration with septin and actin cytoskeleton. SepA ring co-localized with actin and ultimately constricts as the septal wall material is deposited. Because SepA rings collapse in hyphae treated with cytochalasin A, their assembly most likely requires the presence of an intact actin ring. Similarly, the formation of AspB rings also depends on the integrity of the actin cytoskeleton and requires functional SepA (Harris, 2001). Although the role of AspB in mediating the assembly of SepA and actin rings is not yet known, these observations suggest that all three components may function in a interdependent manner to form the septal band (Harris, 2001). It has been established that mitotic signals direct the assembly of the septal band (Wolkow. T.D *et al*., 1996**:** Momany and Hamer 1997**)**. However, if each mitotic nucleus triggered the formation of a septum, hyphal cells would be uninucleate. The multinucleate nature of hyphal cells suggests that septal band assembly in response to mitotic signals is restricted to specific cortical regions. These regions presumably contain morphological landmarks that identify them as potential septation sites (Harris, 2001). Alternatively, all cortical regions may be competent to undergo septum formation, but the assembly of a septal band at one site might block the ability of adjacent mitotic nuclei to trigger the same event.

III. Materials and Methods

1. Equipment and chemicals

Chemicals were purchased from Sigma (Taufkirchen), Roth (Karlsruhe), Boehringer (Mannheim), Roche (Mannheim), AppliChem (Darmstadt), Merck (Darmstadt), BIOMOL (Hamburg), ICN (Eschwege), Gibco (Karlsruhe), Stratagene (Amsterdam, Niederlande), and Difco Laboratories (Detroit, MI, USA). Restriction enzymes and other DNA-modifying enzymes were obtained from New England Biolabs (Frankfurt/Main) and Amersham (Freiburg). The enzymes for PCR were bought from Promega (Mannheim) Qbiogene (Heidelberg) or Roche Diagnostics (Mannheim). The agar for solid medium was used from Roth. DNA Marker was provided by MBI-Fermentas (St. Leon-Roth). Nitrocellulose membrane (Hybond-N) was obtained from Amersham and Pall Gelman Laboratories (Dreieich). Miracloth filter tissue was bought from Calbiochem (Heidelberg). As protein standard for SDS-polyacrylamidgelelectrophoresis Roti-Mark Prestained from Roth (Karlsruhe) was used. For western blot protein transfer, Protein Nitrocellulose Transfer membrane from Schleicher and Schuell (Whatman, Dassel) was used. Developer and Fixer solutions were from Kodak-GmbH (Stuttgart). The DAPI Mix was obtained from Molecular Probes (Vectashield Mounting Medium, H-1200, Burlingame, USA) and Hoechst 33342 was from Molecular Probes (H-3570, Oregon, USA). Autoradiographic films were from Kodak (Rochester, NY, USA) or Fuji (New RX, Fuji, Japan). The agarose for DNA-isolating gels was from Peqgold Agarose (Peqlab, Erlangen). QUIAquick gel extraction kit was from Qiagen (Hilden). Gel-electrophoresis chamber for agarose gels was bought from Peqlab. The photograph of colony was taken from digital camera (Nikon Coolpix). All microscope images were taken from Zeiss Axiophoto Microscope and Zeiss Axioimager Z1 and CCD camera Hamamatsu (ORCA ER) was used.

2. Organisms used in this study and microbiological methods

2.1. Organisms

In this work the following *A. nidulans* and *E. coli* strains were used:

Table III.1: *A. nidulans* strains used in this study. All strains are *veA1*.

Strain	Genotype	Source
TN02A3	*pyrG89*; *argB2, ΔnkuA::argB*; *pyroA4*	[Nayak, T *et al.,* 2006]
RMS011	*pabaA1, yA2*; *ΔargB::trpCΔB*; *pyroA4*	[Stringer, M *et al.,*1991]
SRL1	*ΔkipA::pyr4; pyrG89; pyroA4, (ΔkipA)*	[Konzack, S *et al.,* 2005]
SJW02	*wA3*; *ΔargB::trpCΔB*; *pyroA4*; *alcA(p)::GFP::tubA,* (GFP-MTs)	[Veith, D *et al.,* 2005]
SSK91	SRF200 transformed with pSK76, *ΔteaA::argB*; *pyrG89*; *ΔargB::trpCΔB*; *pyroA4.* (*ΔteaA*)	[Konzack, S *et al.,*2005]
SNT17	*pyrG89; wA3; alcA(p)::GFP::kipA-rigor* (GFP-*KipA*-rigor)	[Takeshita, N *et al.,*2008]
SNT49	TN02A3 transformed with pNT28, (*teaA(p)-mRFP1-TeaA*)	[Takeshita, N *et al.,*2008]
SNT28	TN02A3 transformed with pNT9, (*GFP-SepA*)	[Takeshita, N *et al.,*2008]
SNT4	TN02A3 transformed with pNT5, (*GFP-TeaA*)	Takeshita, N *et al.,*2008]
SNT52	SNT49 crossed to RMS011, (*teaA(p)-mRFP1-TeaA*)	[Takeshita, N *et al.,*2008]
SYH03	TN02A3 with pYH06 (*alcA(p)-GFP-TeaC, pyroA4*)	This study
SYH05	TN02A3 transformed with pYH03 and pYH09, (*YFP^N-SepA* and *YFP^C-TeaC*)	This study
SYH06	TN02A3 transformed with pYH01 and pYH09, (*YFP^N-TeaA* and *YFP^C-TeaC*)	This study

SYH13	SYH03 crossed to SNT52 (*GFP-teaC, teaA(p)-mRFP1-TeaA*)	This study
SYH17	TN02A3 transformed with pYH30 (*teaCp-mRFP1-TeaC*)	This study
SYH18	SYH20 crossed to SNT28 (*teaCp-mRFP1-TeaC* and *GFP-SepA*)	This study
SYH19	SYH20 crossed to SSK91 (*teaC(p)-mRFP1-TeaC ΔteaA*)	This study
SYH20	SYH17 crossed to RMS011(*teaCp-mRFP1-TeaC*)	This study
SYH21	TN02A3 transformed with pYH14 (*ΔteaC*)	This study
SYH22	SYH20 crossed to SJW02 (*GFP-MT, teaCp-mRFP1-TeaC*)	This study
SYH23	SYH20 crossed to SNT17 (*GFP-kipA* [rigor] *teaCp-mRFP1-TeaC*)	This study
SYH24	SYH21 crossed to SNT52 (*teaA(p)-mRFP1-TeaA, ΔteaC*)	This study
SYH25	SYH17 crossed to SRL1 (*ΔkipA, teaCp-mRFP1-TeaC*)	This study
SYH26	SYH28 crossed to SYH27 (*mRFP1-TeaC, GFP-SepA*)	This study
SYH27	TN02A3 transformed with pYH24 (*mRFP1-TeaC*)	This study
SYH28	RMS011 crossed to SNT28 (*GFP-SepA*)	This study
SYH32	TN02A3 transformed with pYH48 (*3xHA-TeaC*)	This study
SYH04	TN02A3 transformed with pYH07 (GFP-*TeaB*)	This study
SYH30	SYH29 crossed to SNT21 (*GFP-TeaC, GFP tubA*)	This study
SYH31	SYH29 crossed to SRF27 (*GFP-TeaC, GFP nucleus*)	This study
SYH36	SYH29 crossed to SNT4 (*alcA(p)-GFP-teaC ΔteaC*)	This study
SYH29	SYH21 crossed to RMS011 (*ΔteaC*)	This study

FGSC: Fungal Genetic Stock Center, Kansas, USA

Table III.2: *E. coli* **strains used in this study**

XL1-Blue	recA1, endA1, gyrA96, thi-1, hsdR17, supE44, relA1, lac [F'proABlacIQZ.M15::Tn10 (TetR)]	Stratagene, Heidelberg
Top10F'	F'[lacIQ, Tn10 (TetR)] mcrA .(mrr-hsdRMS-mcrBC), O80 lacZ .M15.lacX74, deoR, recA1, araD139.(araleu) 7679, galU, galK, rpsL, (StrR) endA1, nupG	Invitrogen, Leek, Netherlands

2.2. Cultivation and growing of microorganisms

Media for *E. coli* were prepared as previously described (Sambrook *et al*., 1999), (Table III.3) and supplemented in function of each experiment, with antibiotics and necessary reagents (Table III.4). Ingredients were added to ddH$_2$O water, poured into bottles with loosen caps and autoclaved 20 min at 15 lb/in2. For solid media, 15 g agar per liter was added. Glassware and porcelain was sterilized in the heat sterilizer for 3 h at 180°C. Heat-sensitive solutions such as antibiotics, amino acids and vitamins were filer-sterilized with 0.22 nm pore filter membrane (Millipore, France), and added to the media after autoclaving. Minimal and complete media for *A. nidulans* growth were prepared according to the protocols (Pontecorvo *et al*., 1953). For protoplast transformation of *A. nidulans*, 0.6 M KCl as osmoprotective substance was added.

2.3. Growth conditions and storage of transformed *E. coli* and *A. nidulans* strains

Cultures of transformed *E. coli* strains were overnight cultivated on LB plates with appropriate antibiotics at 37°C. Liquid culture was inoculated from a single colony and incubated in LB medium containing appropriate antibiotics at 37°C with 180 rpm overnight shaking. For storage of *E. coli* strains, freshly grown bacterial suspension was adjusted to 15% end concentration of sterile glycerol and frozen at –80°C. The   *A. nidulans* strains were grown on minimal or complete medium plates. Colony pieces were cut from an agar plate and suspended in 15-20% sterile glycerol and stored at –80°C.

2.4. Induction of the *alcA* promoter

In this study, some of *A. nidulans* strains were carrying constructs expressed under the control of *alcA* promoter. For induction of this promoter, the strains were grown overnight (12-16 h) in medium with glucose followed by a replacing with a medium containing 2% glycerol or 2% threonine (and lacking glucose), where the promoter can be induced. Also, especially for preparation of samples designated to be used for microscopy, the spores were inoculated overnight or for one day directly in the inducing medium and subsequently observed.

Table III.3: Media for *E. coli*

Medium	Ingredients (per liter)
LB	10 g Bacto-Tryptone; 5 g Bacto-Yeast Extract; 10 g NaCl
SOC	20 g Bacto-Tryptone; 1 g Bacto-Yeast Extract; 5 g NaCl; 0.185 g KCl; 2.03 g $MgCl_2$ x $7H_2O$; 2.46 g $MgSO_4$ x $7H_2O$; 3.6 g Glucose

Table III.4: Antibiotics and supplements for *E. coli* media

Substance	End concentration
Ampicillin (Amp)	100 µg/ml
Kanamycin (Km)	50 µg/ml
X-Gal	40 µg/ml
IPTG	8 µg/ml

Table III.5: Media and stock solutions for *A. nidulans*

Solution	Concentration (per liter)

20x Salt stock solution	120 g NaNO$_3$; 10.4 g KCl; 10.4 g MgSO$_4$ x 7H$_2$O; 30.4 g KH$_2$PO$_4$
1000x Trace elements stock solution	22 g ZnSO$_4$ x 7H$_2$O; 11 g H$_3$BO$_3$; 5 g MnCl$_2$x 4H$_2$O; 5 g FeSO$_4$ x 7 H$_2$O; 1,6 g CoCl$_2$ x 5 H$_2$O; 1,1 g (NH$_4$)$_6$Mo$_7$O$_{24}$ x 4 H$_2$O; 50 g Na$_4$EDTA; adjustet to pH 6.5-6.8 with KOH
Minimal medium (MM)	50 ml Salt stock solution; 1 ml Trace elements stock solution; 20 g Glucose; adjust to pH 6.5 using 10 N NaOH
Complete medium (CM)	Minimal medium with 2 g Peptone; 1 g Yeast extract; 1 g Casaminoacids; 1 ml Vitamin stock solution; 1 ml Trace elements stock solution; adjust to pH 6.5 using 10 N NaOH

Table III.6: Vitamins, amino acids and medium components

Component	Stock Concentration	Volume per liter
PABA (p-amino-benzoic acid)	0.1%	1 ml
Pyridoxin-hydrochloride	0.1%	1 ml
Arginine	500 mM	10 ml
Uracil	-	1 g
Uridine	500 mM	10 g

3. Genetic methods in *A. nidulans*

Genetic tests on *A. nidulans* strains were basically done after the commonly used protocols (Käfer, 1977); (Morris, 1976); (Pontecorvo *et al*., 1953); and (Clutterbuck,1969).

3.1. Crossing of *A. nidulans*

The strains used for crossing were inoculated side by side on to MM plus appropriate markers plates for 2 days, until the mycelium of both strains fused at the borders. Small agar square blocks were cut from these fused edges and transferred to MM plates, where just the growth of a heterokaryon is possible. Plates were sealed with adhesive tape and incubated 10-14 days at 37°C or 30°C in a humid chamber. The fruiting bodies (cleistothecia) developed after this time were isolated with help of a sterile inoculating needle, rolled until completely cleaned from Hülle-cells on the surface of an agar plate, and smashed in an Eppendorf tube with 0.5 ml sterile ddH$_2$0. An aliquot of the ascospore suspension obtained in this way was inoculated onto MM agar plates. After 3 days incubation, the grown colonies were transferred onto MM plates with different appropriate markers, to test for the missing auxotrophic marker. If more strains were analyzed, they were inoculated onto raster plates, which contained 16-32 colonies.

4. Molecular biological methods

4.1. Plasmids

In this study the following plasmids were used:

Table III.7: Plasmids used in this study

Plasmids	Construction	Source
pCR2.1-TOPO	Cloning vector	Invitrogen (NV Leek, The Netherlands)
pMCB17apx	*alcA(p)::GFP*, for N-terminal fusion of proteins to GFP; contains *N. crassa pyr4*	[Efimov, V *et al.*, 2006]
pDM8	GFP replaced mRFP1 in pMCB17apx	[Wolkow, T *et al.*, 1996]
pSCI	*pry4* with *Sfi*I-sites	[Konzack, S *et al.*,

		2005]		
pNT33	N-terminal half of *teaA* cDNA in pGADT7	[Takeshita, *al.,*2008]	N	*et*
pNT34	N-terminal half of *teaA* cDNA in pGABKT7	[Takeshita, *al.,*2008]	N	*et*
pNT35	C-terminal half of *teaA* cDNA in pGADT7	[Takeshita, *al.,*2008]	N	*et*
pSH19	C-terminal half of *teaA* cDNA in pGABKT7	[Takeshita, *al.,*2008]	N	*et*
pNT6	0.7kb *teaA* fragment in pDBM8	[Takeshita, *al.,*2008]	N	*et*
pNT28	1.5 kb *teaA*(p) fragment in pNT6	[Takeshita, *al.,*2008]	N	*et*
pNT6	0.7kb *teaA* fragment from pNT1 inpDM8	[Takeshita, *al.,*2008]	N	*et*
pNT9	1.2 kb *sepA* fragment in pMCB17apx	[Takeshita, *al.,*2008]	N	*et*
pDV7	GFP replaced N-terminal half of YFP in pMCB17apx	[Takeshita, *al.,*2008]	N	*et*
pDV8	GFP replaced C-terminal half of YFP in pMCB17apx	[Takeshita, *al.,*2008]	N	*et*
pYH01	0.7 kb *teaA* fragment from pNT1 in pDV7	[Takeshita, *al.,*2008]	N	*et*
pYH03	1.2 kb *sepA* fragment from pNT9 in pDV7	[Takeshita, *al.,*2008]	N	*et*
pYH06	1.2 kb *teaC* fragment in pMCB17apx	This study		
pYH08	1.2 kb *teaC* fragment from pYH06 in pDV8	This study		
pYH14	*teaC*-deletion construct: flanking regions from pYH33 and pYH34 ligated with *pry4* from pCS1	This study		
pYH16	N-terminal half of *teaC* cDNA in pGADT7	This study		
pYH17	N-terminal half of *teaC* cDNA in pGBK T7	This study		

pYH18	C-terminal half of *teaC* cDNA in pGADT7	This study
pYH19	C-terminal half of *teaC* cDNA in pGBKT7	This study
pYH24	1.2 kb *teaC* fragment in pDM8	This study
pYH30	1.5 kb *teaCp* fragment in pYH24	This study
pYH32	1.0 kb 5´-flanking region of *teaC* with *Sfi*I-site in pCR2.1-TOPO	This study
pYH33	1.0 kb 3´-flanking region of *teaC* with *Sfi*I-site in pCR2.1-TOPO	This study
pYH34	1.2 kb *teaC* fragment in pCR2.1-TOPO	This study
pSM14	GFP replaced C-terminal 3xHA in pMCB17apx	Müller, S, unpublished data
pYH48	1.2kb *teaC* fragment in pSM14	This study
pYH07	0.7kb teaB fragment in pMCB17apx	This study
pYH44	C-terminal half of *teaC* cDNA in pGBKT7	This study

4.2 DNA manipulations

4.2.1. Plasmid DNA preparation from *E. coli* cells

For isolation of plasmid, an alkali-lysis method was used. For DNA small volumes (miniprep), 2.5 ml of overnight liquid culture was centrifuged 1 min at 13000 rpm, the pellet resuspended in 200 µl Tris-EDTA Buffer, then 200 µl of Alkali-lysis buffer added and gently mixed, followed by addition of 200 µl neutralization buffer (Table III.8). After 10 min centrifugation, plasmid DNA-containing supernatant was precipitated with 0.7 vol. isopropanol, followed by 70% EtOH washing. The dried pellet was resuspended in TE buffer. For large DNA volumes (midipreps), plasmid DNA from 50-100 ml *E. coli* overnight liquid culture was extracted using a Macherey-Nagel Nucleobond Plasmid DNA Purification Kit, according to the manufacturer protocols. Plasmid DNA concentration was compared between the intensity of ethidium bromide DNA bands on agarose gels and the intensity of defined standards.

Table III.8: Solutions used for plasmid extraction (miniprep)

Solution	Concentration
Tris-EDTA buffer	10 ml 1M Tris-HCl (pH 7.5); 2 ml 0.5M EDTA (pH 8.0); 10 mg RNAse in 200 ml
Alkali-lysis buffer	0.2 M NaOH; 1% SDS
Neutralization buffer	1.5 M K-acetate, pH 4.8
TE buffer	10 mM Tris-HCl; 1 mM EDTA; pH 8.0

4.2.2 Genomic DNA preparation from *A. nidulans*

Preparation of *A. nidulans* genomic DNA was done by inoculation in a 9 cm plastic petri dish of around 20 ml fresh liquid minimal media with spore suspension from a colony grown on an agar plate, followed by incubation for 12-15 h at 37°C. Then, the mycelium was harvested with a spatula, pressed briefly until dry between paper towels, and frozen in liquid nitrogen. The frozen mycelium was homogenized by a mortar. Homogenized mycelium was transferred to the new tube, followed by incubation for 0.5-2 h at 68°C. Sample was vortexed and centrifuged at 13000 rpm, 5 min at room temperature. Supernatant was transferred to a new tube and 60 µl of 8 M Kalium acetate pH 4.2 was added. Sample was centrifuged at 13000 rpm, 5 min at room temperature. Supernatant was transferred to a new tube and 750 µl of Isopropanol was added and well mixed. Sample was centrifuged at 13000 rpm, 5 min at room temperature. Pellet was washed two times with 70% ethanol, then dried and resuspended in 200 µl H_2O with 0.01 mg/ml Rnase by heating at 68°C 30 min. Genomic DNA concentration was calculated by a comparison between the intensity of ethidium bromide DNA bands on agarose gels and the intensity of defined standards.

Table III.9: Solutions used for genomic DNA preparation from *A. nidulans*

Solution	Concentration
Extraction buffer	10 ml 0.5 M EDTA (pH 8.0) 0.2 g SDS in 100 ml
8 M potassium acetate	29.5 g potassium acetate in 50 ml H_2O + 11.5 ml acetic acid pH 4.2 with HCl in 100 ml H_2O

4.2.3 Digestion of DNA by restriction endonucleases

DNA samples (200 ng – 1 µg) were digested by restriction endonucleases using corresponding reaction buffers. Generally, restriction digests were prepared in 20 µl total volume, with 0.5-1 µl restriction enzyme (1-20 U/µl) and incubated at 37°C from 1 h to overnight. In other cases, enzyme, DNA, buffer volumes and reaction times varied depending on the specific requirements. *A. nidulans* genomic DNA was generally digested overnight. In the case of different enzymes, the restriction digest was carried out first in the buffer with low salt concentration or the buffer compatible to both enzymes.

4.2.4 DNA precipitation

Contamination by small nucleic acid fragment, protein and salt can be reduced to acceptable level by precipitating the DNA. In order to do this, 2.5 volume of ethanol and 1/10 10 M LiCl were added to the DNA solution. The sample was mixed, kept at –80ºC for 10 min and centrifuged for 10 min at 10.000 rpm. The supernatant was discarded and the pellet was washed with 70% EtOH, followed by centrifugation at 10.000 rpm for 5-10 min. The pellet of purified DNA was completely in a speed vacuum and then dissolved in sterile water or TE buffer.

4.2.5. DNA ligation

DNA ligation was performed using T4 ligase (NEB, Frankfurt) at 16 ºC in a volume of 10-20 µl. Around 50 ng vector was used in one ligation. The ratio of vector to insert was 1:2-3 and 1:5-10 respectively for cohesive end ligation. For the cloning of PCR products, restriction enzyme sites were added to both primers, or TA cloned. For TA cloning, the PCR products amplified with Taq (Qbiogene, Heidelberg) or other proof reading polymerases (e.g. Pfu, Promega, Madison, WI, USA) were cloned into pCR2.1 TOPO (Invitrogen, NV Leek, The Netherlands).

4.2.6. DNA agarose gel electrophoresis

The separation and identification of DNA fragments was done by running them through agarose gels (0.8-1.2%), which were prepared by boiling agarose into 0.5x or 1x TAE buffer and pouring it into gel chambers. DNA samples were mixed with 1/6 6x DNA loading buffer. As standard DNA marker an Eco130I-cut λDNA (MBI Fermentas, St. Leon-Rot) was used, and gels were run for 30 min - 2h in gel chambers with 0.5x or 1x TAE buffer. Then, the gel was stained for 15-30 min in 0.5x TAE with 1 µg/µl ethidium bromide. The DNA bands were visualized in the gel at 302 nm UV light. Photos were taken using a camera (INTAS, Goettingen) connected to a video printer.

Table III.10: Solutions used for genomic DNA gel electrophoresis

Solution	concentration
50x TAE buffer (pH 8.0)	40 mM Tris-Acetate; 1 mM EDTA; pH 8.0
10x Loading buffer	20% Ficoll 400; 0.1 M Na_2EDTA (pH 8.0); 1% SDS; 0.25% Bromphenol blue; 0.25% Xylene cyanol

4.2.9. PCR

Polymerase chain reaction (PCR) was performed with Taq (Qbiogene, Heidelberg), Pfu (Promega, Madison, WI, USA) according to manufacturer protocols. Oligonucleotides synthesis was made by MWG Biotech (Ebersberg) and the concentration used for a PCR reaction volume of 10-100 µl was 5-20 pM. As DNA template was used either plasmid DNA (0,2-10 ng) or genomic DNA (10-20 ng). The PCR reactions were carried out in Biometra TRIO Themoblock and annealing temperatures varied in function of each application. PCR programs were generally used with 30-35 cycles, at a denaturation temperature of 95-98°C, and a polymerization temperature of 68-72°C. In the case of oligonucleotides containing restriction sites. Oligonucleotides used in this study (Table III.12) were synthesized by MWG Biotech (Ebersberg).

Table III.11: PCR reaction

Standard PCR reaction

1 µl 2.5 mM dNTP
1 µl DNA template
1 µl 10 x buffer
1 µl 50 mM MgCl$_2$
1 µl each 5 µM Primer A and B
0.2 µl Taq DNA polymerase
1.8 µl autoclaved ddH$_2$O

Table. III.12: Primers used for PCR in this study

Primer	Sequence
TeaC-left-for	(5'-GAACAGTTGCCTTTCGAAAT-3')
TeaC-left-rev-SfiI	(5'-TGGT<u>GGCCATCTAGGCC</u>GTAGCAGGATGTTCAAAGG3')
TeaC-right-for-SfiI	(5-AATA<u>GGCCTGAGTGGCC</u>CCGACTGGCACCACTAC-3')
TeaC-right-rev	(5'-AGAGGCTGGATTCCTTCT-3')
teaC-AF	(5'-TA<u>GGCGCGCC</u>GATGGCTAGACCTAGAATGG-3')
teaC-PR	(5'-C<u>TTAATTAA</u>TTCTTCAACAGCCTTAGTTTT-3')
TeaCp-pro-AvrII	(5'-A<u>CCTAGG</u>TGACCTTGGGTATCGTTG-3')
teaC-pro-KpnI	(5'-A<u>GGTACC</u>ACGAATTATGTAGCAGGAT-3')
Fwd-Kpn-YFP-N	(5´-<u>CGGTACC</u>ATGGTGAGCAAGGGCGAGGAGCTG-3´)
rev-YFP-N-Li-Asc	(5-C<u>GGCGCGCC</u>CGTGGCGATGGAGCGCATGATATAGACG TTGTG GCTGTTGTAG-3´).
fwd-Kpn-YFP-C	(5´-C<u>GG TAC C</u>AT GGC CGA CAA GCA GAA GAA CGG CAT CAA GG-3´)
ev_YFP-C_Li_Asc	(5´C<u>GGCGCGCC</u>GTGGTTCATGACCTTCTGTTTCAGGTCGT TCGGGATCTTGCAGGCCGGGCGCTTGTACAGCTCGTCCA TGCCGAGAGTGATCCC-3´)
TeaC-EF	(5´-GGCC<u>GAATTC</u>ATGGCTAGACCTAGAATGG -3´)
TeaC-BMR	(5'-<u>GGATCC</u>TTACAGTAGGTTCGGAGTGAG -3')
TeaC-EMF	(5´-<u>GAATTC</u>GAAAAGCCGCGCTCAAG-3')
TeaC-BR	(5'-GGCC<u>GGATCC</u>TTATTGACTCGTCGACCTG -3')
GFP for	(5'-ATGAGTAAAGGAGAAGAACTT-3')
mRFP for 100 bp rev	(5'-AGCTTGGCGGTCTGGGT-3')
Pry4 rev 100 bp	(5'-GATGCATGCGGAACCGC-3')
HA-EfimovF2	(5'-<u>GGTACC</u>ATGTACCCATACGATGTTCCTGAC -3')

4.2.10. DNA isolation from agarose gel

The DNA from normal agarose gels was isolated with the QIAEX II Gel Extraction System (Qiagen,Hilden).

4.2.11. DNA sequencing

DNA sequencing was done by commercial sequencing (MWG Biotech,Ebersberg).

4.2.12. Transformation of *E. coli*

The transformation of electrocompentent *E. coli* cell was done as described (Ausubel *et al.,* 1995). After dialyzation of ligation reaction, 2 µl ligation solution and 50 µl *E. coli* electrocompetent cells were mixed and filled into a transformation cuvette (PEQLAB, Erlangen). The plasmids were transformed by electroporation (Gene-Pulser, Bio-Rad) into electrocompentant *E. coli* cells XL1-Blue (Stratagene, La Jolla, USA). Alternatively, chemical competent *E. coli* strain TOP10 F' (Invitrogen, Leek, Netherlands) was used according to the distributor protocols.

4.2.13. Transformation of *A. nidulans*

Standard procedures of *Aspergillus* protoplast transformation were used (Yelton *et al.,* 1984). Spores were harvested from freshly grown plates (~109 conidia), inoculated in 500 ml volume minimal medium with appropriate components, and shaked at 30ºC in water bath for 12-16 h until spores germinated. The culture was filtered through sterile Miracloth followed by washing using Wash solution. The washed mycelium was collected on ice in a sterile 100 ml Erlenmeyer flask with 5 ml of Osmotic medium. After addition of GlucanX (Novozyme) (200 mg/ml sterile water) and 5 min incubation on ice, BSA (6 mg/0.5 ml sterile water) was added into the flask. Subsequently, the digestion mixture was incubated at 30ºC in water bath for 1-3 h until enough protoplasts became free. Then, it was transferred into a 30 ml Corex tube and 10 ml of Trapping buffer was slowly added, followed by a centrifugation at 5000 rpm for 15 min using HB-6 rotor

(Universal 320R, Hettich). The obtained protoplast band was transferred into a new sterile tube, followed by washing two times using STC with centrifugation at 7000 rpm for 8 min. The protoplast pellet was gently resuspended in 200-1000 µl STC for transformation (for the solutions used, see Table III.10). 100 µl protoplasts in STC and 100 µl DNA (10 µg DNA filled up to 100 µl STC) were mixed and incubated 25 min at room temperature in a falcon tube. Then, 2 ml PEG was added and the tube was rolled until the mixture was homogeneous, followed by 20 min incubation at room temperature. Finally, 8 ml STC was added and the entire mixture was spread onto osmotically stabilized medium (MM + 0.6 M KCl) with appropriate selection markers. The plates were incubated at 37ºC until colonies were formed after 3-4 days.

Table III.13: Solutions used for *A. nidulans* transformation

Solution	Concentration
Mycelium wash solution	0.6 M $MgSO_4$
Osmotic medium	1.2 M $MgSO_4$, 10 mM Na_3PO_4 buffer, pH 5.8
Trapping buffer	0.6 M sorbitol, 0.1 M Tris-HCl, pH 7.0
STC	1.2 M sorbitol, 10 mM $CaCl_2$, 10 mM Tris-HCl, pH 7.0
PEG 60%	PEG 4000, 10 mM $CaCl_2$, 10 mM Tris-HCl, pH 7.0

4.2.14. DNA-DNA hybridization (Southern blot analysis)

DNA-DNA hybridization (Southern blot analysis) was performed using DIG labelling probe. The preparation of probes was made by PCR DIG Probe Synthesis Kit from Roche (Mannheim). The DNA samples were isolated through 1% agarose gel. After electrophoresis gel was washed with Denaturation Buffer two times 15 min. The gel was washed with Neutralisation Buffer two times 15 min. The gel was afterwards equilibrated 10 min in 20x SSC at RT. Isolated DNA was transferred to Nitrocellulose Membrane (Pall Gelman Laboratories, Dreieich) overnight. To transfer, Set up the transfer system (bottom to top):→Brdege of whatman paper; presoaked in 20x SSC and making contact to 20x SSC reservoirs at both ends → gel (upside down) → Nitrocellulose Membrane, presoaked in 20x SSC → 3 layers of whatman paper → several layers of tissue → glass

plate on top about 200g weight. Nitrocellulose Membrane was cross-linked under UV-Light (254nm 1 min each side). Pre-hybridize membrane with pre-heated DIG-Standerd-HYB Buffer; at last 1 h 68°C. For hybridisation 2 µl DIG-labelled probe pre ml of DIG-Standard-HYB Buffer was used. Probe was diluted in 40 µl ddH$_2$O and boiled 5 minutes 100 °C in water bath. Boiled probe was then added to DIG-Standerd-HYB Buffer and hybridization was done overnight at 68°C, followed by stringent washing. The first washing step consisted in 2 times of 2 x Washing Buffer for 10 min, and then the second step of 2 times each 10 min 0.5 x Washing Buffer at 68ºC, and third step of wash 5minutes in Washing Buffer. Next, membrane was incubated at 30 min in Blocking Buffer. Anti-DIG-Antibody-AP (Roche, Mannheim) was added 5 µl in 50 ml new Blocking Buffer, followed by incubation for 30 minutes. Membrane was washed two times for 15 min in Washing Buffer, followed by equilibration for 5 min in AP-Buffer. Membrane was transferred to plastic film and substrate (5 µl CDP-Star in 500 µl AP-Buffer) was added. Substrate was distributed evenly on the membrane and incubated for at least 5 min. Signal was detected in the dark room.

Table III.14: Solutions used for Southern blot

Solution	Concentration
DIG Standard Hybridization Buffer	5x SSC; 0.02 % SDS; 1% Blocking Buffer 0.1% (W/V) N-laurylsarcosine
Acidic Buffer	0.25 M HCl
Denaturation Buffer	0.5 M NaOH; 1,5 M NaCl
Neutralization Buffer	0.5M TrisHCl, 1.5M pH7.5
20 x SSC	3M NaCl 0.3M NaCitrat
2 x Washing Buffer	2x SSC 0.1% (W/V) SDS
0.5 x Washing Buffer	0.5x SSC 0.1% SDS
Maleic Acid Buffer	100mM Maleic Acid 150mM NaCl
Blocking buffer	1% Blocking Solution in Maleic Acid Buffer
10x Blocking Solution	10%(W/V) Blocking Reagent (Roche) in Maleic Acid Buffer
AP-Buffer	0.1M TrisHCl pH 9.5 0.1M NaCl 50mM MgCl2

4.3. Description of DNA constructs (plasmids)

Flanking regions of *teaC* were amplified by PCR using genomic DNA and the primers TeaC-left-for and TeaC-left-rev-SfiI for the upstream region of *teaC* and the primers TeaC-right-for-SfiI and TeaC-right-rev for the downstream region and cloned into pCR2.1-TOPO to generate plasmids pYH32 and pYH33, respectively. The SfiI restriction sites are underlined. In a three-fragment ligation, the *N. crassa* pyr-4 gene was released from plasmid pSCI with SfiI and ligated between the two teaC-flanking regions, resulting in the vector pYH14. This plasmid was transformed into the uracil-auxotrophic strain TN02A3 (*nkuA*). The integration events were confirmed by PCR and Southern blotting (Fig.IV.3).

4.3.1 GFP-labeling of alcA-TeaC (pYH06)

To create an N-terminal green fluorescent protein (GFP) fusion construct of TeaC, a 1.2-kb N-terminal fragment of *teaC* (starting from ATG) was amplified from genomic DNA with the primers teaC-AFand teaC-PR and cloned into pCR2.1-TOPO, yielding pYH34. The restriction sites are underlined. The AscI-PacI fragment from pYH34 was subcloned into the corresponding sites of pMCB17apx, yielding pYH06. This plasmid was transformed into the uracil-auxotrophic strain TN02A3 (nkuA). The integration events were confirmed by PCR and Southern blotting.

4.3.2 mRFP-labeling of alcA-TeaC(pYH24) and native promoter TeaC(pYH30)

To create an N-terminal mRFP1 fusion construct of TeaC, the AscI-PacI fragment from pYH06 was subcloned into the corresponding sites of pDM8, yielding pYH24. To produce TeaC N-terminally tagged with mRFP1 expressed from the native promoter, a 1.5-kb fragment of the *teaC* putative promoter region was amplified from genomic DNA with the primers TeaCp-pro-AvrIII and teaC-pro-KpnI digested with AvrI and KpnI, and ligated with AvrI-KpnI-digested pYH24, yielding pYH30 (*alcA* promoter replaced with the teaC promoter in pYH24). Those plasmids were transformed into the

uracil-auxotrophic strain TN02A3 (*nkuA*). The integration events were confirmed by PCR and Southern blotting (results not shown).

4.3.3 HA-labeling of TeaC (pYH48)

To create an N-terminal mRFP1 fusion construct of TeaC, the *Asc*I-*Pac*I fragment from pYH06 was subcloned into the corresponding sites of pSM14, yielding pYH48.

This plasmid was transformed into the uracil-auxotrophic strain TN02A3 (*nkuA*). The integration events were confirmed by PCR.
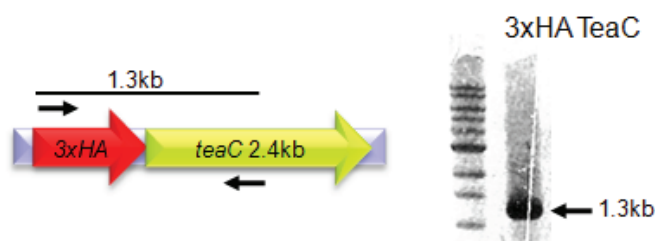
4.3.4 Split-YFP-labeling of TeaC, TeaA and SepA

For bimolecular fluorescence complementation (BiFC) analyses, the N-terminal half of YFP (YFPN) or the C-terminal half of YFP (YFPC) was fused to the N-terminus of the protein of interest. YFPN (154 amino acids of YFP and 5 amino acids linker) was amplified with the primers fwd-Kpn-YFP-N. YFPC (86 amino acids of YFP and 17 amino acids linker) was amplified with the primers fwd-Kpn-YFP-C and ev_YFP-C_Li_Asc. The KpnI-AscI fragment of YFPN or YFPC was ligated into KpnI- and AscI-digested pMCB17apx, yielding pDV7 (GFP replaced with YFPN in pMCB17apx) and pDV8 (GFP replaced with YFPC in pMCB17apx). To create an N-terminal YFPC fusion construct of TeaC, the AscI-PacI fragment from pYH06 was subcloned into the corresponding sites of pDV8, yielding pYH08. To create N-terminal YFPN fusion constructs teaA and sepA fragments from pNT1, pNT9, were subcloned into the corresponding sites of pDV7, yielding pYH01 and pYH03. Those plasmids were transformed into the uracil-auxotrophic strain TN02A3 (*nkuA*). The integration events were confirmed by PCR.

4.3.5 Yeast-two-hybrid analysis

The yeast-two-hybrid analysis was performed by using the MatchMaker3 Gal4 two-hybrid system (BD Clontech). For bait generation, fragments of teaC cDNA corresponding to the N-terminal half of TeaC (356 amino acids) with the primers TeaC-EF and TeaC-BMR or corresponding to the C-terminal half of TeaC (428 amino acids) with the primers TeaC-EMF and TeaC-BR were amplified and cloned into the pGBK7 vector, which contains the Gal4 DNA-BD and the TRP1 marker, yielding pYH17 and pYH19 (BD Clontech). The fragments of teaC cDNA corresponding to the N-terminal half and C-terminal half of TeaC from pYH17 and pYH19 were amplified and cloned into the pGADT7 vector, which contains the GAL4 DNA-AD and the LEU2 marker (BD Clontech), yielding pYH16 and pYH18. pGBK7-associated plasmids were transformed into yeast Y187 (mating type MAT), and pGADT7-associated plasmids were transformed into yeast AH109 (mating type MATa).

5. Biochemical methods

5.1. Isolation of proteins from *A. nidulans*

For protein extraction, spores were incubated overnight in liquid media at 37°C shaking with 200 rpm and for induction of the *alcA* promoter, *A. nidulans* cultures ware shaken in MM containing 2% threonine or 2 % glycerol for 48 h. The mycelium was harvested by filtration through Miracloth (Calbiochem, Heidelberg). The grown mycelium was filtered, dried and grounded in liquid nitrogen. Then, it was resuspended in the same amount of a protein extraction buffer (50 mM Tris-HCl (pH 8), 150 mM NaCl with 1 mM phenylmethylsulfonyl fluoride, 10 µM leupeptin, 1 µM pepstatin). The slurry was centrifuged at 13.000 rpm at 4°C for 5-10 min and the total protein concentration of the supernatant measured according to Bradford (Bradford, 1976). After centrifugation, the supernatant was stored at -80°C or aliquots selected for analysis were heated at 95°C for 10 min together with loading buffer (240 mM Tris/HCl, pH6.8; 8 % SDS; 40 %

Glycerol; 12 % DTT; 0.004 % Bromophenole blue) prior to loading. Protein concentration was quantified with the Roti-Quant kit (Roth, Karlsruhe).

5.2 SDS-polyacrylamide gel electrophoresis (SDS-PAGE)

The SDS-PAGE gel consisted of a resolving gel topped by a stacking gel. The separating gel was casted between the glass plates using Bio-Rad Mini PROTEAN 3 system and overlayed with a thin layer of ddH$_2$O. After gel polymerisation, the water was removed and the gel chamber was filled up with stacking gel. The protein samples were diluted to appropriate concentrations using 4 x Laemmli sample buffer, heated at 95ºC for 10 min and loaded onto the gel. Electrophoresis took place at room temperature, first at 50 V until the sample moved out from the wells and then 100-120 V until tracking dye reached the bottom of separating gel (for the solutions used, see Table III.15).

Table III.15: Solutions used for SDS-polyacrylamide gel preparation

Solution	Stacking gel	Separating gel
	4%	7.5 %
30% Acrylamid Mix	0.83 ml	2.475 ml
1M Tris-HCl pH6.8	0.63 ml	-
1M Tris-HCl ph8.8	-	2.5 ml
H$_2$O	3.4 ml	4.825 ml
10% SDS	0.05 ml	0.1 ml
10% APS	0.05 ml	0.1 ml
TEMED	0.005 ml	0.008 ml

10x Electrophoresis running buffer	**30.3 g Tris; 144 g Glycine; 2 g SDS in 1 liter of ddH$_2$O.**

5.3. Western blotting

For immunodetection of the proteins a Western blot was performed. After SDS-PAGE the proteins were transferred from the gel to nitrocellose membrane from Schleicher and Schuell (Dassel, Germany). Electroblotting was performed in a "sandwich" assembly in Transfer buffer for 3 h to overnight at 60 V at 4°C using Mini Trans-Blot Electrophoretic Transfer Cell (Bio-Rad, USA). After transfer, the membrane was stained for 5 min in PonceauS solution, and then washed with water until the protein bands were distinctly visible. The membrane was washed in TBS-T solution 4 x 5 min, blocked in Blocking solution for 1 h, then hybridized for 1-2 h at room temperature or overnight at 4°C with the primary antibody diluted in Blocking solution. Afterwards, the membrane was washed again 4 x 5 min in TBS-T, incubated with the secondary antibody for 1 h at room temperature, followed by 4 x 5 min washing in TBS-T (for the solutions used, see Table III.16). GFP-fusion protein was detected with rabbit polyclonal anti-GFP (Sigma-Aldrich, Munich, Germany; dilution 1:4000) and a secondary polyclonal anti-rabbit antibodies coupled to peroxidase (Product A 0545; Sigma-Aldrich, Munich, Germany; dilution 1:4000).

Table III.16: Solutions used for Western blot

Solution	Concentration
10 x Transfer buffer	15 g Tris; 72 g glycine in 1 g SDS 1 liter of ddH$_2$O.
Transfer buffer	800 ml H$_2$O, 100 ml 10 x Transfer buffer, 200 ml methanol
Ponceau S	0.1% Ponceau-S in 1% acetic acid, reusable
10 x TBS	24.2 g Tris, 80 g NaCl in 1 liter of ddH$_2$O, pH 7.5
Blocking solution	TBS-T with 3% BSA
TBS-T	1 x TBS, 0.1% Tween 20 (100%)

6. Microscopic method

6.1. Light/fluorescence Microscopy

For live-cell imaging of germlings and young hyphae, cells were grown on cover slips in 0.5 ml MM + 2% glycerol (derepression of the *alcA* promoter and thus moderate expression of the gene), MM + 2 % threonine (activation of the gene thus high expression levels) or MM + 2% glucose (repression of the *alcA* promoter). Cells were incubated at room temperature for 1-2 days. For pictures of young hyphae of each gene-deletion strain, the spores were inoculated on microscope slides coated with MM + 2% glucose + 0.8% agarose and grown at 30°C for 1 day. Images were captured at room temperature using an Axioimager microscope (Zeiss, Jena, Germany). Images were collected and analyzed with the AxioVision system (Zeiss).

6.2. FM4-64, Hoechst 33342, Calcofluor white, Benomyl and Cytochalasin A treatment

FM4-64 was used at a concentration of 10 µM in the medium. Cover slips were incubated for 5 min and washed. Benomyl, (methyl 1-(butylcarbamoyl)-2-benzimidazole carbamate; Aldrich) was used at a final concentration of 2.5 µg/ml in the medium from a stock solution of 1 mg/ml in ethanol. Cytochalasin A (Sigma) was used at a final concentration of 2 µg/ml in the medium from a stock solution of 100 mg/ml in dimethyl sulfoxide (DMSO). Calcofluor white was used at a final concentration of 60 µg/ml in the medium. Hoechst 33342 (Molecular Probes, USA) used at a final concentration of 10 µg/ml in the medium.

6.3. BiFC (Bimolecular fluorescent complementation analysis)

Protein-protein interactions were detected by using the BiFC-analysis. This method was developed by Hu *et al.*, 2002, and has been meanwhile applied in animals, plants, fungi and bacteria (Atmakuri *et al.*, 2003; Blumenstein *et al.*, 2005; Bracha-Drori *et al.*, 2004;

Grinberg *et al.*, 2004; Hoff & Kuck, 2005; Hynes *et al.*, 2004; Walter *et al.*, 2004) Hereby half of split YFP fusion protein comes closer enough to another half of target split YFP fusion protein when there interacted functional YFP is accomplish. In this study Split-YFP was fused downstream of the *alcA*-promoter. For microscopic observations the conditions are described in material and methods (6.1).

7. Yeast-Two-Hybrid analysis

As another proof for protein-protein interactions, the Yeast two hybrid analysis was used. In this method DNA-construct and experiment protocol was used MatchmakerR Library Construction & Screening Kit from Clontech (Mountain View, CA, USA).

IV. Results

1. TeaC is required for polarized growth

I searched the *A. nidulans* genome database at the Broad Institute (Cambridge, MA)(http://www.broad.mit.edu/annotation/genome/aspergillus_group/MultiHome.html) for proteins with similarity to the cell end marker protein Tea4 from *S. pombe* and identified one open reading frame (AN1099.3)(Galagan *et al*., 2005). DNA and cDNA sequences were confirmed and five introns of 66, 60, 66, 46, and 45 bp length determined. I named the gene *teaC*, although sequence similarity between the 687 amino acid long *A. nidulans* protein and the 810 amino acids long *S. pombe* protein was restricted to a conserved SH3 domain **(Fig. IV. 1)**. Within this 86 amino acid long domain the identity was 63 % with an e-value of 6e-27. Outside this region, the homology was very low and the overall identity only 12.5 %. Sequence similarity to the *S. cerevisiae* Bud14 protein, which shares some functional relationship with Tea4, was even lower.
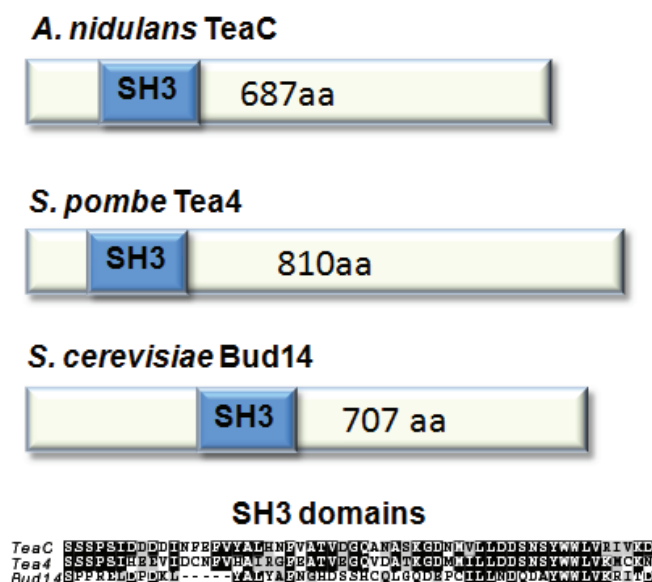
Fig. IV. 1: **Comparison of TeaC with related proteins from *S. pombe* and *S. cerevisiae*.** Scheme of *A. nidulans* TeaC, *S. pombe* Tea4 and *S. cerevisiae* Bud14, indicating the location of the SH3 domain. The alignment of the three SH3 domains is displayed below the scheme.

In other *Aspergilli*, proteins with high identities to *A. nidulans* TeaC were found **(Fig. IV. 2)**. The identity to corresponding proteins from other ascomycetous fungi was again much lower, e.g. *Penicillium chrysogenum* 43 %, and to *Magnaporthe grisea* only 22 %. Sequence identity to basidiomycetous species was below 10 %. These results indicate that TeaC sequences are only poorly conserved between different genera.
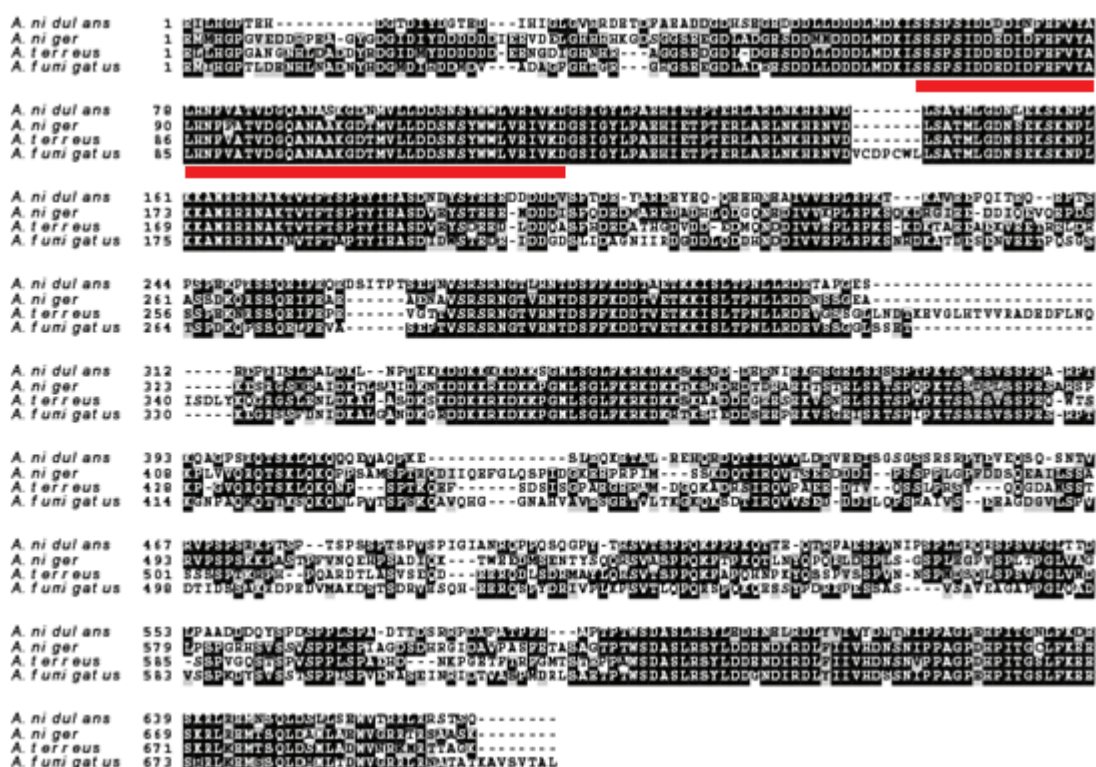
Fig. IV. 2: **Comparison of TeaC with related proteins from four other *Aspergilli*.** Alignment of TeaC homologues from four *Aspergillus* species as indicated. The SH3 domain is highlighted with the red line below the sequences. The alignments were done with Clustal W with standard parameters. Identical amino acids were shaded in black and chemically conserved amino acids in grey using the program box shade.

2. Deletion and phenotype analysis

Flanking regions of teaC were amplified by PCR using genomic DNA and the primers TeaC-left-for and TeaC-left-rev-SfiI for the upstream region of *teaC* and the primers TeaC-right-for-SfiI and TeaC-right-rev for the downstream region and cloned into pCR2.1-TOPO to generate plasmids pYH32 and pYH33, respectively. In a three-fragment ligation, the N. crassa *pyr4* gene was released from plasmid pSCI with *SfiI* and ligated between the two *teaC*-flanking regions, resulting in the vector pYH14 The cellular function of *teaC* was investigated through the construction of a null mutant by homologous recombination **(Fig. IV. 3, A see Materials and Methods)**. The each *teaC* region was disrupted by insertion of the nutritional marker gene *pyr4* **(Fig IV. 3, A)**. Colony purified uridine and urasil prototrophic transformants of strain TN02A3 were tested for the integration event at the teaC locus by Southern blot analysis using different restriction digests **(Fig. IV. 3, B)** and checked by PCR **(Fig. IV. 3, C and D)**. 20 strains were analyzed from which eight showed the *teaC*-deletion pattern. All eight deletion strains displayed the same phenotypes. One *teaC*-deletion strain was selected for further studies and named SYH21. Coupling of the observed phenotypes with the gene-deletion event was confirmed by crosses, re-complementation with *teaC*-derived clones and by down regulation of the gene through the suppressed *alcA* promoter **(Fig. IV. 8).**
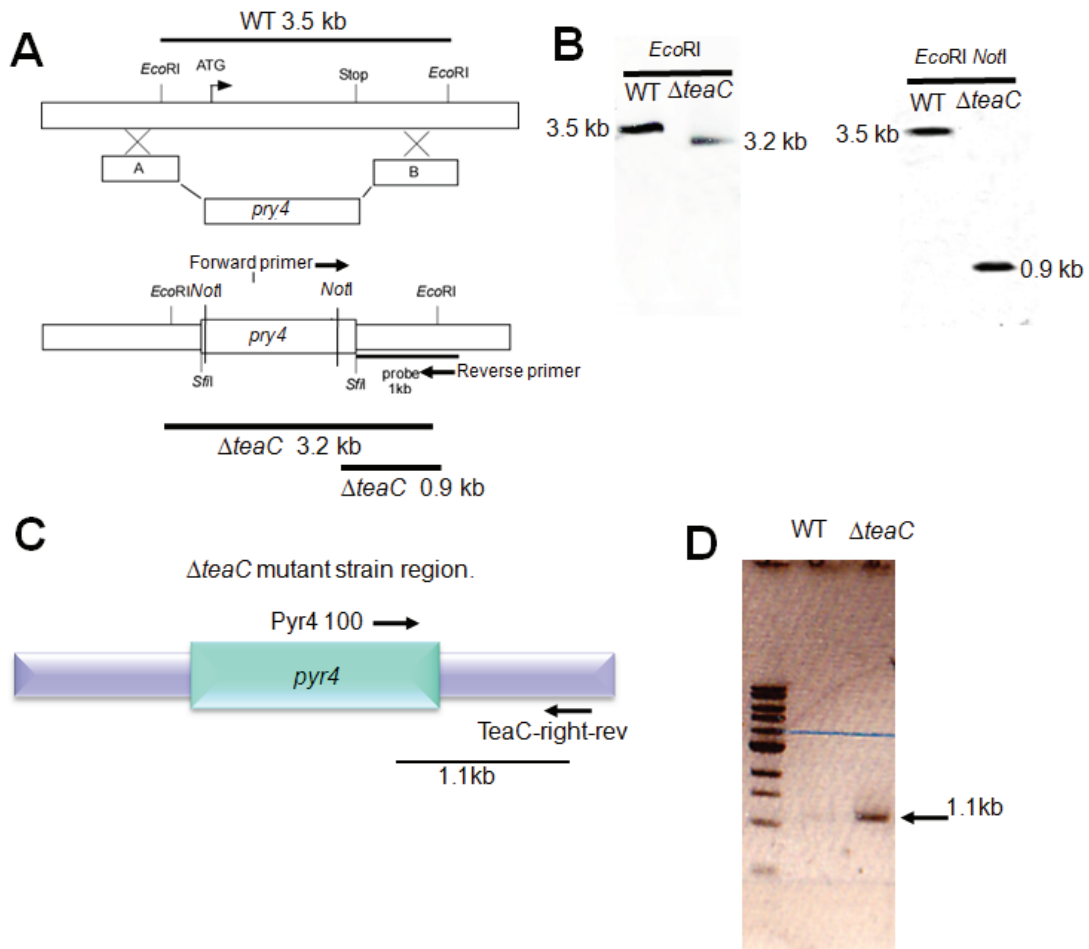
Fig. IV. 3: Construct for the deletion of *teaC*. (A) Scheme of the deletion construct and the expected replacement. The lines indicate the expected band sizes after the corresponding restriction digest. **(B)** Southern blot of WT (TN02A3) and SYH21. Genomic DNA was digested with *Eco*RI or *Eco*RI and *Not*I. The blot was hybridized with the probe indicated in (A). **(C)** Scheme of the deletion construct and the expected replacement. **(D)** PCR of WT (TN02A3) and (SYH21). Genomic DNA of WT (TN02A3) and Δ*teaC* (SYH21) was used with the primers indicate in (C).

To analyze the function of *teaC* in *A. nidulans*, I constructed a *teaC*-deletion strain (SYH21) and compared it to a ∆*teaA*-deletion strain constructed previously (Takeshita *et al*., 2008). In comparison to wild type, the growth defect was slightly more severe in the ∆*teaA*-deletion strain **(Fig. IV. 4, A)**. In both ∆*teaA*-deletion and ∆*teaC*-deletion strains hyphae displayed a zig-zag growth phenotype in comparison to straight hyphae in the wild type **(Fig. IV. 4, B)**. The effect on the maintenance of growth directionality was also stronger in the ∆*teaA* strain. The mutant phenotype was mainly seen in young hyphae. Both strains produced compact and small colonies (75-85 % of the diameter) compared to the wild tip. Another polarity defect has been detected in the way the second germ tube emerges from a conidiospore. In wild type, the second hypha emerges opposite to the first germ tube (bipolar) in 83 % of the spores. In contrast, the second hyphae emerged at random positions in 56% of the spores in the ∆*teaC*-mutant strain. A similar defect was observed in 55 % of the spores in the ∆*teaA* mutant **(Fig. IV. 4, C : n = 100)**. This suggests that *teaA* and *teaC* are required for the selection of the site of polarity initiation.
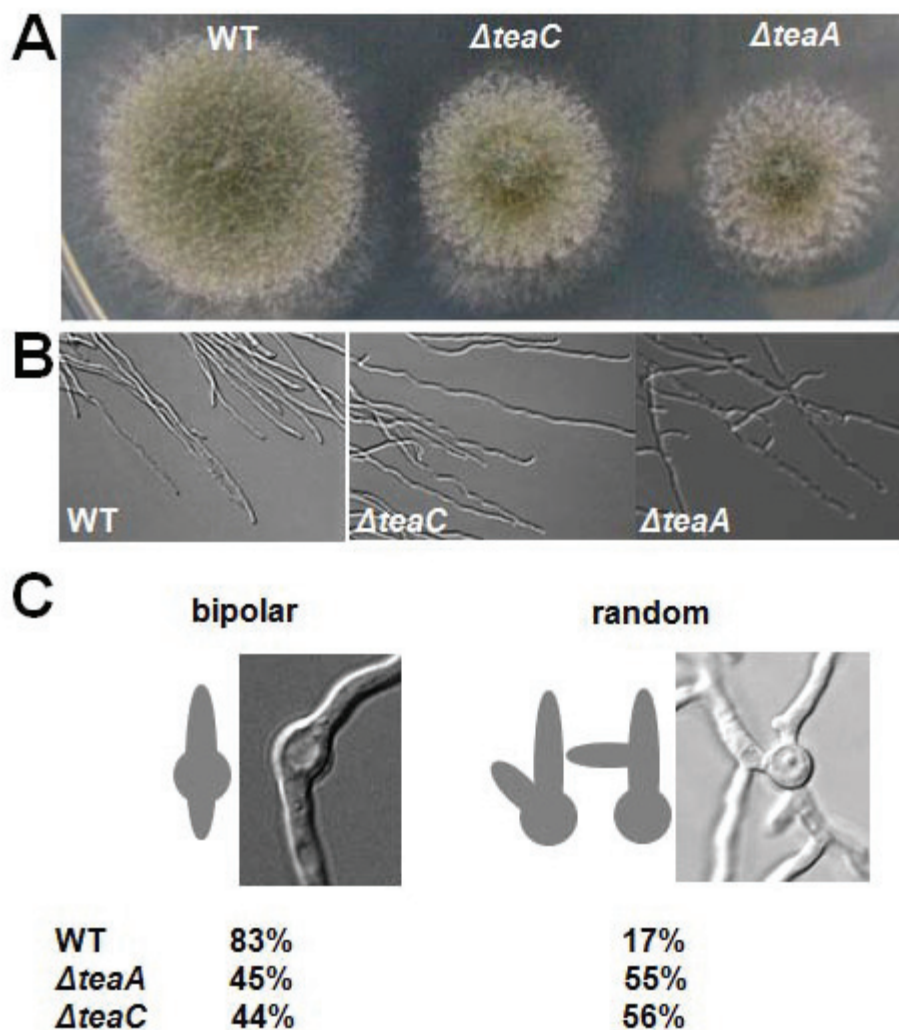
Fig. IV. 4: Phenotypic comparison of wild type (WT) with ∆*teaC* and ∆*teaA* strains. (A) Colonies of WT (TN02A3), ∆*teaA* (SSK91) and∆ *teaC* (SYH21) strains. Strains were grown on minimal medium glucose agar plates for 2 days. **(B)** Hyphae of a wild type,∆ *teaA*, and a∆ *teaC* strain were grown on microscope slides coated with minimal medium with 2% glucose and 0.8 % agarose for 1 day. Images were taken with differential interference contrast (DIC). Hyphae are 3-4 μm in diameter. **(C)** Quantification of the effect of different gene deletions on second germ tube formation. Conidia of each strain were germinated in minimal medium with glucose and analyzed for the emergence of the second germ tube. For each strain, 100 germlings were counted.

The ∆*teaC* mutants also showed an increased number of septa and branches, probably due to the reduced extension rate of the hyphae and not specific for the *teaC* deletion **(Fig. IV. 5, and Fig. IV. 6)**. In addition, I counted number of nuclei in one compartment, which were stained with Calcofluor white and Hoechst 33343. I noticed some small compartments (5 µm; 8%. n = 100), which did not contain any nucleus **(Fig. IV 7, A)**. This did not occur in wild type or in slower growing *A. nidulans* strains **(Fig. IV 7, C)**. I also construct GFP-nuclei in *teaC*-deletion to see Hoechst 33343 staining is complementary with GFP target nuclei and I confirmed same aspect **(Fig. IV 8, B)**.
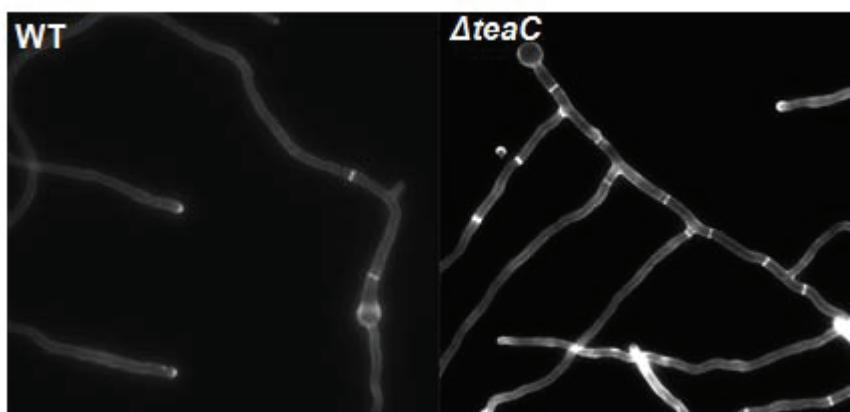
Fig. IV. 5: Relationship of ∆*teaC* and septation site. Z-stack image of WT (TN02A3) and the ∆*teaC* (SYH21) strain grown on minimal medium with 2% glucose for 1 day and stained with Calcofluor white.

A
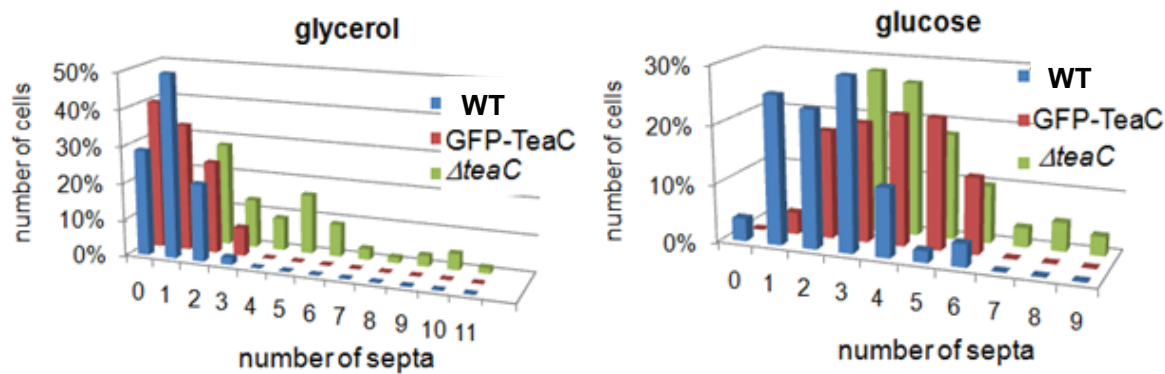
B
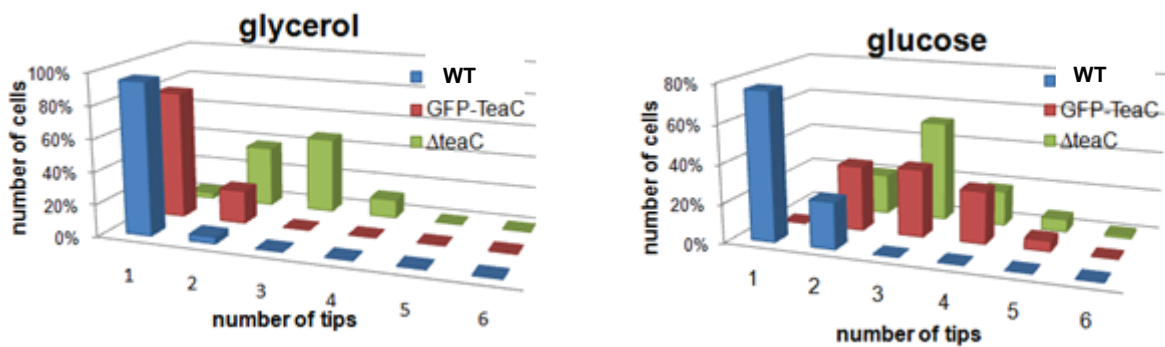
Fig. IV. 6: Deletion of *teaC*. (A) Quantification of the number of septa in WT (TN02A3), the Δ*teaC* strain (SYH21), and the *alcA(p)-GFP-teaC* strain (SYH03) in minimal medium with glycerol and glucose. **(B)** Quantification of the number of tips in WT (TN02A3), the Δ*teaC* strain (SYH21), and the *alcA(p)-GFP-teaC* strain (SYH03) in minimal medium with glycerol and glucose as indicated.

51
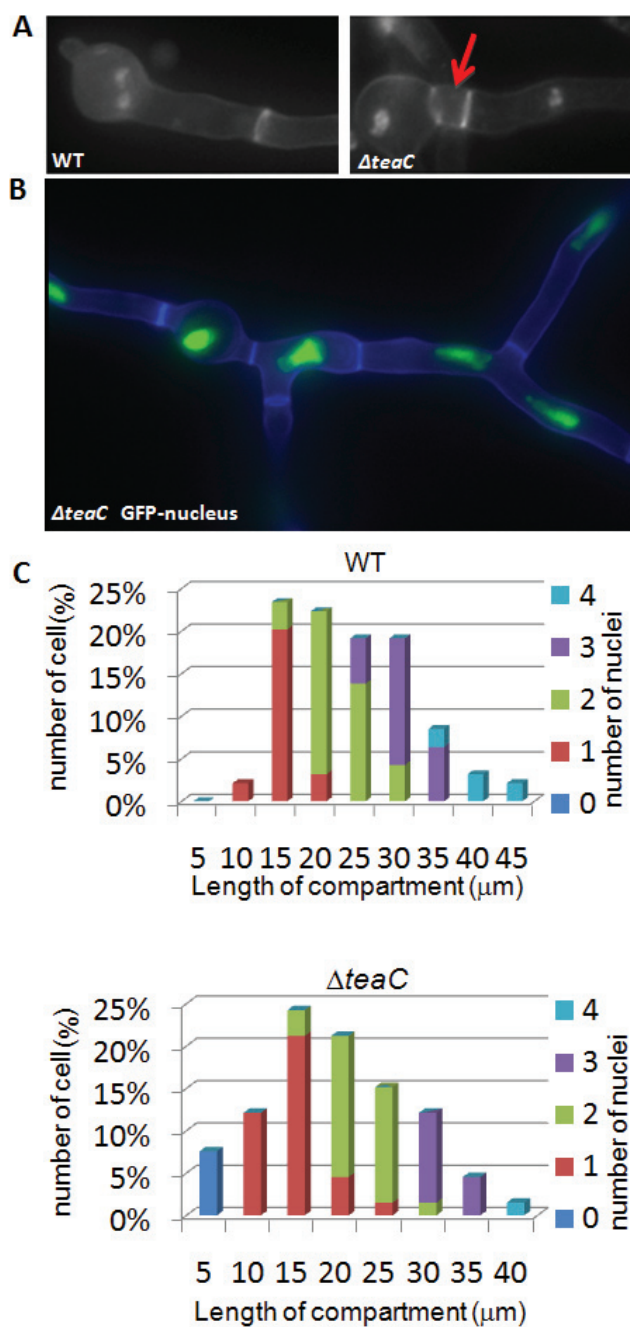
Fig. IV. 7: Relationship of ΔteaC and septation site. (A) Z-stack image of WT (TN02A3) and the ΔteaC strain (SYH21) grown on glucose minimal medium and stained with Calcofluor white and Hoechst 33343. The arrow points to a short, anucleate hyphal compartment. **(B)** Localization pattern of GFP nuclei in ΔteaC mutant. **(C)** Quantification of the number of septa in WT (TN02A3), the ΔteaC strain (SYH21), in minimal medium with glycerol and stained with Calcofluor white and Hoechst 33343. Hyphae are 3-4 µm in diameter.

3. Localization of TeaC

3.1. Tagging of proteins with GFP or mRFP1

To localize TeaC in *A. nidulans*, a N-terminal fusion protein with GFP or mRFP1 was constructed. Approximately 1.2 kb from the 5' region of the coding sequence was cloned downstream of GFP or mRFP1. The target gene was expressed under the control of the inducible alcA promoter (p) **(Fig. IV.8)**. *A. nidulans* TN02A3 was transformed with the circular plasmid pYH06 and transformants were screened for GFP or mRFP1 fluorescence under inducing conditions (glycerol as carbon source). These strains were analyzed for the integration of the plasmid and a strain with a single ectopic integration as well as a strain with a single homologous integration were chosen for further analysis. The ectopic copy results in an aberrant, non-functional fusion protein, whereas homologous integration results in a duplication of the region where the plasmid integrated. Transformants are confirmed by PCR and Southern blot analysis **(Fig. IV. 9 and 10)**.
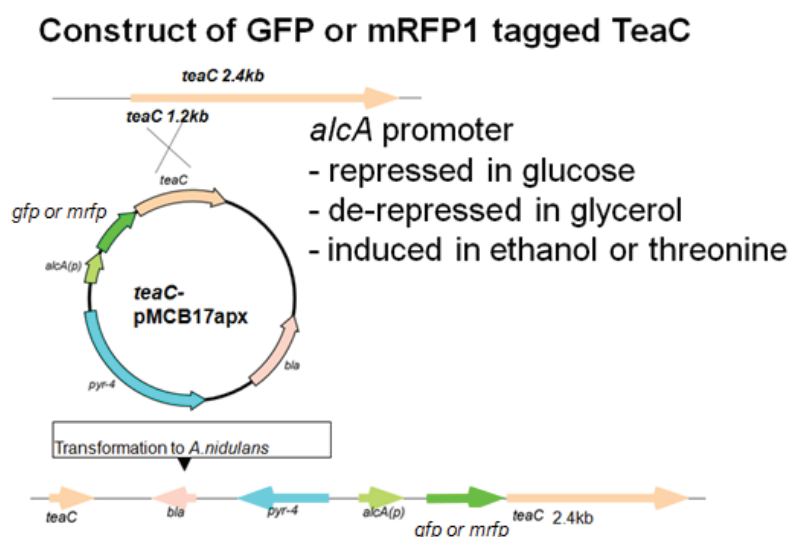
Fig. IV. 8: Construct of GFP-TeaC.

Scheme of the GFP or mRFP1-TeaC construct and the expected
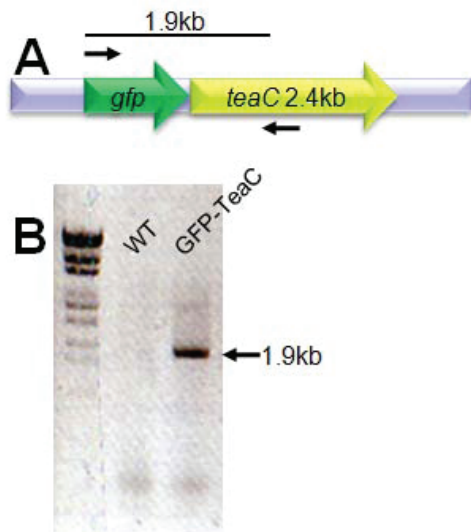
Fig. IV. 9: Construct of GFP-TeaC. (A) Scheme of the GFP-TeaC construct and the expected replacement. (B) PCR of WT (TN02A3) and GFPSYH06. Genomic DNA was used WT (TN02A3) and GFP-TeaC (SYH21).
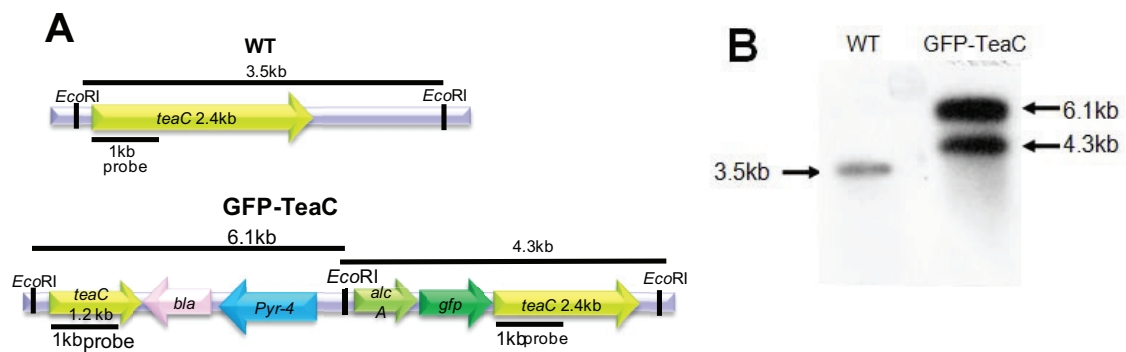
Fig. IV.10: Construct of GFP teaC. (A) Scheme of the GFP-TeaC construct and the expected integration. The lines indicate the expected band sizes after the corresponding restriction digest. (B) Southern blot of WT (TN02A3) and SYH06 (GFP-TeaC). Genomic DNA was digested with *Eco*RI. The blot was hybridized with the probe indicated in (A).

3.2. TeaC localized at new septa and hyphal tips

To investigate the subcellular localization of TeaC, I constructed an *A. nidulans* strain expressing a GFP-TeaC fusion protein under the control of the *alcA* promoter **(see Fig. IV. 9 and Materials and Methods)**. The construct was transformed into strain TN02A3 and a transformant selected in which the construct was integrated into the *teaC* locus

(SYH03). This leads to duplication of the 5' end of the gene under the control of the endogenous promoter and the *GFP-teaC* fusion construct under the control of the *alcA* promoter. Under repressing conditions, the strain displayed the Δ*teaC*-deletion phenotype, which showed compact colonies and zigzag hyphe **(Fig. IV. 11, A and B)** and increased number of septa and branches **(Fig. IV. 6 and Fig. V. 11, B)**. Under de-repressed conditions, wild type hyphal morphology was obtained. This experiment showed that the observed phenotypes in the Δ*teaC*-deletion strain were indeed caused by the deletion and not by another mutation and it showed that the GFP-TeaC fusion protein was functional.
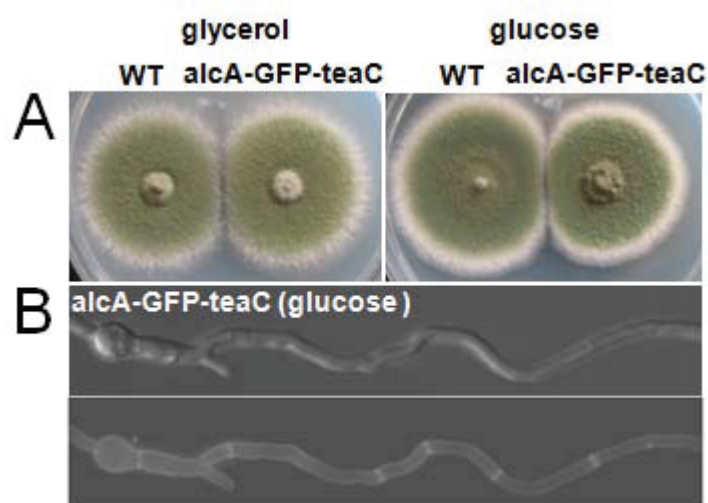
Fig. IV. 11: Phenotypic comparison of wild type (WT) and alcA-GFP-TeaC strain repressing condition. Comparison of a colony of strain SYH03 (*alcA(p)-GFP-teaC*) and WT on glycerol- or glucose-containing medium after 4 days of growth at 37°C. **(B)** Z-stack image of strain SYH03 (*alcA(p)-GFP-teaC*) grown on minimal medium with glucose as carbon source WT (TN02A3) a for 1 day and stained with Calcofluor white. Hyphae are 3-4 μm in diameter.

GFP-TeaC localized to one bright point at all hyphal tips and at newly forming septa **(Fig. IV 12, A)**. In addition, some weaker points were observed. The GFP-TeaC points always localized close to the plasma membrane or appeared attached to it.

In growing tips, the Spitzenkörper has an important role as vesicle supply center. To compare the localization of TeaC with the Spitzenkörper, I stained hyphae with FM4-64, which has been used in several fungi to stain the Spitzenkörper (Fischer-Parton *et al*., 2000: Takeshita *et al.,* 2008). The Spitzenkörper appeared to colocalize with GFP-TeaC **(Fig. IV. 12, B)**, although from these pictures it was not unambiguously clear whether TeaC is part of the Spitzenkörper or only attached to the membrane and therefore very close to the Spitzenkörper.

To confirm TeaC localization and to prove that the observed localization was not an artifact of the expression under *alcA*-promoter control, I constructed a strain (SYH17) producing mRFP1-TeaC under the control of the native promoter. SYH17, in which mRFP1-TeaC is the only source of TeaC, did not show the phenotype observed in the Δ*teaC* mutant, indicating that mRFP1-TeaC at this expression level was also biologically functional. Although signals of mRFP1 appeared much weaker, mRFP1-TeaC still localized to one point and weaker signals were observed along the apex and at forming septa **(Fig. IV. 12, C)**. The single spot of mRFP1-TeaC normally localized at the center of the hyphal apex **(Table. IV. 1)**. At a small number of tips (13%, n = 100), mRFP1-TeaC localized along the tip membrane. For further experiments, I normally used strains producing mRFP1-TeaC under the native promoter, when I analyzed the localization of TeaC.
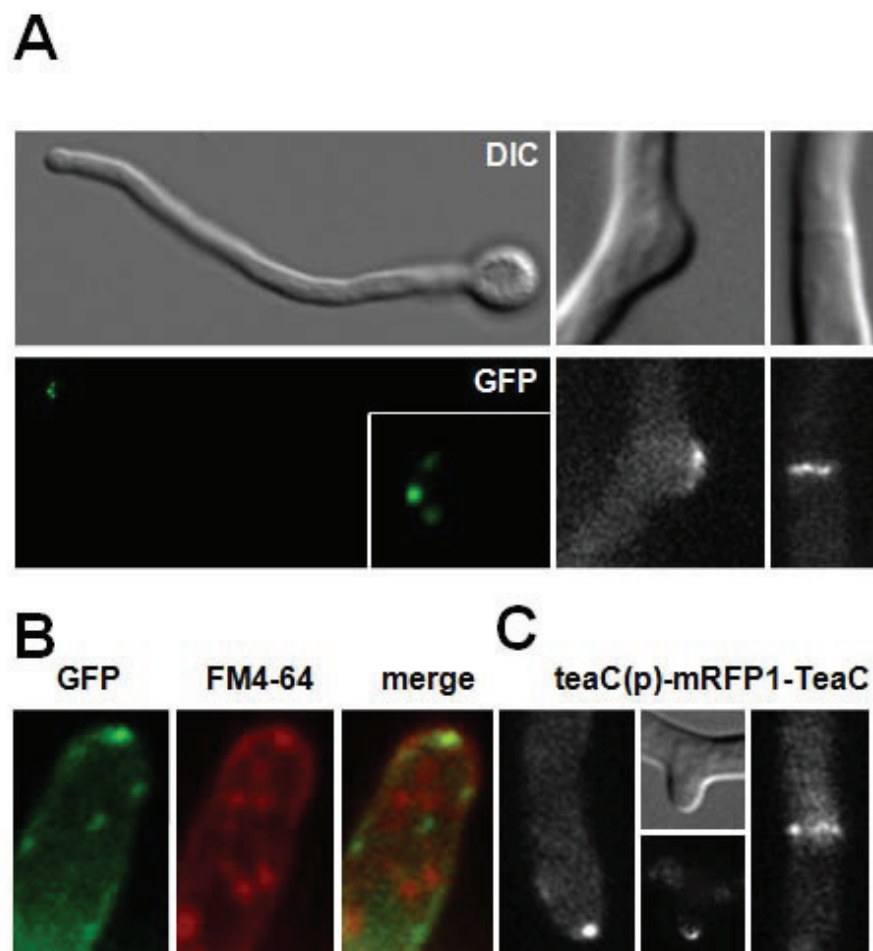
Fig. IV. 12: Subcellular localization of TeaC. (A) Hyphae of strain SYH03 (*alcA(p)-GFP-teaC*) grown on minimal medium with glycerol as carbon source. Upper row: DIC pictures; lower row: same hyphae in the GFP channel. GFP-TeaC localized to one point in the hyphal apex (enlarged in the insert), branching site and at septa. **(B)** Localization of TeaC (GFP) and the Spitzenkörper (visualized with FM4-64). **(C)** mRFP1-TeaC expressed under the control of the native promoter (SYH17). Fluorescent signals were observed at the hyphal tip and new branches, and at septa. Hyphae are 3-4 μm in diameter.

3.3. TeaC at the hyphal tip depends on microtubules but not on the kinesin KipA

To test whether TeaC localization at the hyphal tip depends on microtubules (MTs), I studied a strain with GFP-labeled alpha-tubulin and mRFP1-TeaC (SYH22) and found

that TeaC localized to the plus end of the MTs, although the signal intensity was close to the detection limit **(Fig. IV. 13, A)**.

Next, I used the MT-destabilizing drug benomyl. After this treatment (2.5 μg benomyl/ml), almost all fluorescence of GFP-MTs was diffused into the cytoplasm within 5 min (data not shown) and the mRFP1-TeaC point at the tips was sometimes divided into several points and disappeared after 30-40 min from >80 % of the tips (n = 100) **(Fig. IV. 13, B and Table. IV. 1).** The delay between the disappearance of the TeaC spot and the disassembly of the MTs suggests that TeaC is rather stable at the cortex.

I investigated also the effect of cytochalasin A (2 µg/ml in 0.02 % DMSO), an inhibitor of actin polymerization, on TeaC localization. mRFP1-TeaC dispersed around the tips within 50% of the tips (n = 100) after 2-10 minutes after the treatment **(Fig. IV. 13, C and Table. IV. 1)** in comparison to the control strain only treated with 0.02 % DMSO. Taken together, our results suggest that TeaC localization depends on the MT and the actin cytoskeleton.
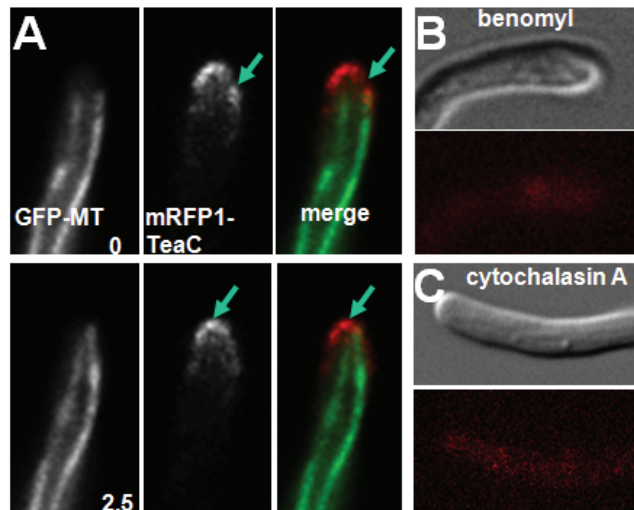
Fig. IV. 13: Relationship between TeaC and microtubules (MT). (A) Observation of GFP-labeled MTs and mRFP1-labeled TeaC (SYH22). The arrows point to the MT plus ends. The same hyphae was observed at time 0 and after 2.5 sec as indicated in the pictures. **(B)** Effect of benomyl on the localization of TeaC in strain SYH22 (*teaC(p)-mRFP1-teaC*). *A. nidulans* was grown in minimal medium with glycerol for 1 day and shifted to medium containing 2.5 μg/ml benomyl for 30 min. **(C)** Effect of cytochalasin A on TeaC localization. SYH17 was grown in minimal medium with glycerol for 1 day and shifted to medium containing 2 μg/ml cytochalasin A for 2 min. Hyphae are 3-4 µm in diameter.

To test whether TeaC is transported by microtubules (MTs) to the septation site, I investigate a strain with GFP-labeled alpha-tubulin and mRFP1-TeaC (SYH22) and found that TeaC localized to the plus end of the MTs at septation site, although the signal intensity was close to the detection limit **(Fig. IV. 14, A)**. Moreover after treatment of MT-destabilizing drug benomyl, TeaC ring formation at the septa was sometimes half or one point in 0.1 µg/ml benomyl and not appeared 0.3 µg/ml benomyl **(Fig. IV.14, B and Table. IV. 2).**
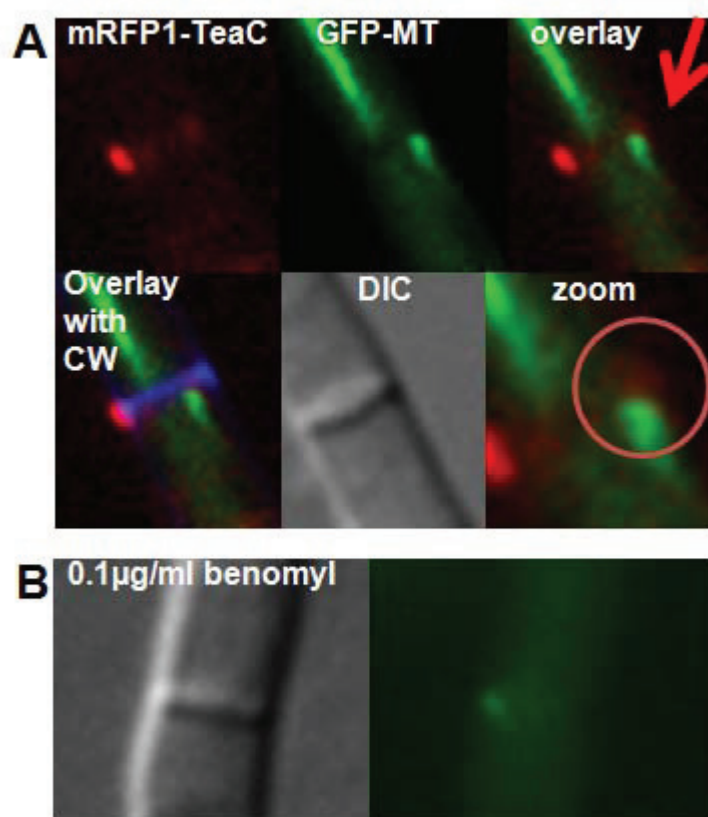
Fig. IV. 14: Relationship between TeaC and microtubules (MT) at septa. (A) Observation of GFP-labeled MTs and mRFP1-labeled TeaC (SYH22) at septa. The arrows point to the MT plus ends. **(B)** Effect of benomyl on the localization of TeaC in strain SYH22 (*teaC(p)-mRFP1-teaC*). *A. nidulans* was grown in minimal medium with glycerol for 1 day 0.1 – 0.3 µg/ml benomyl for overnight.

To analyze if TeaC is transported in a kinesin-7-dependent way to the MT plus end, I studied TeaC localization in a ΔkipA mutant. mRFP1-TeaC still localized to one point at nearly 80 % of the tips (n = 100), indicating KipA-independent polarization. However, the mRFP1-TeaC point did not localize to the center of the apex and moved away to the side of the hypha **(Fig. IV. 15, A and Table. IV. 1)**. I further studied this effect by localization of TeaC in a KipA^{rigor} mutant, in which KipA (fused to GFP) harbors a point mutation in the ATP-binding domain (Konzack *et al.,* 2005: Zekert *et al.,* 2009). GFP-KipA^{rigor} binds but does not move along MTs, and thus decorates them. In this strain (SYH23) mRFP1-TeaC still localized at 90% of the tips, but the mRFP1-TeaC point often moved away to the side of the apex and sometimes divided into two points **(Fig. IV. 15, B Table. IV. 1)**. These results indicate that TeaC can be transported independently of KipA to the tip and that probably other KipA-transported proteins are required for exact positioning of TeaC. I are assuming that the key for further understanding of the cell end marker protein complex lies in the characterization of cargoes of the KipA motor protein.
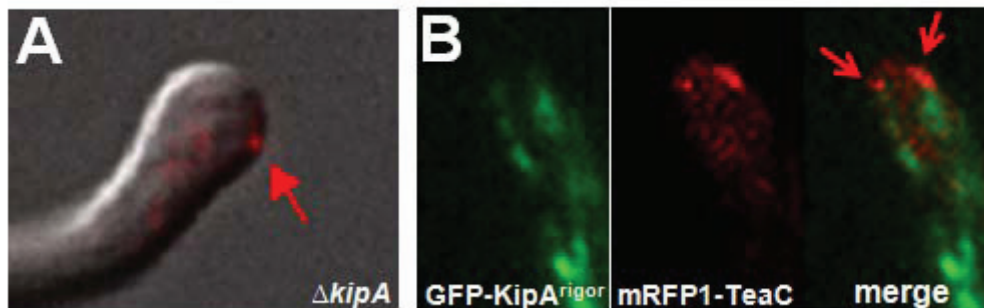
Fig. IV 15: Relationship between TeaC and kipA. (A) In the Δ *kipA* mutant SYH25 TeaC moved away from the center of the apex to the side of the tip (arrow). **(B)** In the GFP-KipA^{rigor} mutant SYH23 TeaC still localized at tips, but the mRFP1-TeaC point often moved away to the side of the apex and sometimes divided into two points**.** Hyphae are 3-4 μm in diameter.

Table. IV. 1: Localization pattern of mRFP1-TeaC. The localization pattern of mRFP1-TeaC of 100 to 200 hyphal tips was analyzed and grouped into six different categories. The construct was expressed from the *teaC* promoter. The numbers indicate the percentages of the hyphal tips of these groups. Hyphae were grown on minimal medium with glycerol as a carbon source for 1 day. For drug treatment, hyphae were incubated in the presence of 2.5 µg of benomyl/ml for 30 min or 2 µg of cytochalasin A/ml for 2 to 10 min.

Category	mRFP1-TeaC localization pattern (%)				
WT	72	3	13	13	2
WT with benomyl	19	0	6	4	71
ΔkipA	44	33	4	18	1
KipA^{rigor}	57	8	28	4	3
WT with cytochalasin A	25	5	7	13	50
ΔteaA mutant	0	4	0	2	94

Table. IV. 2: Localization pattern of mRFP1-TeaC. The localization pattern of mRFP1-TeaC of 150 septation site was analyzed and grouped into four different categories. The construct was expressed from the *teaC* promoter. The numbers indicate the percentages of the hyphal tips of these groups. Hyphae were grown on minimal medium with glycerol as a carbon source for 1 day. For drug treatment, hyphae were incubated in the presence of 0.1 - 0.3 µg of benomyl/ml overnight.

0.01 %DMSO	30%	11%	13%	46%
0.1 µg/ml	8%	6%	19%	67%
0.3 µg/ml	1%	3%	6%	90%
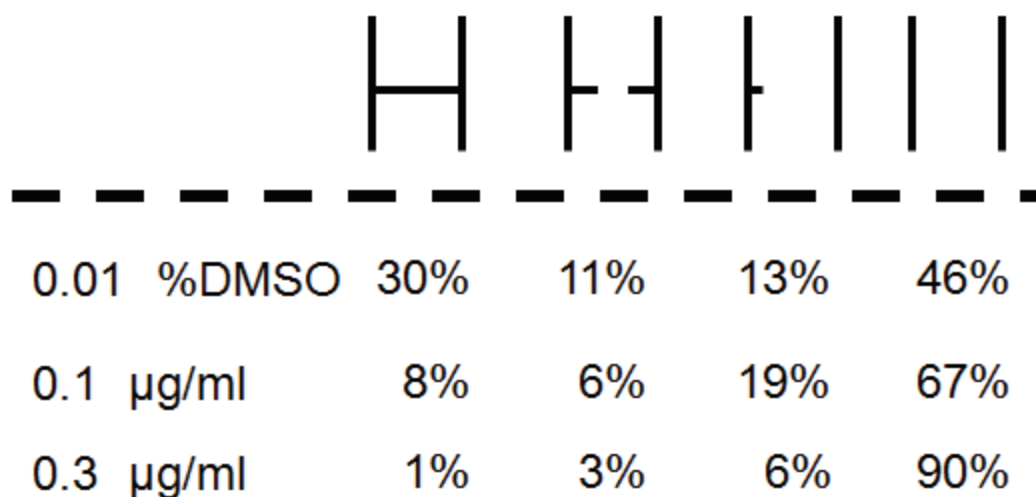
3.4. Overexpression of TeaC inhibits septum formation

I next tested whether overexpression of TeaC would also cause any morphological phenotype. I expressed *teaC* using the control of the *alcA* promoter under inducing conditions (threonine; see Materials and Methods). When the GFP-TeaC strain was grown on threonine MM colonies appeared smaller than the ones from wild type (Fig. IV. 16A). The high expression level of TeaC was shown by Western blotting and an increase in GFP fluorescence **(Fig. IV. 16, B and C; see also below)**.
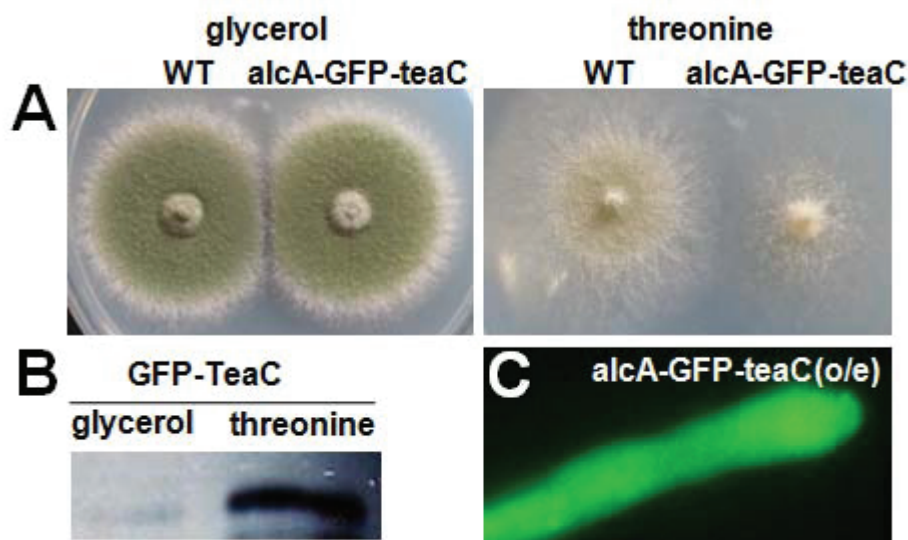
Fig. IV. 16: Effect of overexpression of *teaC*. (A) Comparison of a colony of strain SYH03 (*alcA(p)-GFP-teaC*) and WT on glycerol- or threonine-containing medium after 4 days of growth at 37°C. **(B)** Western blot of hyphae of SYH03 grown on minimal medium with glycerol or threonine as carbon source. 10 μg of total protein extract were loaded onto the gel and processed for the western blot as described in Materials and Methods. **(C)** Fluorescence microscopic picture of a hypha of SYH03 after induction with threonine for one day.

Under inducing conditions, I often observed lysis at the hyphal tips **(Fig. IV. 17, A or B)** and rarely branching of hyphae. Furthermore, the number of conidia that produced a second germ tube was reduced from 66% to 17% (n = 100) **(Fig. IV. 17, C)**. Some conidia without a second germ tube grew continuously isotropic up to 20 μm in diameter after 2 days. Some hyphae appeared to be empty, probably because of leakage of the cytoplasm. This was visualized by calcofluor white staining of the cell wall and GFP staining of the cytoplasm. Whereas the spore on the right side in Fig. IV. 17 A. showed fluorescence in both channels, the left spore showed only fluorescence of the cell wall, indicating an empty spore.
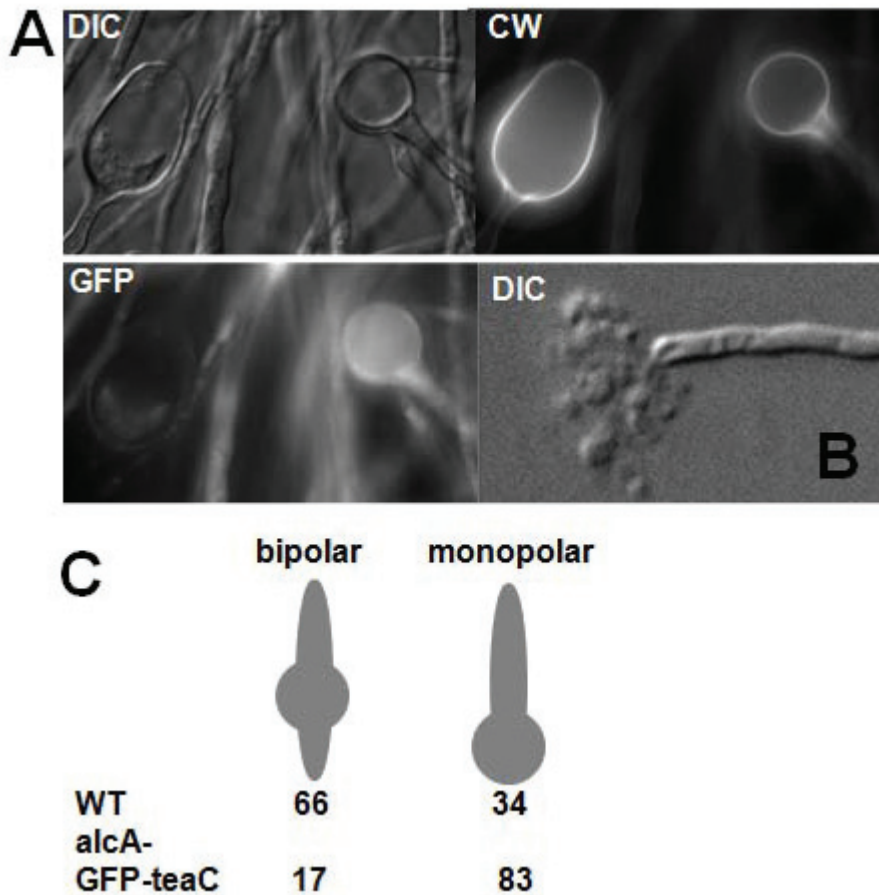
Fig. IV. 17: Phenotype of overexpression of *teaC*. (A) Germinated conidia of SYH03 grown on minimal medium with threonine as carbon source for 48 hr observed in differential interference contrast (DIC). The conidium had lysed. **(B)** Quantification of the effect of teaC overexpression on the emergence of the second germ tube. For each strain, 100 germlings were counted. **(C)** Germinated conidia of SYH03 grown on minimal medium with threonine as carbon source for 48 hr observed in differential interference contrast (DIC), stained with calcofluor white (CW) or observed in the GFP channel.

GFP amino acid is 238, this not small size for TeaC amino acid which is 687 amino acid. To construct of 3xHA-TeaC overexpression strain, I confirmed whether GFP-TeaC overexpression is functional. It is considered that 27 amino acid 3xHA-tag is not affect for TeaC function. I expressed teaC using the control of the *alcA* promoter under inducing conditions **(threonine; see Materials and Methods)**. When the

3xHA-TeaC strain was grown on threonine MM colonies appeared as the same morphological phenotype with GFP-TeaC overexpression. **(Fig. IV. 18)**.
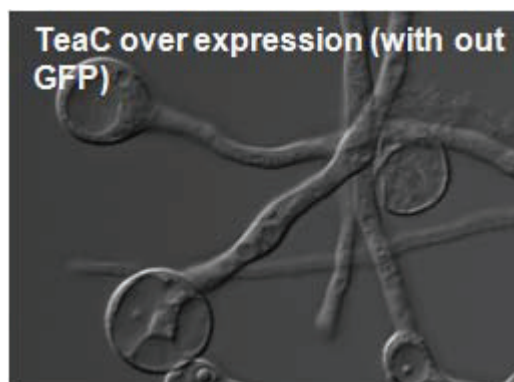
Fig. IV. 18: Effect of overexpression of *teaC* without GFP. Germinated conidia of SYH48 grown on minimal medium with threonine as carbon source for 48 hr observed in differential interference contrast (DIC).

When I analyzed the number of septa, I found that teaC overexpression repressed almost completely septation **(Fig. IV. 13, A)**. Because TeaC interacts with SepA and possibly regulates the localization and/or the activity (see below), I sought to determine which phenotype would be caused by overexpression of TeaC, together with the overexpression of SepA. The displayed phenotype was similar to the phenotype of teaC overexpression, namely, very few septa **(Fig. IV. 19, B and C)**. In addition, conidia were swollen, hyphae had an irregular shape, and hyphal tips appeared very large **(Fig. IV. 20)**. To quantify this effect, I counted the number of septa in germlings, which were between 100 and 300 μm in length (n = 50) **(Fig. IV. 19, C)**. Overexpression of SepA alone did not cause a reduction of the number of septa, and the morphology was less severely affected
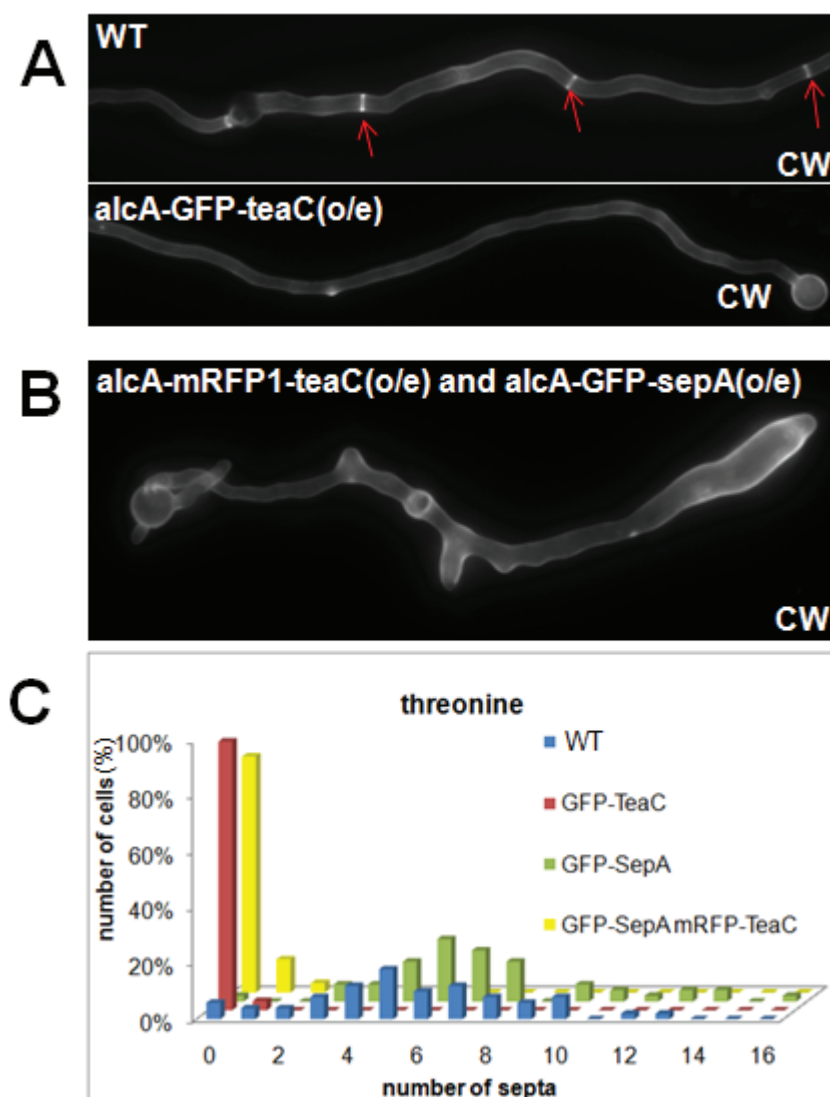
Fig. IV. 19: Effect of overexpression of *teaC* on septation. (A) Strain SYH17 (teaC(p)-mRFP1-teaC)(WT) and SYH03 (alcA(p)-GFP-teaC) grown on threonine minimal medium and stained with Calcofluor white (CW). The red arrows point to the stained septa. Hyphae are 3-4 μm in diameter. (B) Strain SYH26 (alcA(p)-GFP-sepA and alcA(p)-mRFP1-teaC) grown on minimal medium with threonine as carbon source for 48 hr and stained with CW. The ring-like structure is a small branch observed from the top. (C) Quantification of the number of septa in SYH17 (considered as wild type), SYH03, SNT28 (alcA(p)-GFP-sepA), and SYH26 grown in threonine minimal medium. 50 germlings were counted for each strain.
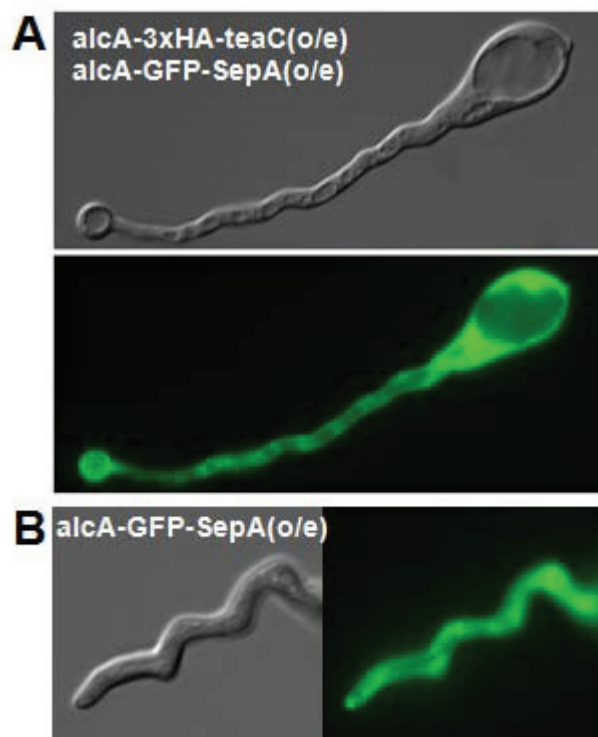
Fig. IV. 20: Effect of overexpression of *teaC* and *sepA*. (A) Germinated conidia of SYH36 (alcA(p)-3xHA-teaC and alcA(p)-GFP-sepA) grown on minimal medium with threonine as carbon source for 24 hr observed in differential interference contrast (DIC) upper one and GFP channel the lower one. **(B)** Hyphae of SNT28 (alcA(p)-GFP-sepA) grown on minimal medium with threonine as carbon source for 24 hr observed in differential interference contrast (DIC) left and GFP channel right. Hyphae are 3-4 µm in diameter.

3.5. TeaC connects TeaA and SepA

To investigate whether *A. nidulans* TeaC co-localizes with TeaA, I constructed a strain (SYH13) expressing mRFP1-TeaA and GFP-TeaC, and compared their localization patterns. The mRFP1-TeaA point at the apex co-localized with that of GFP-TeaC. If mRFP1-TeaA localized at two points (10 %, n = 100) TeaC also co-localized with the same spots **(Fig. IV. 21, A)**. Likewise, I tested co-localization of TeaC with SepA. I constructed a strain (SYH18) expressing GFP-SepA and *teaC(p)-mRFP1-teaC*. TeaC and SepA did not obviously co-localize at the hyphal apex. When SepA localized at the

hyphal apex, TeaC appeared adjacent to the SepA signal (11 %, n = 100). When TeaC localized at the hyphal apex at one point, SepA did not localize at the hyphal apex (89 %, n = 100) **(Fig. IV. 21, B)**.

I also found no obvious co-localization at septa **(Fig. IV. 21, C)**. It appeared that TeaC surrounded SepA **(Fig. IV. 21, C)**.
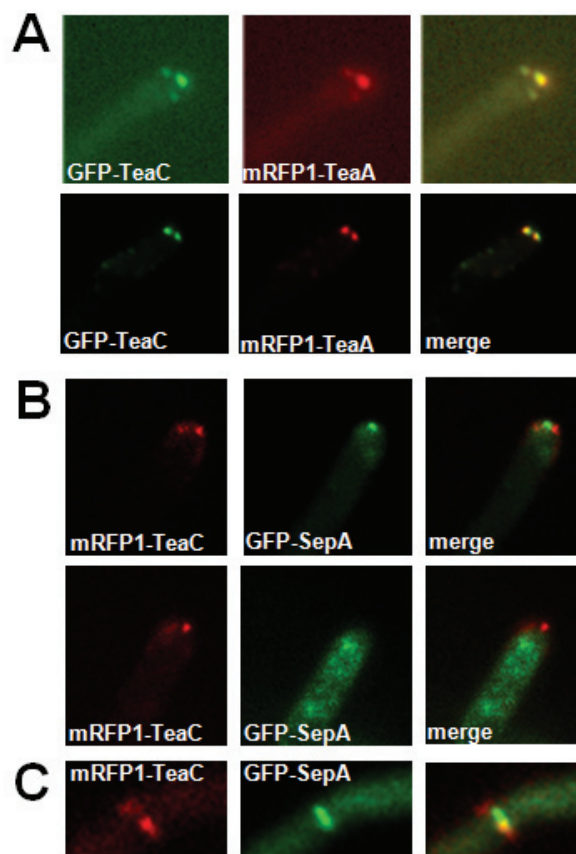
Fig. IV 21: Co-localization of TeaC with TeaA and SepA. (A) Co-localization of TeaC and TeaA in strain SYH18. **(B)** Visualization of TeaC and SepA in strain SYH13 at the hyphal tip. **(C)** Partially co-localization of TeaC and SepA in strain SYH13 at septa.

Doing time course-experiments I found that SepA and TeaC follow a constricting ring, but that TeaC constriction was slightly delayed in comparison to SepA **(Fig. IV 22 A, B).**
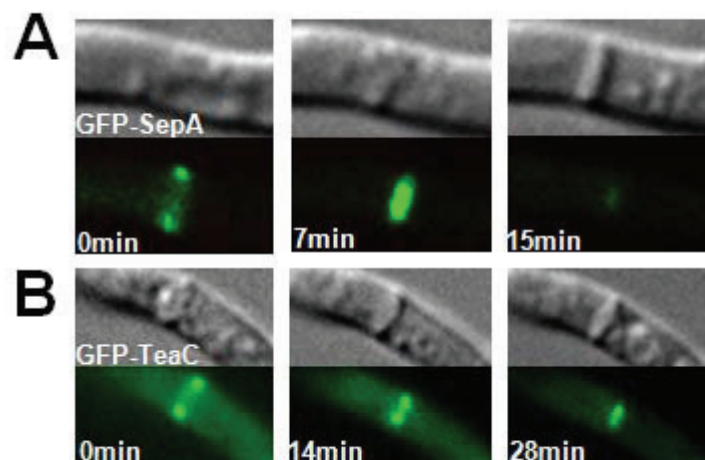
Fig. IV 22: Localization pattern of GFP-TeaC and GFP-SepA at septation site (A) Localization of SepA in strain SNT28. **(B)** Localization of TeaC in strain SYH03.

Tagging of proteins with split-YFP

Next I asked whether TeaA/TeaC and TeaC/SepA would interact. This was studied by bimolecular fluorescence complementation (BiFC). The N-terminal half of YFP (YFP^N) was fused to SepA and TeaA, and the C-terminal half of YFP (YFP^C) was tagged with TeaC **(Fig. IV. 23, A)**. Strains expressing only YFP^N-SepA, YFP^N-TeaA or YFP^C-TeaC showed no YFP fluorescence. In contrast, in the strain expressing both YFP^N-SepA and YFP^C-TeaC produced YFP signals as a single point and along the apex and at hyphal septa **(Fig. IV. 23, B).** In the case of the combination of YFP^N-TeaA and YFP^C-TeaC, YFP signals were detected only at the hyphal tip **(Fig. IV. 23, C)**. I also tested YFP^N-TeaR (the membrane anchor protein) and YFP^C-TeaC interaction, but no YFP fluorescence was observed (data not shown).
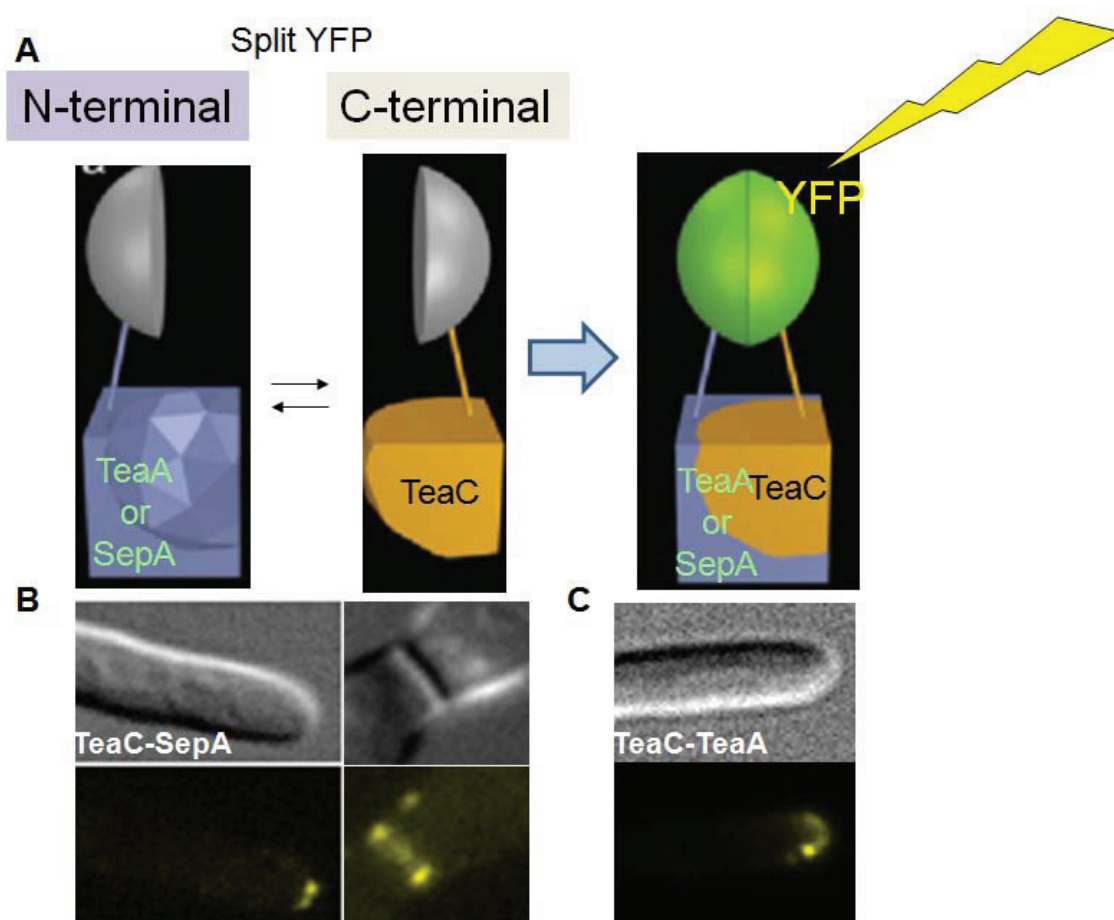
Fig. IV 23: TeaC/TeaA and TeaC/SepA interaction was identified by bimolecular fluorescence complementation (BiFC). (A) Scheme of Bimolecular fluorescence complementation (B) Interaction of TeaC with SepA (strain SYH05) shown in the bimolecular fluorescence complementation assay. (C) Interaction of TeaC with TeaA (strain SYH06) shown in the bimolecular fluorescence complementation assay. Hyphae are 3-4 µm in diameter.

Yeast two-hybrid analysis

The yeast two-hybrid analysis was performed using the MatchMaker3 Gal4 two-hybrid system (BD Clontech). For bait generation, fragments of *teaC* cDNA corresponding to the N-terminal half of TeaC (356 aa) with primers TeaC-EF and TeaC-BMR or corresponding to the C-terminal half of TeaC (428 aa) with primers TeaC-EMF and TeaC-BR were amplified and cloned into the pGBK7 vector, which contains the Gal4

DNA-BD and the *TRP1* marker, yielding pYH17 and pYH19 (BD Clontech). The fragments of *teaC* cDNA corresponding to the N-terminal half and C-terminal half of TeaC from pYH17 and pYH19, were amplified and cloned into the pGADT7 vector, which contains the GAL4 DNA-AD and the *LEU2* marker (BD Clontech), yielding pYH16 and pYH18. pGBK7 associated plasmids were transformed into yeast Y187 (mating type MATα) and pGADT7 associated plasmids were transformed into yeast AH109 (mating type MATa). The system utilizes two reporter genes (*HIS3* and *LacZ*) under the control of the GAL4-responsive UAS. Beta-galactosidase activity was analyzed by liquid culture assays using ONPG (o-nitrophenyl β-D-galactopyranoside)(Sigma), as substrate. The activity was calculated in Miller Units (Miller 1972). Experiments were repeated three times.

The observed interactions were analyzed with the yeast-two hybrid system. TeaA showed self-interaction and interaction with TeaC. In both cases, the C-termini of TeaA and TeaC were important for the interaction **(Fig. IV. 25)**. Interaction of TeaC and SepA could not be detected in this assay, because TeaC-N terminal interact with empty vector of pGADT7 and induced the expression of the yeast two hybrid reporters **(Fig. IV. 24).**

Fig. IV. 24: Yeast two-hybrid assay to analyze the interactions. Colonies of the yeast strains. The mated yeasts were selected on SD/-Leu/–Trp and SD-Leu-Trp-His plates. The proteins fused to the binding domain (BD) and the activation domain (AD)
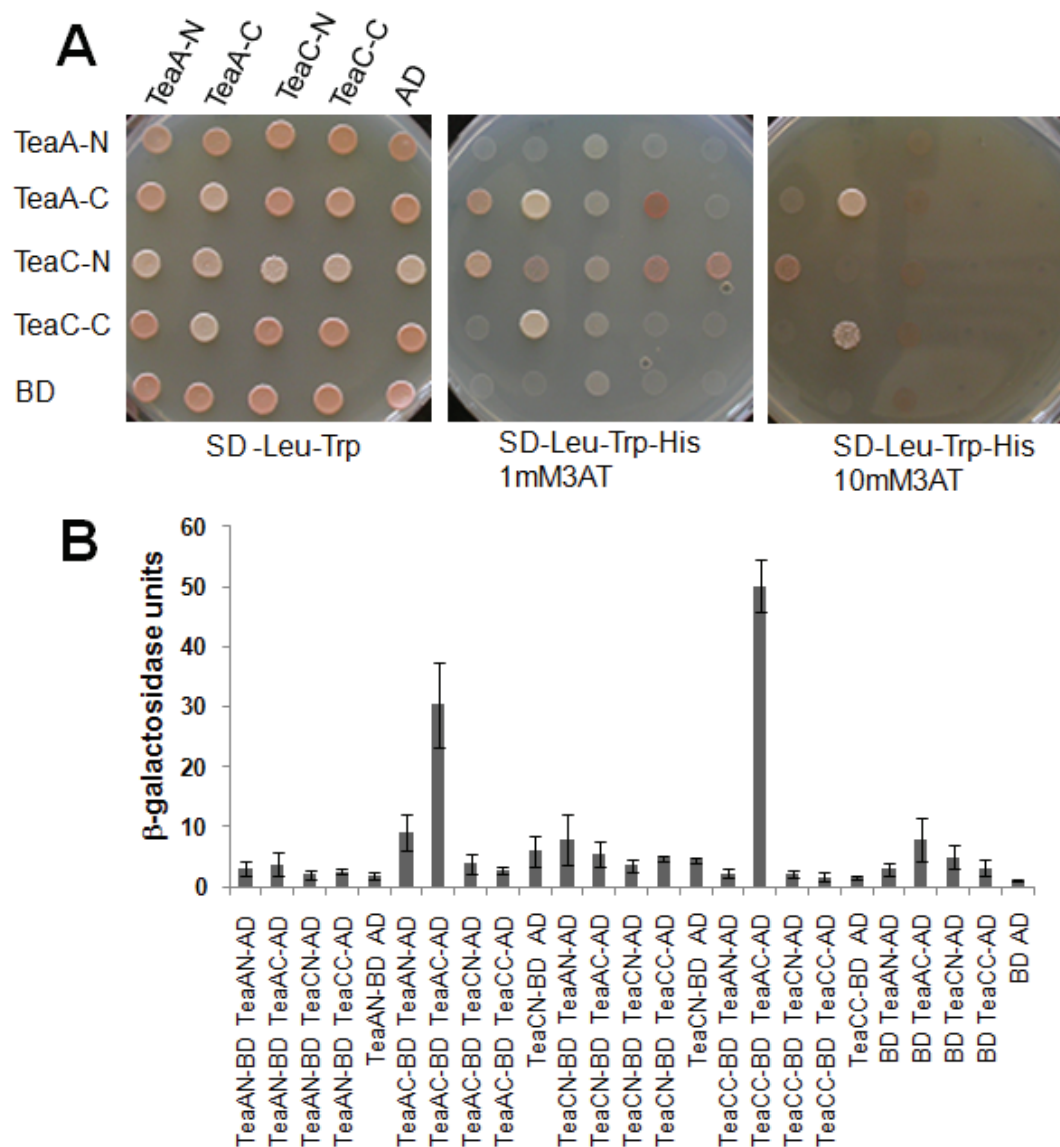
Fig. IV. 25: Yeast two-hybrid assay to analyze the interactions. (A) Colonies of the yeast strains. The proteins indicated on the left side were fused to the binding domain (BD) and the proteins indicated above the picture with the activation domain (AD). The mated yeasts were selected on SD/-Leu/–Trp-His plates and grown on SD medium (SD-Leu-Trp) supplemented with 1 mM or 10 mM 3AT (3-Amino-1,2,4-triazole). **(B)** Beta-galactosidase activity was analyzed from liquid cultures using ONPG as substrate and is expressed as Miller Units. The data are expressed as the mean of three independent experiments. The standard deviation is given in brackets.

3.6. Localization dependency

Localization dependency of TeaC and TeaA

I analyzed TeaC localization in a Δ*teaA* mutant and found that the correct positioning of TeaC depends on TeaA **(Fig. IV 26 A; Table. IV 1)**. In the absence of TeaA, TeaC appeared dispersed in the cytoplasm. I also analyzed TeaA localization in a Δ*teaC* mutant. mRFP1 tagged TeaA did not concentrate in one point in the apex but appeared as several points along the membrane **(Fig. IV 26 B)**.
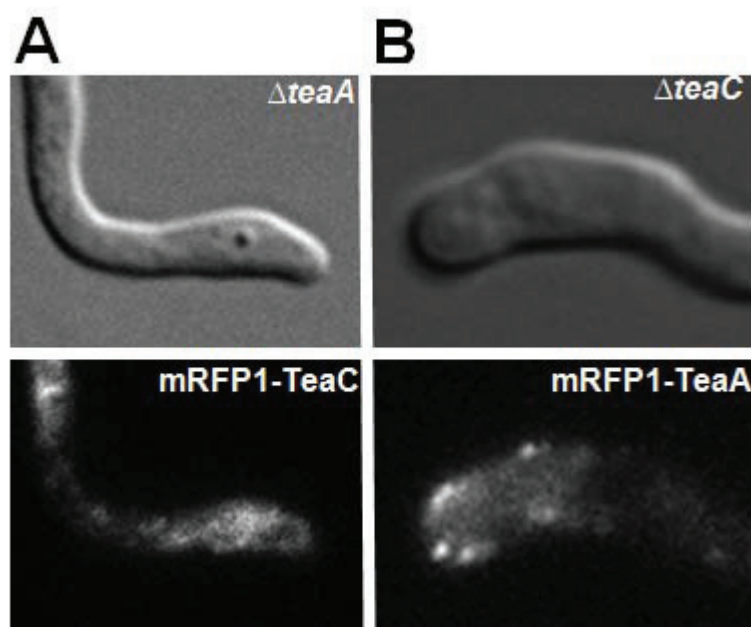
Fig. IV. 26. Localization dependency of TeaC and TeaA. (A) TeaC localization in the Δ*teaA* mutant (SYH19). **(B)** TeaA localization in the Δ*teaC* mutant (SYH24). Hyphae are 3-4 µm in diameter.

Overexpression of TeaA in Δ*teaC* mutant

TeaA constructs component with several another cell end marker proteins (Takeshita *et al.*, 2008). It suggests that huge amount of TeaA recover zigzag phenotype or localizes correct position of hyphal tip without TeaC protein condition. Then I tested whether overexertion of TeaA recovers zigzag phenotype in Δ*teaC* mutant, so I expressed *teaA* using the control of the *alcA* promoter under inducing conditions (threonine; see Materials and Methods). Whereas TeaA overexpression did not recover zigzag phenotype and correct position of hypal tip localization **(Fig. IV. 27)**.

Fig. IV. 27. Overexpression of TeaA in Δ*teaC* mutant.

SYH36(alcA-GFP-TeaA, Δ*teaC*) in threonine MM. Hyphae are 3-4 μm in diameter.

mRFP1-TeaC localization in SepA repressing condition

The interaction partner TeaA deletion affects TeaC localization. I tried to identify whether another interaction partner of SepA localization affects TeaC localization. I used SYH18 (*alcA(p)-GFP-sepA, teaC(p)-mRFP1-teaC*) strain and using the control of the *alcA* promoter under repressing conditions (glucose; see Materials and Methods). In SepA repressing condition, TeaC localized at the hyphal tip and cell septation, which is the normal TeaC localization pattern **(Fig. IV. 28)**.
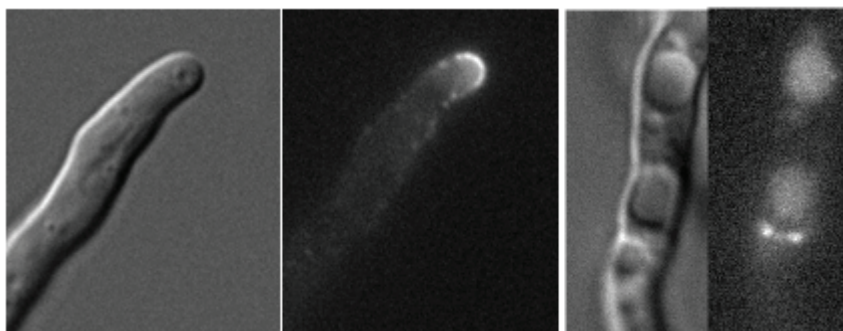
Fig. IV. 28. mRFP1-TeaC localization in SepA repressing condition.
SYH18 (*alcA(p)-GFP-sepA, teaC(p)-mRFP1-teaC*) in glucose MM. Hyphae are 3-4 μm in diameter.

GFP-MT in *∆teaC* mutant

I also analyzed GFP-MT localization in a ∆*teaC* mutant. In the tip of the wild type, MTs elongated toward the apex and normally converge in one point at the center of the tip **(Fig. IV. 13)**, and they paused there without elongating until a catastrophe event caused depolymerization. In the ∆*teaC* mutant, MTs reached the tip cortex, but sometimes they did not converge to one, but attached to several points **(Fig. IV. 29)**.
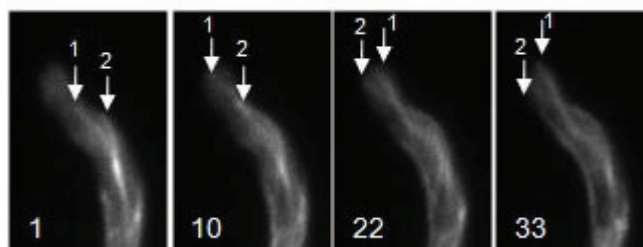
Fig. IV. 29. ∆*teaC* mutant GFP-MT. In strain SYH (∆*teaC*, GFP-MT), GFP-MTs did not merge in one point at the apex but instead attached to a few points (arrows indicate points where MT attached). Elapsed time is given in seconds.

4. Partial characterization of TeaB

I searched the *A. nidulans* genome at the Broad Institute (Cambridge, MA)(http://www.broad.mit.edu/annotation/genome/aspergillus_group/MultiHome.html) for proteins with similarity to the cell end marker protein Tea3 from *S. pombe*. However, the sequence is apparently not conserved in *A. nidulans.* Therefore, I searched for functional similarity of Tea3 protein in *A. nidulans* and found an open reading frame AN0813.3 with kelhi1 and kelhi2 domains and a BTB/POZ domain, which is a putative TeaA binding protein **(Fig. IV. Add, 1)**.
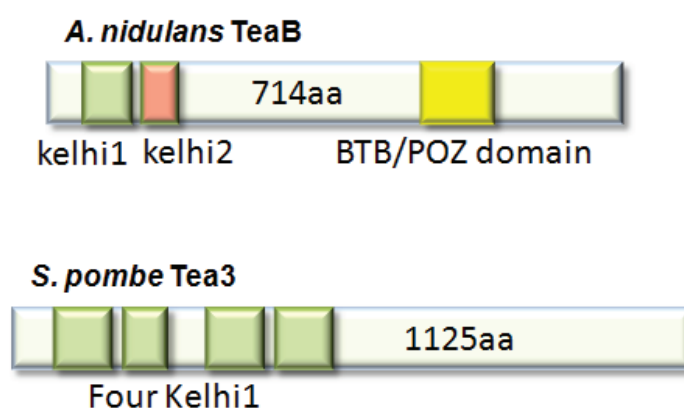
Fig. IV. Add. 1: **Comparison of TeaB with putative functional related proteins from *S. pombe.*** Scheme of *A. nidulans* TeaB, *S. pombe* Tea3 indicating the location of the kehi1 domain.

Tagging of TeaB with GFP

To localize TeaB in *A. nidulans*, a N-terminal fusion protein with GFP was constructed. Approximately 750 bp from the 5' region of the coding sequence was cloned downstream of GFP. The target gene was expressed under the control of the inducible alcA promoter (p) **(Fig. IV. Add, 2).** *A. nidulans* TN02A3 was transformed with the circular plasmid pYH07 and transformants were screened for GFP fluorescence under inducing conditions (glycerol as carbon source). These strains were analyzed for the integration of the plasmid and a strain with a single ectopic integration. The ectopic

copy results in an aberrant, non-functional fusion protein, whereas homologous integration results in a duplication of the region where the plasmid integrated.
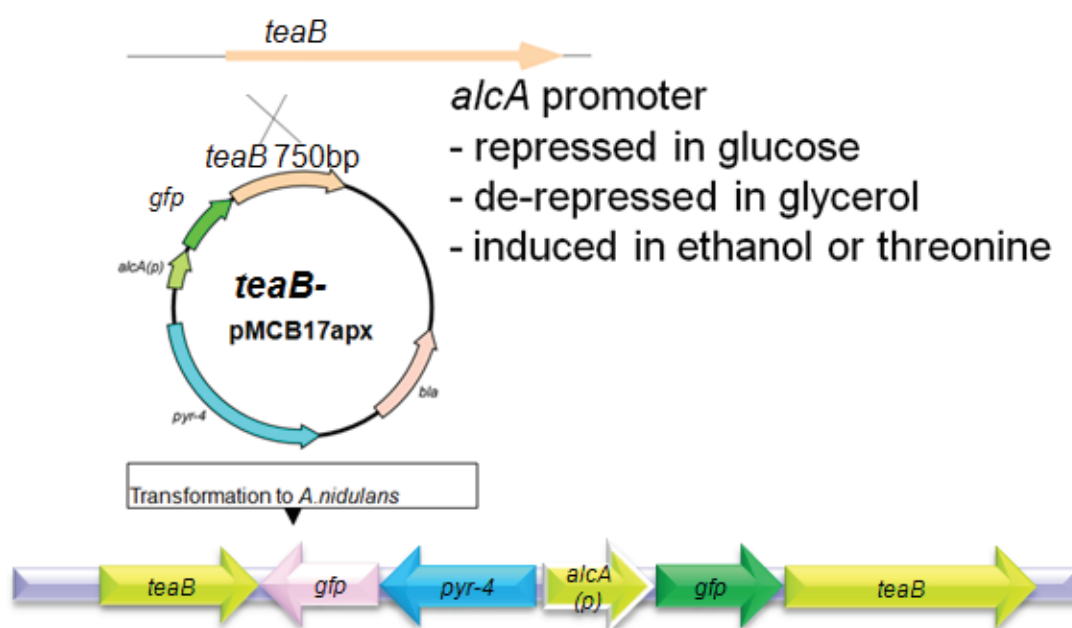
Fig. IV. Add. 2: Construct of GFP-TeaB.

Scheme of the GFP-TeaB construct and the expected integration.

TeaB localized at new septa and hyphal tips

To investigate the subcellular localization of TeaB, I constructed an *A. nidulans* strain expressing a GFP-TeaB fusion protein under the control of the *alcA* promoter **(see Fig. IV. Add. 2 and Materials and Methods).** The construct was transformed into strain TN02A3 and a transformant selected in which the construct was integrated into the *teaB* locus (SYH03). This leads to duplication of the 5' end of the gene under the control of the endogenous promoter and the *GFP-teaB* fusion construct under the control of the *alcA* promoter. Under repressing conditions, the strain showed Zigzag hyphae **(Fig. IV. Add. 3, B).** Under de-repressed conditions, wild type hyphal morphology was obtained. This experiment, GFP-TeaB localized to one bright point at

all hyphal tips and at old septa **(Fig. IV. Add. 3, A)**. The observed interactions were analyzed with the Yeast-two hybrid system. The N-terminus of TeaA and C-terminus of TeaB interacted **(Fig. IV. Add. 3, C)**. However, interaction between TeaB and TeaA was not so strong when analzed in yeast liquid cultures and TeaB and TeaR did not interact (data not shown). Therefore, I did not investigate further TeaB.
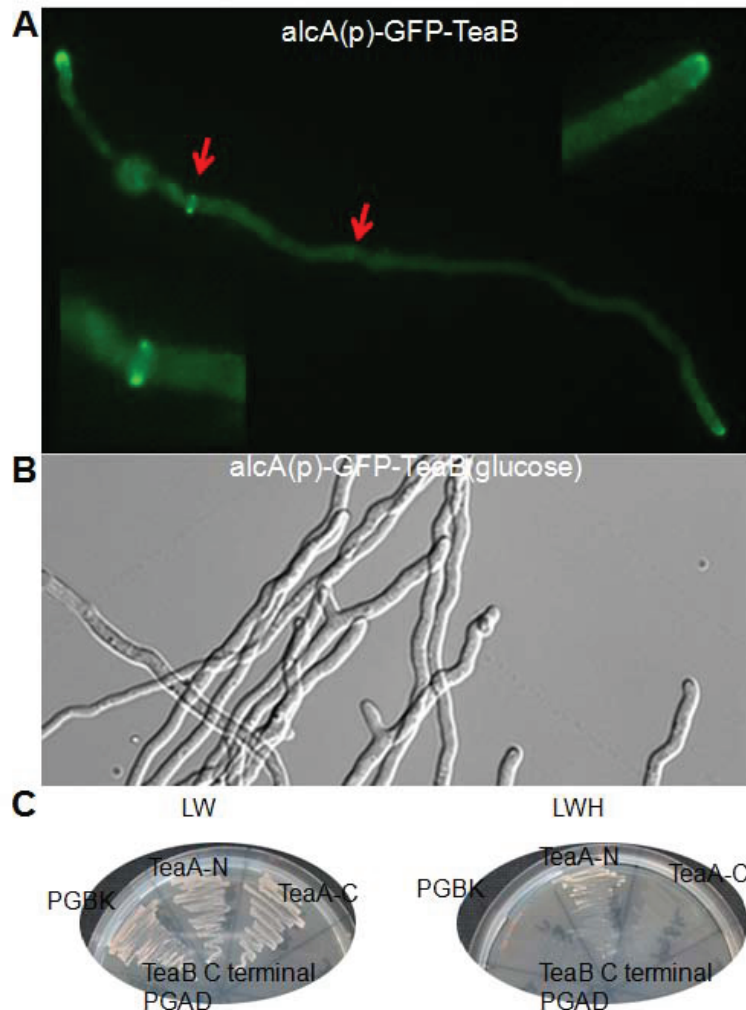
Fig. IV. Add. 3: Subcellular localization of TeaB and yeast two-hybrid assay to analyze the interactions. (A) Hyphae of strain SYH (*alcA(p)-GFP-teaB*) grown on minimal medium with glycerol as carbon source. Upper row: DIC pictures; lower row: same hyphae in the GFP channel. GFP-TeaB localized to one point in the hyphal apex (enlarged in the insert). **(B)** Hyphae of strain SYH (*alcA(p)-GFP-teaB*) grown on minimal medium with glucose a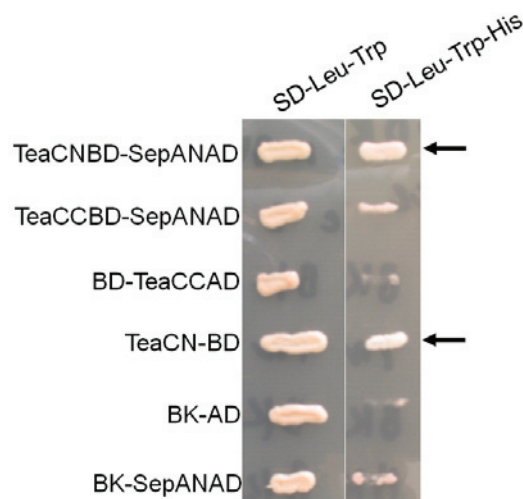s carbon source WT (TN02A3) a for 1 day. Hyphae are 3-4 µm in diameter. **(C)** Yeast two-hybrid assay to analyzed the interaction. Colonies of the yeast strains. The mated yeasts were selected on SD/-Leu/–Trp-His plates and grown on SD medium (SD-Leu-Trp).

V. Discussion

Polarized growth of *A. nidulans* is achieved through a collaborative action of the MT and the actin cytoskeleton. At the beginning of this research, it was unclear whether the machinery discovered in *S. pombe,* consisting of cell end marker proteins, which coordinate the MT and the actin cytoskeleton, was conserved in filamentous fungi, because only some components could be identified by sequence comparisons. However, meanwhile four genes have been analyzed in *A. nidulans,* among which is the *tea4* homologue, TeaC, studied in this work. These genes will be a basis to identify novel components in future research. Tea4 is involved in the transmission of positional information through the interaction with both Tea1 and the formin For3 (Martin *et al*., 2005). Here I show that in *A. nidulans* TeaC serves similar functions in polarized growth and in addition, I discovered a role of the protein in septation. The role of TeaC will be discussed in the light of recent findings for *S. pombe* Tea4 and the closest *S. cerevisiae* homologue Bud14.

1. TeaC localization

TeaC localized at hyphal tips and at forming septa. Furthermore TeaC colocalized with the Spitzenkörper at the hyphal apex and with TeaA at one point at hyphal tips **(Fig. IV. 12, B)**. Interaction studies revealed that TeaC interacted with TeaA at hyphal tips **(Fig. IV. 23, C and 25)**. TeaC did not localize at hyphal tips in *ΔteaA* mutants. These results suggest that TeaC interacts with TeaA at hyphal tips. However, TeaA did not localize at septation sites. This result shows that TeaA is not required for TeaC recruitment at septation sites.

Another TeaC interaction partner, SepA, was observed by BiFC analysis **(Fig. IV. 23, B)** TeaC and SepA localized at hyphal tips and cell septation sites **(Fig. IV. 21, B and C)**. Interestingly, those proteins did not obviously colocalize at hyphal tips. This may be explained by the mechanism of actin polymerization by formin. In *S. pombe*, it was suggested that For3 is activated and promotes actin filament assembly at the cell

79

cortex for only some seconds and then For3 is inactivated and released from the cortex by retrograde flow along actin filaments (Martin and Chang, 2006). On the other hand, it can also be that SepA is very dynamic at the tip and the interaction with TeaC is only weak and transient. Another aspect of TeaC localization is that TeaC surrounded SepA at the septation site **(Fig. IV. 21, C)**. Doing time course-experiment I found that SepA and TeaC follow a constricting ring, but that TeaC constriction was slightly delayed in comparison to SepA **(Fig. IV. 22)**. In *S. pombe*, For3 deletion did not affect Tea4 localization (Martin *et al*., 2005). Likewise, depletion of SepA did not affect TeaC localization in *A. nidulans* **(Fig. IV. 28)**. These results suggest that TeaC localization does not depend on SepA at hyphal tip and also not at septa. TeaC localization involeved in TeaA ant hyphal tips but sutill not clear at the septation site. Probabley some other TeaC conecting protein exist in septation site.

In *S.pombe* the Tea4 interacting partner Tea1 is transported by Tea2 to extending MT plus ends which deliver Tea1 to both cell ends. In *tea2* deletion strains, Tea1 did not localize at cell ends and on MTs (Browning *et al*, 2003). In contrast, *A. nidulans* TeaA localized at the hyphal apex in *ΔkipA* mutants. However, TeaA did not localize at the center of the apex and moved away to the side of the hyphae (Takeshita *et al*, 2008). TeaC showed the same localization pattern in *ΔkipA* mutants. In *S. pombe,* Tea4 is concentrated at both cell tips and could also be observed as dots at MTs plus ends (Martin *et al.,* 2005). The cell end localization of Tea4 was abrogated by a β-tubulin mutation (Tatebe *et al.,* 2005). In *A. nidulans,* TeaC localized at MT plus ends, although the signal intensity was close to the detection limit **(Fig. IV. 13, A)**. After treatment with the MT-destabilizing drug benomyl, the TeaC point at the tip was sometimes divided into several points and disappeared **(Fig. IV. 13, B).** These results suggest that TeaC travels with the MT plus ends to the cortex but that the accumulation at the MT plus end is apparently independent of the motor KipA. I have evidence that TeaC also serves a function in MT organization. MTs elongated toward the apex and normally converge in one point at the center of the tip, but in *ΔteaC* mutant, MTs reached the tip cortex, however sometimes they did not converge to one pint, but attached to several points **(Fig. IV. 26, B)**. This is very similar to the MT organization in *teaA* mutants, suggesting that the TeaC-TeaA protein complex

regulates MT organization (Takeshita *et al.*, 2008). Whether TeaC has also a role on MT organization at septa is less clear. After treatment of *A. nidulans* with benomyl, TeaC ring formation at the septation sites was sometimes half and almost did not appear **(Fig. IV.14, B and Table. IV. 2).** However, treatments of benomyl affects also mitosis and a mitotic signal is required for septation. Septation in *A. nidulans* depends on mitosis and the position of the nucleus (Xiang *et al.*, 1994: Wolkow *et al.*, 1996) and there for the benomyl effect on septation could be indirect.

TeaC localization was not only affected by MT destabilization but also by actin inhibition. CytochalasinA treatment caused that SepA points dispersed around the tips within 10min. TeaA localization was also partially affected by cytochalasinA but remained concentrated at >70% of the tips after the 30 to 40min (Takeshita *et al.,* 2008). TeaC points dispersed around the tips within 50% of the tips after 10min treatment, which is inbetween the effect on SepA and TeaA, respectively.

2. A novel role of TeaC in septation

A. nidulans hyphae normally grow straight. Deletion of *teaC* caused a growth defect and a zig-zag hyphal phenotype, similar to but not identical with the one of *teaA* deletion (Takesita N *et al.*, 2008). The zigzag hyphal phenotype in the *teaC* deletion strain was weaker than in the *teaA*-deletion mutant, suggesting that the contribution of TeaC to the function of polarity maintenance is lower than that of TeaA. TeaA probably serves additional functions. In fact, in *S.pombe* and *A. nidulans,* Tea1 and TeaA interact with several proteins involved in polarized growth (Snaith and Sawin, 2003: Snaith *et al.*, 2005: Takesita N *et al.,* 2008). A severe effect on polarized growth was also observed upon overexpression of *teaC*. Normally TeaC localized at hyphal tips and forming septa, however after overexpression, large amounts of TeaC localized at hyphal tips and in the cytoplasm **(Fig. IV. 16, C)**. This suggests that not all TeaC could localize only at tips and thus remained in cytoplasm. I often observed lysis at the hyphal tips and rarely branching of hyphae **(Fig. IV. 17, A and B)**. In addition, the frequency of monopolar germination was increased. **(Fig. IV. 17, C)**. Some conidia without a second germ tube grew continuously isotropic up to 20 µm in diameter after 2

days. Some hyphae appeared to be empty, probably because of leakage of the cytoplasm. The lysis results sugget that TeaC is able to recruit further components required for cell wall extension. The effect on branching may be explained by the second severe effect of *teaC overexpression*, namely the inhibition of septation. Whereas deletion caused an increase in the number of septa in comparison to wild type, overexpression suppressed septation. The increase of the number of septa could be simply explained by the growth delay of *ΔteaC,* which leads to an apparent increase of septation and branching. However, it appears more likely that TeaC is also involved in septum site selection.

 (i) Recently, it was shown that *S. cerevisiae* Bud14 negatively controls the activity of the formin Bnr1 (Chesarone *et al*., 2009). Bud14 as a high-affinity inhibitor of the yeast formin Bnr1 that rapidly displaces the Bnr1 FH2 domain from growing barbed ends. If TeaC negatively controls SepA at septa, then overexpression would cause a reduction of the number of septa. Contradictory to this idea is the finding that in *S. pombe* overexpression of Tea4 led to long actin cables (Martin *et al.*, 2005).

(ii) A large amount of TeaC protein in the cytoplasm could trap SepA in the cytoplasm and prevent specific localization at septation sites. In agreement with this hypothesis is that I did not see any SepA-GFP rings when TeaC and SepA were overexpressed and the germlings displayed in observed in the GFP channel (data not shown).

(iii) In *S. pombe,* the position of interphase nuclei determines the cleavage site through a protein called Mid1. Mid1 is a nuclear protein, which moves out of the nucleus upon phosphorylation and marks the cell cortex in the vicinity of the nucleus for septum formation (Huang *et al* 2007: Motegi *et al* 2004）. Likewise, septation in *A. nidulans* depends on mitosis and the position of the nucleus (Wolkow *et al*., 1996 : Xiang *et al*., 1994). However, as a difference to *S. pombe*, septation does not follow every mitosis, with the result of multinucleate hyphal compartments (Wolkow *et al*., 1996). Given the importance of Mid1 for septum formation in *S. pombe,* I searched the *A. nidulans* genome for potential homologues, but were unable to find one. Since there are several

examples that e.g. cell end marker proteins are poorly conserved although they serve similar functions, a Mid1-homologue could still exist in filamentous fungi. However, the activity of this postulated protein should be further regulated, because not all nuclear division planes are used for cytokinesis. TeaC might be involved in this selection by controlling the activity of a putative Mid1 homologue. Such a function for Tea4 has been shown recently as the mechanism for tip occlusion of septation in *S. pombe* (Huang *et al*., 2007). *teaC* deletion would thus impair site selection of septation. Indeed I observed some short and empty compartments. Nevertheless, I did not find more septa close to the hyphal tip in *teaC* deletion strains, indicating that as yet unknown factors need to locally control the activity of a putative Mid1 homologue along the hyphae in addition to TeaC.

Another possibility to explain the role of TeaC in polarized growth and septation is the recruitment of other proteins involved in both processes. One candidate is the protein phosphatase 1 BimG, the *A. nidulans* homologue of *S. pombe* Dis2 and the *S. cerevisiae* homologue Glc7 (Alvarez-Tabarés *et al* 2007: Fox *et al*., 2002). This phosphatase localizes to different places in *A. nidulans*, among which is the membrane at growing tips and septa. The involvement in different processes, such as mitosis and hyphal growth, probably depends on several pathway-specific targets. Although there is evidence in *S. pombe* that Tea4 interacts with Dis2, the localization pattern of BimG and TeaC at the tip looks different. Whereas BimG localizes along the membrane and excludes the very tip, TeaC appears to be restricted to the very tip. Therefore, a direct link to TeaC remains to be shown.

Recent research shows, that the entry into mitosis depends on a concentration gradient of the protein kinase Pom1, which inhibits entry into mitosis (Sawin, 2009). Normally, Pom1 localizes with high concentration at both cell ends and forms a concentration gradient towards the middle of the cell. After cell extension, the Pom1 concentration decreases at the cell centre (Sawin, 2009). Tea4 did not show physical interaction with Pom1 but Pom1 localization at cell ends depends on Tea4 (Tatebe *at al*., 2005). *S. pombe* Pom1 is conserved in *A. nidulans* (AN7678.3, research in progress). TeaC overexpression could retain Pom1 in the cytoplasm thus lead to an inhibition of septation.

83

3. Outlook

In this research, it was discovered that the *S. pombe* cell end marker gene *tea4* homologue, *teaC* is conserved in *A. nidulans*. TeaC coordinates the MT and actin cytoskeleton together with four other proteins KipA, TeaA, TeaR and SepA. Mainly TeaC acts as connecting protein, which interacts with TeaA at the tip and SepA at cell tip and cell septation site. TeaC probably acts as regulator for the formin SepA. The identification and characterization cell end marker proteins in *A. nidulans* opens now new avenues to identify further components required for polarized growth. In recent research in our group, KipA and TeaA interacting proteins were isolated and one of them, KatA (KipA and TeaA interacting protein) interacted with both. A homologue of this protein was shown before to be involved in kinetochore attachment in *S. pombe* and other eukaryotes. This finding suggests that MT attachment at chromosomes and MT attachment at the cortex share some components (Herrero *et al*., 2009, in preparation). Moreover, TeaA was identified as an interaction partner of AlpA, which is important for suppressing MT catastrophe (Takeshita *et al*., 2009, submitted).

VI. Literature

Alberti-Segui C., Dietrich F., Altmann-Jöhl R, Hoepfner D. & Philippsen P. (2001). "Cytoplasmic dynein is required to oppose the force that moves nuclei towards the hyphal tip in the filamentous ascomycete *Ashbya gossypii*." *J Cell Sci* **114(Pt 5)**: 975-986.

Alvarez-Tabarés I., Grallert A.,Ortiz JM & Hagan IM. (2007). "Schizosaccharomyces pombe protein phosphatase 1 in mitosis, endocytosis and a partnership with Wsh3/Tea4 to control polarised growth." *J Cell Sci* **120 (Pt 20)**: 3589-3601.

Araujo-Bazan L., Peñalva MA. & Espeso EA. (2008). "Preferential localization of the endocytic internalization machinery to hyphal tips underlies polarization of the actin cytoskeleton in *Aspergillus nidulans*." *Mol Microbiol* **67(4)**: 891-905.

Arellano M., Niccoli T. & Nurse P. (2002). "Tea3p is a cell end marker activating polarized growth in *Schizosaccharomyces pombe*." *Curr Biol* **12**: 751-756.

Feierbach B. & Chang F. (2001). „Roles of the fission yeast formin for3p in cell polarity, actin cable formation and symmetric cell division". *Curr biol* **11**: 1656–1665.

Bender, A. (1993). "Genetic evidence for the roles of the bud-site-selection genes BUD5 and BUD2 in control of the Rsr1p (Bud1p) GTPase in yeast." *Proc Natl Acad Sci (USA)* **90(21)**: 9926-9929.

Bretscher, A. (2003). "Polarized growth and organelle segregation in yeast: the tracks, motors and receptors." *J Cell Biol* **160**: 811-816.

Browning H., Hackney DD. & Nurse P. (2003). "Targeted movement of cell end factors in fission yeast." *Nat Cell Biol* **5(9)**: 812-818.

Butty AC., Perrinjaquet N., Jaquenoud M., Segall JE., Hofmann K., Zwahlen C. & Peter M. (2002). "A positive feedback loop stabilizes the guanine-nucleotide exchange factor Cdc24 at sites of polarization." *EMBO J* **21(7)**: 1565-1576.

Castagnetti S., Novác B. & Nurse P. (2007). "Microtubules offset growth site from the cell centre in fission yeast." *J Cell Sci* **120**: 2205-2213.

Chang, F. & Peter M. (2003). "Yeasts make their mark." *Nat Cell Biol* **5(4)**: 294-299.

Chesarone M., Gould CJ., Moseley JB. & Goode BL. (2009). "Displacement of formins from growing barbed ends by Bud14 is critical for actin cable achitecture and function." *Dev Cell* **16**: 202-302.

Efimov V., Zhang J., & Xiang X. (2006). "CLIP-170 homologue and NUDE play overlapping roles in NUDF localization in *Aspergillus nidulans*." *Mol Biol Cell* **17**(**4**): 2021-2034.

Feierbach G., Verde F. & Chang F. (2004). "Regulation of a formin complex by the microtubule plus end protein tea1p." *J Cell Biol* **165(5)**: 697-707.

Fischer-Parton, S., R. M. Parton, P. C. Hickey, J. Dijksterhuis, H. A. Atkinson, and N. D. Read. (2000). "Confocal microscopy of FM4-64 as a tool for analyzing endocytosis and vesicle trafficking in living fungal hyphae." *J. Microsc*. **198**:246-259

Fischer, R., N. Zekert & Takeshita N. (2008). "Polarized growth in fungi - interplay between the cytosekelton, positional markers and membrane domains." *Mol Microbiol* **68(4)**: 813-826.

Fox H., Hickey PC., Fernández-Abalos JM., **Lunness P**., **Read ND**. & **Doonan JH. (2002).** "Dynamic distribution of BIMG^{PP1} in living hyphae of *Aspergillus* indicates a novel role in septum formation." *Mol Microbiol* **45(5)**: 1219-1230.

Galagan JE., Calvo SE., Cuomo C., **Ma LJ**., **Wortman JR**., **Batzoglou S**., **Lee SI**., **Baştürkmen M**., **Spevak CC**., **Clutterbuck J**., **Kapitonov V**., **Jurka J**., **Scazzocchio C**., **Farman M**., **Butler J**., **Purcell S**., **Harris S**., **Braus GH**., **Draht O**., **Busch S**., **D'Enfert C**., **Bouchier C**., **Goldman GH**., **Bell-Pedersen D**., **Griffiths-Jones S**., **Doonan JH**., **Yu J**., **Vienken K**., **Pain A**., **Freitag M**., **Selker EU**., **Archer DB**., **Peñalva MA**., **Oakley BR**., **Momany M**., **Tanaka T**., **Kumagai T**., **Asai K**., **Machida M**., **Nierman WC**., **Denning DW**., **Caddick M**., **Hynes M**., **Paoletti M**., **Fischer R**., **Miller B**., **Dyer P**., **Sachs MS**., **Osmani SA**. & **Birren BW. (2005).** "Sequencing of *Aspergillus nidulans* and comparative analysis with *A. fumigatus* and *A. oryzae*." *Nature* **438**: 1105-1115.

Giasson L. & Kronstad JW. (1995). "Mutations in the *myp1* gene of *Ustilago maydis* attenuate mycelial growth and virulence." *Genetics* **141**: 491-501.

Girbardt M. (1979): "A microfilamentous septal belt (FSB) during induction of cytokinesis in Trametes versicolor (L. ex Fr.)". *Exp Mycol* **3**: 215-228.

Harris SD. (2001). "Septum formation in *Aspergillus nidulans*." *Curr Opin Microbiol* **4(6)**: 736-739.

Harris SD., Hamer L., Sharpless KE. & Hamer JE. (1997). "The *Aspergillus nidulans sepA* gene encodes an FH1/2 protein involved in cytokinesis and the maintenance of cellular polarity." *EMBO J* **16**(12): 3474-3483.

Harris, S. D. & Momany M. (2004). "Polarity in filamentous fungi: moving beyond the yeast paradigm." *Fungal Genet Biol* **41**: 391-400.

Harris, SD., Morrell JL. & Hamer JE. (1994). "Identification and characterization of *Aspergillus nidulans* mutants defective in cytokinesis." *Genetics* **136**: 517-532.

Harris SD., Read ND.,Roberson RW., Shaw B., Seiler S., Plamann M. & Momany M. (2005). "Polarisome meets Spitzenkörper: microscopy, genetics, and genomics converge." *Eukaryot Cell* **4(2)**: 225-229.

Höög JL., Schwartz C., Noon AT., O'Toole ET., Mastronarde DN., McIntosh JR. & Antony C. (2007). "Organization of interphase microtubules in fission yeast analyzed by electron tomography." *Dev Cell* **12(3)**: 349-361.

Howard RJ. (1981). "Ultrastructural analysis of hyphal tip cell growth in fungi: Spitzenkörper, cytoskeleton and endomembranes after freeze-substitution." *J Cell Sci* **48**: 89-103.

Howard RJ. & Aist JR. (1980). "Cytoplasmic mirotubules and fungal morphogenesis: ultrastructural effects of methyl benzimidazole-2-ylcarbamate determined by freeze-substitution of hyphal tip cells." *J Cell Biol* **87**: 55-64.

Huang Y., Chew TG., GE W. & Balasubramanian MK. (2007). "Polarity determinants Tea1p, Tea4p, and Pom1p inhibit division-septum assembly at cell end in fission yeast." *Dev Cell* **12**: 987-996.

Jaspersen SL. & Winey M. (2004). "The budding yeast spindle pole body: structure, duplication, and function." *Annu Rev Cell Dev Biol* **20**: 1-28.

Käfer E. (1977). "Meiotic and mitotic recombination in *Aspergillus* and its chromosomal aberrations." *Adv Genet* **19**: 33-131.

Keating, TJ. & Borisy GG. (1999). "Centrosomal and non-centrosomal microtubules." *Biol Cell* **91(4-5)**: 321-329.

Kohno H., Tanaka K., Mino A., Umikawa M., Imamura H., Fujiwara T., Fujita Y., **Hotta K**., **Qadota H**., **Watanabe T**., **Ohya Y**. & **Takai Y. (1996).** "Bni1p implicated in cytoskeletal control is a putative target of Rho1p small GTP binding protein in *Saccharomyces cerevisiae*". *EMBO J* **15**: 6060-6068.

Konzack, S., P. Rischitor, Enke C. & Fischer R. (2005). "The role of the kinesin motor KipA in microtubule organization and polarized growth of *Aspergillus nidulans*." *Mol Biol Cell* **16**: 497-506.

Kron SJ. & Gow NA. (1995). "Budding yeast morphogenesis: signalling, cytoskeleton and cell cycle". *Curr Opin Cell Biol* **7**: 845-855.

Kovar DR. (2006). "Cell polarity: Formin on the move." *Curr Biol* **16(14)**: R535-538.

Madden K. & Snyder, M. (1998). "Cell polarity and morphogenesis in budding yeast." *Ann Rev Microbiol* **52**: 687–744.

Martin SG. & Chang F. (2003). "Cell polarity: a new mod(e) of anchoring." *Curr Biol* **13(18)**: R711-730.

Martin SG. & Chang F. (2005). "New End Take Off: Regulating Cell Polarity during the Fission Yeast Cell Cycle." *Cell Cycle* **4(8)**: 1046-1049.

Martin SG. & Chang F. (2006). "Dynamics of the formin for3p in actin cable assembly." *Curr Biol* **16(12)**: 1161-1170.

Martin SG., McDonald WH. , Yates JR. & Chang F. (2005). "Tea4p links microtubule plus ends with the formin for3p in the establishment of cell polarity." *Dev Cell* **8(4)**: 479-491.

Martin SG., Rincon SA., Basu R., Pérez P. & Chang F. (2007). "Regulation of the formin for3p by cdc42p and bud6p." *Mol Biol Cell* **18(10)**: 4155-4167.

Mitchison, T. J. & Nurse P. (1985). "Growth in cell length in the fission yeast *Schizosaccharomyces pombe*." *J Cell Sci* **75**: 357-376.

Momany M. & Hamer JE. (1997). "Relationship of actin, microtubules, and crosswall synthesis during septation in *Aspergillus nidulans*." *Cell Motil Cytoskeleton* **38**: 373-384.

Morris NR. (1975). "Mitotic mutants of *Aspergillus nidulans*." *Genet Res* **26**: 237-254.

Morris NR & Enos AP. (1989). "Mitotic gold in a mold: Aspergillus genetics and the biology of mitosis." *Trends Genet* **8**(1):32-7.

Moseley JB. & Goode BL. (2005). "Differential activities and regulation of *Saccharomyces cerevisiae* formin proteins Bni1 and Bnr1 by Bud6." *J Biol Chem* **280(30)**: 28023-28033.

Motegi, F., Mishra M., Balasubramanian MK. & Mabuchi I. (2004). "Myosin-II reorganization during mitosis is controlled temporally by its dephosphorylation and spatially by Mid1 in fission yeast." *J Cell Biol* **265(5)**: 685-695.

Nayak, T., Szewczyk E., Oakley CE., Osmani A., Ukil L., Murray SL., Hynes MJ., Osmani SA. & Oakley BR. (2006). "A versatile and efficient gene targeting system for *Aspergillus nidulans*." *Genetics* **172(3)**: 1557-1566.

Ni L. & Snyder M. (2001). "A genomic study of the bipolar bud site selection pattern in *Saccharomyces cerevisiae*." *Mol Biol Cell* **12(7)**: 2147-2170.

Nierman WC., May G., Kim HS., Anderson MJ., Chen D. & Denning DW. (2005). "What the Aspergillus genomes have told us". *Med Mycol* **43 Suppl 1**: S3–5.

Osmani SA. & Mirabito PM (2004). "The early impact of genetics on our understanding of cell cycle regulation in Aspergillus nidulans". *Fungal Genet Biol* **41(4)**: 401–10.

Park HO. & Bi E. (2007). "Central roles of small GTPases in the development of cell polarity in yeast and beyond." *Microbiol Mol Biol Rev* **71(1)**: 48-96.

Pel HJ., de Winde JH., Archer DB., Dyer PS., Hofmann G., Schaap PJ., Turner G., de Vries RP., Albang R., Albermann K., Andersen MR., Bendtsen JD., Benen JA., van den Berg M., Breestraat S., Caddick MX., Contreras R., Cornell M., Coutinho PM., Danchin EG., Debets AJ., Dekker P., van Dijck PW., van Dijk A., Dijkhuizen L., Driessen AJ., d'Enfert C., Geysens S., Goosen C., Groot GS., de Groot PW., Guillemette T., Henrissat B., Herweijer M., van den Hombergh JP., van den Hondel CA., van der Heijden RT., van der Kaaij RM., Klis FM., Kools HJ., Kubicek CP., van Kuyk PA., Lauber J., Lu X., van der Maarel MJ., Meulenberg R., Menke H., Mortimer MA., Nielsen J., Oliver SG., Olsthoorn M., Pal K., van Peij NN., Ram AF., Rinas U., Roubos JA., Sagt CM., Schmoll M., Sun J., Ussery D., Varga J., Vervecken W., van de Vondervoort PJ., Wedler H., Wösten HA., Zeng AP., van Ooyen AJ., Visser J. & Stam H. (2007). "Genome sequencing and analysis of the versatile cell factory *Aspergillus niger* CBS 513.88." *Nat Biotechnol.* **25(2)**: 221-231.

Philips, J. & Herskowitz I. (1998). "Identification of Kel1p, a kelch-domain-containing protein invovled in cell fusion and morphology inSaccharomyces cerevisiae." *J Cell Biol* **143**: 375-389.

Pontecorvo G., ROPER JA., **HEMMONS LM**., **MACDONALD KD. & BUFTON AW**. **(1953).** "The genetics of *Aspergillus nidulans*." *Adv Genet* **5**: 141-238.

Pruyne, D. & Bretscher A. (2000). "Polarization of cell growth in yeast." *J Cell Sci* **113(4)**: 1013-1015.

Rida PC., Nishikawa A., Won GY. & Dean N. (2006). "Yeast-to-hyphal transition triggers formin-dependent Golgi localization to the growing tip in *Candida albicans*." *Mol Biol Cell* **17(10)**: 4364-4378.

Sawin KE. & Tran PT. (2006). "Cytoplasmic microtubule organization in fission yeast." *Yeast* **23**(13): 1001-1014.

Sawin KE. (2009). „Cell cycle: Cell division brought down to size." *Nature* **459**: 782-783.

Schenkman LR., Caruso C., Pagé N. & **Pringle JR**. **(2002).** "The role fo cell cycle-regulated expression in the localization of spatial landmark proteins in yeast." *J Cell Biol* **156(5)**: 829-841.

Seiler S., Nargang FE., Steinberg G. & Schliwa M. (1997). "Kinesin is essential for cell morphogenesis and polarized secretion in *Neurospora crassa*." *EMBO J* **16**(11): 3025-3034.

Sharpless KE. & Harris SD. (2002). "Functional characterization and localization of the *Aspergillus nidulans* formin SEPA." *Mol Biol Cell* **13**: 469-479.

Snaith HA., Samejima I. & Sawin KE. (2005). "Multistep and multimode cortical anchoring of tea1p at cell tips in fission yeast*." EMBO J* **24**: 3690-3699.

Snaith HA. & Sawin KE. (2003). "Fission yeast mod5p regulates polarized growth through anchoring of tea1p at cell tips." *Nature* **423**: 647-651.

Stringer MA., Dean RA., Sewall TC. & Timberlake WE. (1991). "*Rodletless*, a new *Aspergillus* developmental mutant induced by directed gene inactivation." *Genes Dev* **5**: 1161-1171.

Taheri-Talesh N., Horio T., Araujo-Bazán L., Dou X., Espeso EA., Peñalva MA., Osmani SA. & Oakley BR. (2008). "The tip growth apparatus of *Aspergillus nidulans*." *Mol Biol Cell* **19(4)**: 1439-1449.

Takeshita N., Higashitsuji Y., Konzack S. & Fischer R. (2008). "Apical sterol-rich membranes are essential for localizing cell end markers that determine growth directionality in the filamentous fungus *Aspergillus nidulans*." *Mol Biol Cell* **19**: 339-351.

Tatebe H., Shimada K., Uzawa S., Morigasaki S. & Shiozaki K. (2005). "Wsh3/Tea4 is a novel cell-end factor essentail for bipolar distribution of Tea1 and protects cell polarity under environmental stress in *S. pombe*." *Curr Biol* **15(11)**: 1006-1015.

Veith D., Scherr N., Efimov VP. & **Fischer R**. **(2005).** "Role of the spindle-pole body protein ApsB and the cortex protein ApsA in microtubule organization and nuclear migration in *Aspergillus nidulans*." *J Cell Sci* **118**: 3705-3716.

Verde F., Mata J. & Nurse P. (1995). "Fission yeast cell morphogenesis: identification of new genes and analysis of their role during the cell cycle." *J Cell Biol* **131**: 1529-1538.

Wedlich-Söldner R. & Li R. (2003). "Spontaneous cell polarization: undermining determinism." *Nat Cell Biol* **5(4)**: 267-270.

94

Wolkow TD., Harris SD. & Hamer JE. (1996). "Cytokinesis in *Aspergillus nidulans* is controlled by cell size, nuclear positioning and mitosis." *J Cell Sci* **109**: 2179-2188.

Xiang X., Beckwith SM. & Morris NR. (1994). "Cytoplasmic dynein is involved in nuclear migration in *Aspergillus nidulans*." *Proc Natl Acad Sci (USA)* **91(6)**: 2100-2104.

Yelton MM., Hamer JE. & Timberlake WE. (1984). "Transformation of *Aspergillus nidulans* by using a *trpC* plasmid." *Proc Natl Acad Sci (USA)* **81**: 1470-1474.

Zekert, N. & Fischer R. (2009). "The *Aspergillus nidulans* kinesin-3 UncA motor moves vesicles along a subpopulation of microtubules." *Mol Biol Cell* **20**: 673-684.

CURRICULUM VITAE

Name: Yuhei Higashitsuji

Address: Stephanienstr. 23   D-76133 Karlsruhe, Germany
e-mail: h_yuhei@hotmail.com
Birth date: June 18, 1980

Education and Qualifications
07/2006-09/2009

PhD , Department of applied Microbiology, University of Karlsruhe, Germany

PhD thesis title: On the Role of the cell end marker protein TeaC in the   filamentous fungus Aspergillus nidulans

04/2005 – 03/2006

Exchange student, Mannheim University of Applied Sciences, Germany

Study: Microbiology, molecular biology and English

Progyect title: RibR, a possible regulator of the Bacillus subtilis riboflavin biosynthetic operon, in vivo interacts with the 5'-untranslated leader of rib mRNA.

04/2003 – 03/2005

Masters in Molecular Biology, Shinsyu-u University, Japan

Study: Microbiology and molecular biology

Progyect title: Post-translational control of vegetative cell separation enzymes through a direct interaction with specific inhibitor IseA in *Bacillus subtilis.*

04/1999 – 03/2003

Bachelor in Molecular Biology, Soujyou University, Japan

Study: Microbiology, molecular biology and Biochemistry

Progyect title: *Bacillus subtilis* transformation in solid medium.

04/1996 – 03/1999

Gojyou High School, Japan

Study: Biology, Chemistry and English

Acknowledgement

First and foremost I would like to deeply thank Prof. Dr. Reinhard Fischer for trusting me and offering me the opportunity to work in his team as a PhD student at an interesting topic, and for his tireless support through suggestions and discussions concerning the scientific research.

My special thanks go to Dr. Norio Takeshita for everything at work, science and life.

To all my colleagues, formerly (Dr. Daniel Veith, Dr. Janina Purschwitz, Sabrina Hettinger) presently (Dr. Elisabeth Poth, Dr. Saturnino Herrero de Vega, Dr. Friederike Bathe, Dr. Julio Rodriguez, Dr. Debjani Saha, Nadine Zekert, Sylvia Müller, Christian Kastner, Sonja Sand, Tobias Schunck, Jan Siebenbrock, Tanja Sauerbrunn, Maren Hedtke, Daniel Mania, Ramona Demir, Constanze Seidel, Claudia Kempf) in the group . I would like to say a sincere "Vielen Danke!", for the nice and friendly atmosphere given to the lab and to everyday work.

All my deep gratitude belongs to my family, to my parents who always guided me towards discovering new beginnings, to my wife Yuki who is sharing with me the life around and to my son Rin.

The Cell End Marker Protein TeaC Is Involved in Growth Directionality and Septation in *Aspergillus nidulans*[∇][†]

Yuhei Higashitsuji, Saturnino Herrero, Norio Takeshita, and Reinhard Fischer*

*University of Karlsruhe and Karlsruhe Institute of Technology, Institute of Applied Biosciences–Microbiology, Hertzstrasse 16,
D-76187 Karlsruhe, Germany*

Polarized growth in filamentous fungi depends on the correct spatial organization of the microtubule (MT) and actin cytoskeleton. In *Schizosaccharomyces pombe* it was shown that the MT cytoskeleton is required for the delivery of so-called cell end marker proteins, e.g., Tea1 and Tea4, to the cell poles. Subsequently, these markers recruit several proteins required for polarized growth, e.g., a formin, which catalyzes actin cable formation. The latest results suggest that this machinery is conserved from fission yeast to *Aspergillus nidulans*. Here, we have characterized TeaC, a putative homologue of Tea4. Sequence identity between TeaC and Tea4 is only 12.5%, but they both share an SH3 domain in the N-terminal region. Deletion of *teaC* affected polarized growth and hyphal directionality. Whereas wild-type hyphae grow straight, hyphae of the mutant grow in a zig-zag way, similar to the hyphae of *teaA* deletion (*tea1*) strains. Some small, anucleate compartments were observed. Overexpression of *teaC* repressed septation and caused abnormal swelling of germinating conidia. In agreement with the two roles in polarized growth and in septation, TeaC localized to hyphal tips and to septa. TeaC interacted with the cell end marker protein TeaA at hyphal tips and with the formin SepA at hyphal tips and at septa.

Filamentous fungi represent fascinating model organisms for studying the establishment and maintenance of cell polarity, because cell growth takes place at the tip of the extremely elongated hyphae. Hyphal extension requires the continuous expansion of the membrane and the cell wall and is driven by continuous fusion of secretion vesicles at the tip (8, 12). The transportation of vesicles is probably achieved by the coordinated action of the MT and the actin cytoskeleton. According to one model, vesicles first travel along MTs, are unloaded close to the hyphal tip, where they form a microscopically visible structure the "Spitzenkörper," which is also called the "vesicle supply center," referring to the assumed function (24, 25). For the last step, vesicle transportation from the Spitzenkörper to the apical membrane, actin-myosin-dependent movement is used. Anti-cytoskeletal drug experiments have shown that hyphae can grow for some time in the absence of MTs but not in the absence of the actin cytoskeleton (14, 27, 30a).

In *Schizosaccharomyces pombe* it was shown clearly that the polarization of the actin cytoskeleton depends on the MT cytoskeleton (2, 7). In 1994, polarity mutants of *S. pombe* were isolated and subsequent cloning of one of the genes identified the polarity determinant Tea1 (19, 29). Because this protein labels the growing cell end, this and other subsequently isolated proteins of this class were named cell end markers. It was shown that cell end localization of Tea1 requires the activity of a kinesin motor protein, Tea2, which transports the protein to the MT plus end (3). Together with the growing MT, Tea1 reaches the cortex, where it is unloaded and binds to a prenylated and membrane-anchored receptor protein, Mod5 (28). The formin For3, which catalyzes actin cable formation, is recruited to the tip through binding to another cell end marker protein, Tea4, which confers tethering to Tea1 (7, 18, 33). Tea4 is required for For3 localization at the cell tip, specifically during initiation of bipolar growth (18).

Recently, it was shown that components of this polarity determination machinery are conserved in the filamentous fungus *A. nidulans* (8). The first component identified was the Tea2 homologue, KipA, a kinesin-7 motor protein (16). Deletion of the gene did not affect hyphal tip extension but polarity determination. Instead of growing straight, hyphae grew in curves. KipA moves along MTs and accumulates at the MT plus end. The identification of Tea1 and a Mod5 homologue was more difficult, because the primary structure of these cell end marker proteins is not well conserved in filamentous fungi. A Tea1 homologue, TeaA, only displayed 27% sequence identity. However, the presence of Kelch repeats in both proteins suggested conserved functions (31). A Mod5 homologue was identified by a conserved CAAX prenylation motif at the C terminus. Systematic analyses of proteins with such a motif in the *A. nidulans* genome led to the identification of TeaR. Like Tea1 and Mod5, TeaA and TeaR localize at or close to the hyphal membrane at the growing cell end (31). However, correct localization of TeaR requires TeaA. In addition, sterol-rich membrane domains define the place of TeaR attachment to the hyphal tip. In contrast to *S. pombe*, TeaA and TeaR are still transported to the hyphal tip in the absence of the motor protein KipA, but their localization is disturbed in comparison to wild type. This suggests that other proteins are necessary for exact TeaA positioning, whose localization depends on KipA.

We characterized a homologue of the *S. pombe* cell end

TABLE 1. *A. nidulans* strains used in this study

Strain[a]	Genotype	Source or reference
TN02A3	*pyrG89*; *argB2* Δ*nkuA::argB*; *pyroA4*	22
RMS011	*pabaA1 yA2*; Δ*argB::trpC*Δ*B*; *pyroA4*	30
SRL1	Δ*kipA::pyr4*; *pyrG89*; *pyroA4* (Δ*kipA*)	16
SJW02	*wA3*; Δ*argB::trpC*Δ*B*; *pyroA4*; *alcA(p)::GFP::tubA* (GFP-MTs)	6
SSK91	SRF200 transformed with pSK76, Δ*teaA::argB*; *pyrG89*; Δ*argB::trpC*Δ*B*; *pyroA4* (Δ*teaA*)	16
SNT17	*pyrG89*; *wA3*; *alcA(p)::GFP::kipA-rigor* (GFP-kipA-rigor)	31
SNT49	TN02A3 transformed with pNT28 [*teaA(p)-mRFP1-teaA*]	31
SNT28	TN02A3 transformed with pNT9 (*GFP-sepA*)	31
SNT52	SNT49 crossed to RMS011 [*teaA(p)-mRFP1-teaA*]	31
SYH03	TNO2A3 with pYH06 [*alcA(p)-GFP-teaC*]	This study
SYH05	TN02A3 transformed with pYH03 and pYH09 (*YFP^N-sepA* and *YFP^C-teaC*)	This study
SYH06	TN02A3 transformed with pYH01 and pYH09 (*YFP^N-teaA* and *YFP^C-teaC*)	This study
SYH13	SYH03 crossed to SNT52 [*GFP-TeaC, teaA(p)-mRFP1-TeaA*]	This study
SYH17	TN02A3 transformed with pYH30 [*teaC(p)-mRFP1-TeaC*]	This study
SYH18	SYH20 crossed to SNT28 [*teaC(p)-mRFP1-TeaC* and *GFP-SepA*]	This study
SYH19	SYH20 crossed to SSK91 [*teaC(p)-mRFP1-TeaC* and Δ*teaA*]	This study
SYH20	SYH17 crossed to RMS011 [*teaC(p)-mRFP1-TeaC*]	This study
SYH21	TN02A3 transformed with pYH14 (Δ*teaC*)	This study
SYH22	SYH20 crossed to SJW02 [*GFP-MT* and *teaC(p)-mRFP1-TeaC*]	This study
SYH23	SYH20 crossed to SNT17 [*GFP-kipA* rigor and *teaC(p)-mRFP1-TeaC*]	This study
SYH24	SYH21 crossed to SNT52 [*teaA(p)-mRFP1-teaA* and Δ*teaC*]	This study
SYH25	SYH17crossed to SRL1 [Δ*kipA* and *teaC(p)-mRFP1-TeaC*]	This study
SYH26	SYH28 crossed to SYH27 (*mRFP1-TeaC* and *GFP-SepA*)	This study
SYH27	TN02A3 transformed with pYH24 (*mRFP1-TeaC*)	This study
SYH28	RMS011 crossed to SNT28 (*GFP-sepA*)	This study

[a] All strains are *veA1*.

marker protein, Tea4, and found that the protein is required for the maintenance of straight polar growth but that it also appears to be involved in septation.

MATERIALS AND METHODS

Strains, plasmids, and culture conditions. Supplemented minimal medium (MM) and complete medium for *A. nidulans* were prepared as described earlier, and the standard strain construction procedures have also been described elsewhere (13). A list of *A. nidulans* strains used in the present study is given in Table 1. Standard laboratory *Escherichia coli* strains (XL1-Blue and Top10F′) were used. Plasmids are listed in Table 2.

Molecular techniques. Standard DNA transformation procedures were used for *A. nidulans* (37) and *E. coli* (26). For PCR experiments, standard protocols were applied using a Biometra TRIO Thermoblock for the reaction cycles. DNA sequencing was done commercially (MWG Biotech, Ebersberg, Germany). Genomic DNA was extracted from *A. nidulans* with the DNeasy plant minikit (Qiagen, Hilden, Germany). DNA analyses (Southern hybridizations) were performed as described previously (26).

Deletion of *teaC*. Flanking regions of *teaC* were amplified by PCR using genomic DNA and the primers TeaC-left-for (5′-GAA CAG TTG CCT TTC GAA AT-3′) and TeaC-left-rev-SfiI (5′-TGG TGG CCA TCT AGG CCG TAG CAG GAT GTT CAA AGG-3′) for the upstream region of *teaC* and the primers TeaC-right-for-SfiI (5-AAT AGG CCT GAG TGG CCC CGA CTG GCA CCA CTA C-3′) and TeaC-right-rev (5′-AGA GGC TGG ATT CCT TCT-3′) for the downstream region and cloned into pCR2.1-TOPO to generate plasmids pYH32 and pYH33, respectively. The SfiI restriction sites are underlined. In a three-fragment ligation, the *N. crassa pry-4* gene was released from plasmid pSCI with SfiI and ligated between the two *teaC*-flanking regions, resulting in the vector pYH14.

Transformants of strain TN02A3 were screened by PCR for the homologous integration event. Single integration of the construct was confirmed by Southern blotting (see Fig. S1 in the supplemental material). A total of 20 strains were analyzed, of which 8 showed the *teaC* deletion pattern. All eight deletion strains displayed the same phenotypes. One *teaC* deletion strain was selected for further studies and named SYH21. Coupling of the observed phenotypes with the gene deletion event was confirmed by crosses, recomplementation with *teaC*-derived clones, and downregulation of the gene through the inducible *alcA* promoter.

Tagging of proteins with GFP and mRFP1. To create an N-terminal green fluorescent protein (GFP) fusion construct of TeaC, a 1.2-kb N-terminal frag-

ment of *teaC* (starting from ATG) was amplified from genomic DNA with the primers teaC-AF(5′-TAG GCG CGC CGA TGG CTA GAC CTA GAA TGG-3′) and teaC-PR(5′-CTT AAT TAA TTC TTC AAC AGC CTT AGT TTT-3′) and cloned into pCR2.1-TOPO, yielding pYH34. The restriction sites are underlined. The AscI-PacI fragment from pYH34 was subcloned into the corresponding sites of pCMB17apx, yielding pYH06. To create an N-terminal mRFP1 fusion construct of TeaC, the AscI-PacI fragment from pYH06 was subcloned into the corresponding sites of pDM8, yielding pYH24. To produce TeaC N-terminally tagged with mRFP1 expressed from the native promoter, a 1.5-kb fragment of the *teaC* putative promoter region was amplified from genomic DNA with the primers TeaCp-pro-AvrII (5′-ACC TAG GTG ACC TTG GGT ATC GTT G-3′) and teaC-pro-KpnI (5′-AGG TAC CAC GAA TTA TGT AGC AGG AT-3′), digested with AvrI and KpnI, and ligated with AvrI-KpnI-digested pYH24, yielding pYH30 (*alcA* promoter replaced with the *teaC* promoter in pYH24). Using the same approach as for TeaC, N-terminal GFP fusion constructs of TeaC were created. All plasmids were transformed into the uracil-auxotrophic strain TN02A3 (Δ*nkuA*). The integration events were confirmed by PCR and Southern blotting (results not shown).

For bimolecular fluorescence complementation (BiFC) analyses, the N-terminal half of YFP (YFP^N) or the C-terminal half of YFP (YFP^C) was fused to the N terminus of the protein of interest. YFP^N (154 amino acids of YFP and 5 amino acids linker) was amplified with the primers fwd-Kpn-YFP-N (5′-CGG TAC CAT GGT GAG CAA GGG CGA GGA GCT G-3′) and rev-YFP-N-Li-Asc (5-CGG CGC GCC CGT GGC GAT GGA GCG CAT GAT ATA GAC GTT GTG GCT GTT GTA G-3′). YFP^C (86 amino acids of YFP and 17 amino acids linker) was amplified with the primers fwd-Kpn-YFP-C (5′-CGG TAC CAT GGC CGA CAA GCA GAA GAA CGG CAT CAA GG-3′) and ev_YFP-C_Li_Asc (5′-CGGCGCGGCCGTGGTTCATGACCTTCTGTTTCAGGTCGT TCGGGATCTTGCAGGCCGGGCGCTTGTACAGCTCGTCCATGCCGAG AGTGATCCC-3′). The KpnI-AscI fragment of YFP^N or YFP^C was ligated into KpnI- and AscI-digested pCMB17apx, yielding pDV7 (GFP replaced with YFP^N in pCMB17apx) and pDV8 (GFP replaced with YFP^C in pCMB17apx). To create an N-terminal YFP^C fusion construct of TeaC, the AscI-PacI fragment from pYH06 was subcloned into the corresponding sites of pDV8, yielding pYH08. To create N-terminal YFP^N fusion constructs *teaA* and *sepA* fragments from pNT1, pNT9, were subcloned into the corresponding sites of pDV7, yielding pYH01 and pYH03.

Yeast two-hybrid analysis. The yeast two-hybrid analysis was performed by using the MatchMaker3 Gal4 two-hybrid system (BD Clontech). For bait generation, fragments of *teaC* cDNA corresponding to the N-terminal half of TeaC

TABLE 2. Plasmids used in this study

Plasmid	Construction	Source or reference
pCR2.1-TOPO	Cloning vector	Invitrogen (NV Leek, The Netherlands)
pCMB17apx	*alcA(p)::GFP*, for N-terminal fusion of GFP to proteins of interest; contains *N. crassa pyr4*	5
pDM8	GFP replaced mRFP1 in pCMB17apx	34
pSCI	*pry4* with SfiI sites	16
pNT33	N-terminal half of *teaA* cDNA in pGADT7	31
pNT34	N-terminal half of *teaA* cDNA in pGABKT7	31
pNT35	C-terminal half of *teaA* cDNA in pGADT7	31
pSH19	C-terminal half of *teaA* cDNA in pGABKT7	31
pNT6	0.7-kb *teaA* fragment in pDBM8	31
pNT28	1.5-kb *teaA(p)* fragment in pNT6	31
pNT6	0.7-kb *teaA* fragment from pNT1 inpDM8	31
pNT9	1.2-kb *sepA* fragment in pCMB17apx	31
pDV7	GFP replaced N-terminal half of YFP in pCMB17apx	31
pDV8	GFP replaced C-terminal half of YFP in pCMB17apx	31
pYH01	0.7-kb *teaA* fragment from pNT1 in pDV7	31
pYH03	1.2-kb *sepA* fragment from pNT9 in pDV7	31
pYH06	1.2-kb *teaC* fragment in pCMB17apx	This study
pYH08	1.2-kb *teaC* fragment from pYH06 in pDV8	This study
pYH14	*teaC* deletion construct: flanking regions from pYH33 and pYH34 ligated with *pry4* from pCS1	This study
pYH16	N-terminal half of *teaC* cDNA in pGADT7	This study
pYH17	N-terminal half of *teaC* cDNA in pGBK T7	This study
pYH18	C-terminal half of *teaC* cDNA in pGADT7	This study
pYH19	C-terminal half of *teaC* cDNA in pGBKT7	This study
pYH24	1.2-kb *teaC* fragment in pDM8	This study
pYH30	1.5-kb *teaC(p)* fragment in pYH24	This study
pYH32	1.0-kb 5′-flanking region of *teaC* with SfiI site in pCR2.1-TOPO	This study
pYH33	1.0-kb 3′-flanking region of *teaC* with SfiI site in pCR2.1-TOPO	This study
pYH34	1.2-kb *teaC* fragment in pCR2.1-TOPO	This study

(356 amino acids) with the primers TeaC-EF (5′-GGC C<u>GA ATT C</u>AT GGC TAG ACC TAG AAT GG-3′) and TeaC-BMR (5′-<u>GGA TCC</u> TTA CAG TAG GTT CGG AGT GAG-3′) or corresponding to the C-terminal half of TeaC (428 amino acids) with the primers TeaC-EMF (5′-<u>GAA TTC</u> GAA AAG CCG CGC TCA AG-3′) and TeaC-BR (5′-GGC C<u>GG ATC C</u>TT ATT GAC TCG TCG ACC TG-3′) were amplified and cloned into the pGBK7 vector, which contains the Gal4 DNA-BD and the *TRP1* marker, yielding pYH17 and pYH19 (BD Clontech). The fragments of *teaC* cDNA corresponding to the N-terminal half and C-terminal half of TeaC from pYH17 and pYH19 were amplified and cloned into the pGADT7 vector, which contains the GAL4 DNA-AD and the *LEU2* marker (BD Clontech), yielding pYH16 and pYH18. pGBK7-associated plasmids were transformed into yeast Y187 (mating type *MATα*), and pGADT7-associated plasmids were transformed into yeast AH109 (mating type *MAT***a**). The system utilizes two reporter genes (*HIS3* and *lacZ*) under the control of the GAL4-responsive UAS. The β-galactosidase activity was analyzed by liquid culture assays using ONPG (*o*-nitrophenyl-β-D-galactopyranoside; Sigma) as a substrate. The activity was calculated in Miller units (20). Experiments were repeated three times.

Light and fluorescence microscopy. For live-cell imaging of germlings and young hyphae, cells were grown on coverslips in 0.5 ml of MM plus 2% glycerol (derepression of the *alcA* promoter and thus moderate expression of the gene), MM plus 2% threonine (activation of the gene thus high expression levels), or MM plus 2% glucose (repression of the *alcA* promoter). Cells were incubated at room temperature for 1 to 2 days. For pictures of young hyphae of each gene deletion strain, the spores were inoculated on microscope slides coated with MM plus 2% glucose plus 0.8% agarose and grown at 30°C for 1 day. Images were captured at room temperature by using an Axioimager microscope (Zeiss, Jena, Germany). Images were collected and analyzed by using the AxioVision system (Zeiss).

FM4-64, Hoechst 33342, calcofluor white, benomyl, and cytochalasin A treatment. FM4-64 was used at a concentration of 10 μM in the medium. Coverslips were incubated for 5 min and washed. Benomyl [methyl 1-(butylcarbamoyl)-2-benzimidazole carbamate; Aldrich] was used at a final concentration of 2.5 μg/ml in the medium from a stock solution of 1 mg/ml in ethanol. Cytochalasin A (Sigma) was used at a final concentration of 2 μg/ml in the medium from a stock solution of 100 mg/ml in dimethyl sulfoxide. Calcofluor white was used at a final

concentration of 60 μg/ml in the medium. Hoechst 33342 (Molecular Probes) used at a final concentration of 10 μg/ml in the medium.

Protein extracts and Western blotting. For induction of the *alcA* promoter, *A. nidulans* cultures ware shaken in MM containing 2% threonine or 2% glycerol for 48 h. The mycelium was harvested by filtration through Miracloth (Calbiochem, Heidelberg, Germany), dried by pressing between paper towels, and immediately frozen in liquid nitrogen. After the mycelium was ground in liquid nitrogen, the material was resuspended in protein extraction buffer (50 mM Tris-HCl [pH 8], 150 mM NaCl) supplemented with protease inhibitors (1 mM phenylmethylsulfonyl fluoride, 10 μM leupeptin, 1 μM pepstatin). Protein extracts ware clarified twice by centrifugation (centrifuge 5403; Eppendorf, Hamburg, Germany) at 13,000 rpm at 4°C for 10 min. The protein concentration was quantified with a Roti-Quant kit (Roth, Karlsruhe, Germany). After denaturation of the samples, protein extracts were loaded on a 7.5% sodium dodecyl sulfate-polyacrylamide gel. For blotting, nitrocellulose membranes from Schleicher & Schuell (Dassel, Germany) were used. For Western blotting, we used rabbit polyclonal anti-GFP (Sigma-Aldrich, Munich, Germany) at a dilution of 1:4,000 and polyclonal anti-rabbit antibodies coupled to peroxidase (product A0545; Sigma-Aldrich) at a dilution of 1:4,000.

RESULTS

Isolation and deletion of *teaC*. We searched the *A. nidulans* genome at the Broad Institute (Cambridge, MA) (http://www.broad.mit.edu/annotation/genome/aspergillus_group/MultiHome.html) for proteins with similarity to the cell end marker protein Tea4 from *S. pombe* and identified one open reading frame (AN1099.3) (11). DNA and cDNA sequences were confirmed, and five introns with lengths of 66, 60, 66, 46, and 45 bp were determined. We named the gene *teaC*, although sequence similarity between the 687-amino-acid *A. nidulans* protein and the 810-amino-acid *S. pombe* protein

A
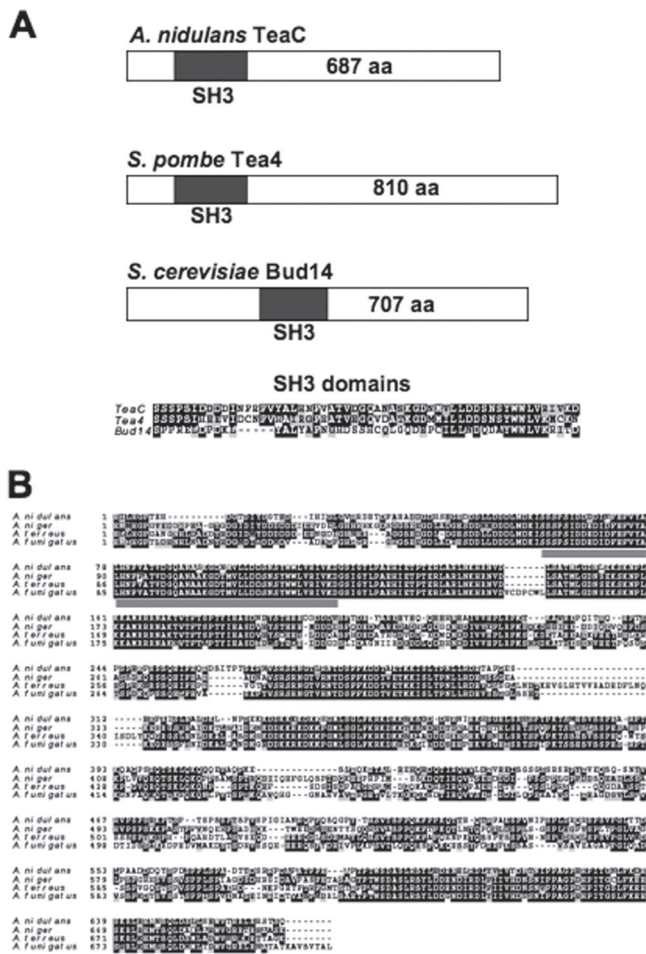
FIG. 1. Comparison of TeaC with related proteins from other fungi. (A) Scheme of *A. nidulans* TeaC, *S. pombe* Tea4, and *S. cerevisiae* Bud14, indicating the location of the SH3 domain. The alignment of the three SH3 domains is displayed below the scheme. (B) Alignment of TeaC homologues from four *Aspergillus* species as indicated. The SH3 domain is highlighted with the red line below the sequences. The alignments were done with CLUSTAL W with standard parameters. Identical amino acids are shaded in black, and chemically conserved amino acids are shaded in gray using the program box shade. aa, amino acids.

was restricted to a conserved SH3 domain (Fig. 1A). Within this 86-amino-acid domain the identity was 63% with an e-value of 6e−27. Outside this region, the homology was very low, and the overall identity was only 12.5%. The sequence similarity to the *S. cerevisiae* Bud14 protein, which shares some functional relationship with Tea4, was even lower. In other aspergilli, proteins with high identities to *A. nidulans* TeaC were found (Fig. 1B). The identity to corresponding proteins from other ascomycetous fungi was again much lower, e.g., *Penicillium chrysogenum* (43%) and *Magnaporthe grisea* (only 22%). Sequence identity to basidiomycetous species was less than 10%. These results indicate that TeaC sequences are only poorly conserved within fungi.

To analyze the function of *teaC* in *A. nidulans*, we constructed a *teaC* deletion strain (SYH21; see Materials and Methods) and compared it to a Δ*teaA* deletion strain con-
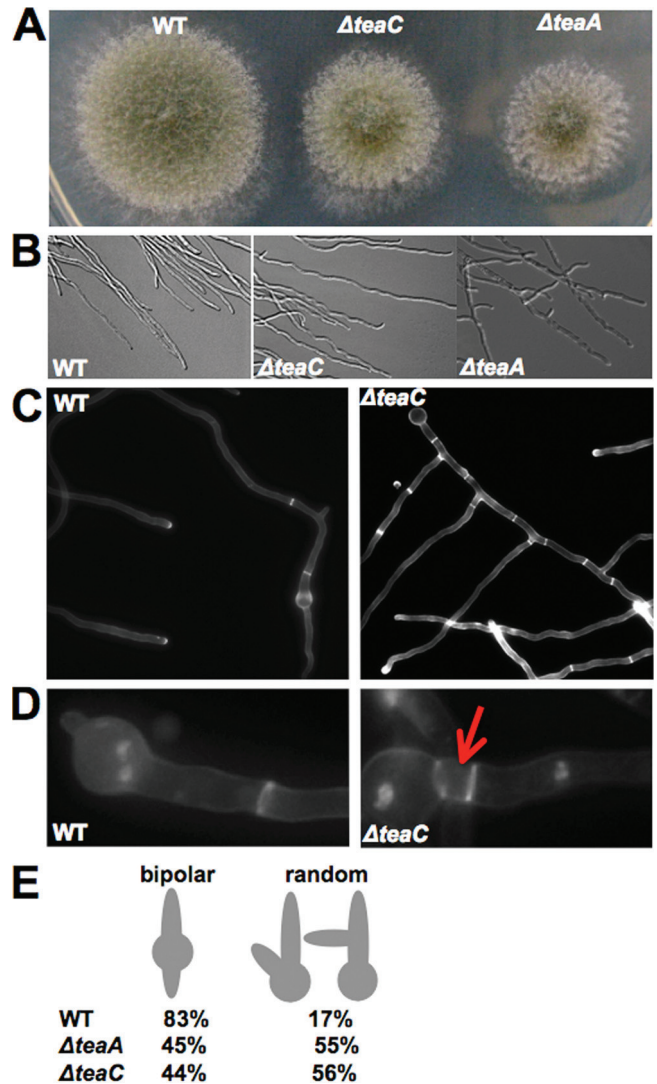
FIG. 2. Phenotypic comparison of wild-type with Δ*teaC* and Δ*teaA* strains. (A) Colonies of wild-type (TN02A3), Δ*teaA* (SSK91), and Δ*teaC* (SYH21) strains. Strains were grown on MM glucose agar plates for 2 days. (B) Hyphae of wild-type, Δ*teaA*, and Δ*teaC* strains were grown for 1 day on microscope slides coated with MM with 2% glucose and 0.8% agarose. Images were taken with differential interference contrast. Hyphae are 3 to 4 μm in diameter. (C) Z-stack image of wild-type (TN02A3) and Δ*teaC* (SYH21) strains grown on MM with 2% glucose for 1 day and stained with calcofluor white. (D) Z-stack image of wild-type (TN02A3) and Δ*teaC* (SYH21) strains grown on glucose MM and stained with calcofluor white and Hoechst 33343. The arrow points to a short, anucleate hyphal compartment. Hyphae are 3 to 4 μm in diameter. (E) Quantification of the effect of different gene deletions on second germ tube formation. Conidia of each strain were germinated in MM with glucose and analyzed for the emergence of the second germ tube. For each strain, 100 germlings were counted. WT, wild type.

structed previously (31). Both strains produced compact and small colonies (75 to 85% of the diameter) compared to the wild type. The growth defect was slightly more severe in the Δ*teaA* deletion strain (Fig. 2A). In both strains hyphae displayed a zig-zag growth phenotype compared to straight hyphae in the wild type (Fig. 2B). The effect on the maintenance
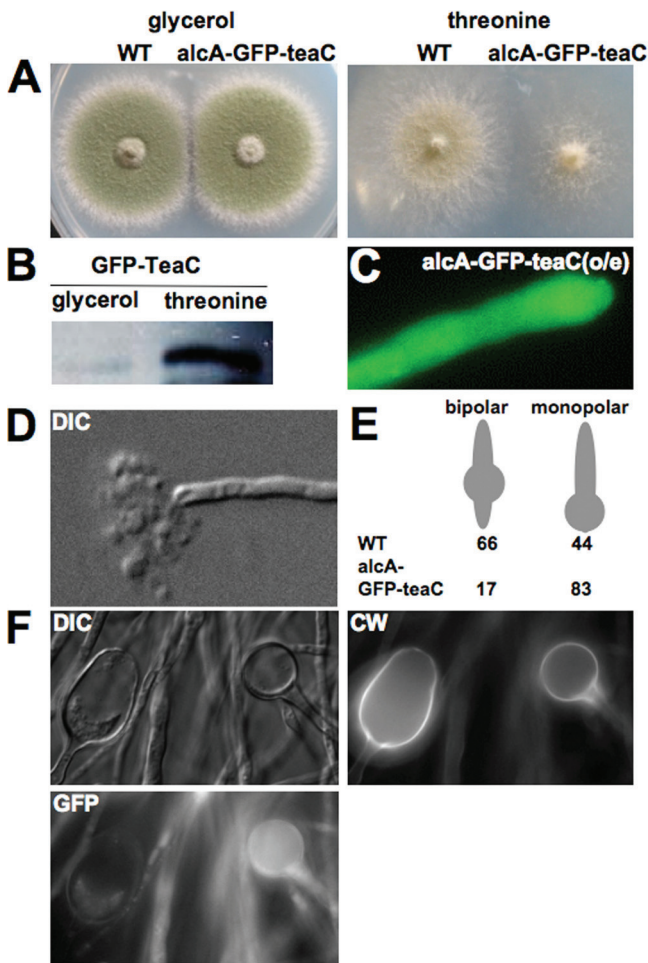
FIG. 3. Effect of overexpression of *teaC*. (A) Comparison of colonies of SYH03 [*alcA(p)-GFP-teaC*] and wild-type strains on glycerol- or threonine-containing medium after 4 days of growth at 37°C. (B) Western blot of hyphae of SYH03 grown on MM with glycerol or threonine as a carbon source. Portions (10 μg) of total protein extract were loaded onto the gel and processed for the Western blot as described in Materials and Methods. (C) Fluorescence microscopic picture of a hypha of SYH03 after induction with threonine for 1 day. (D) Germinated conidia of SYH03 grown on MM with threonine as a carbon source for 48 h observed using differential interference contrast. The hyphal tip had lysed. (E) Quantification of the effect of *teaC* overexpression on the emergence of the second germ tube. For each strain, 100 germlings were counted. (F) Germinated conidia of SYH03 grown on MM with threonine as carbon source for 48 h observed using differential interference contrast, stained with calcofluor white (CW), or observed in the GFP channel. WT, wild type; DIC, differential interference contrast.

of growth directionality was also stronger in the Δ*teaA* strain. The mutant phenotype was mainly seen in germlings.

The Δ*teaC* mutants also showed an increased number of septa and branches, probably due to the reduced extension rate of the hyphae and not specific for the *teaC* deletion (Fig. 2C and see Fig. S2 in the supplemental material). In addition, we noticed some small compartments (5 μm; 8% [*n* = 100]), which did not contain any nucleus (Fig. 2D). This did not occur in the wild type or in slower-growing *A. nidulans* strains.

Another polarity defect has been detected in the way the second germ tube emerges from a conidiospore. In the wild type, the second hypha emerges opposite to the first germ tube (bipolar) in 83% of the spores. In contrast, the second hyphae emerged at random positions in 56% of the spores in the Δ*teaC* mutant strain. A similar defect was observed in 55% of the spores in the Δ*teaA* mutant (*n* = 100) (Fig. 2E). This suggests that *teaA* and *teaC* are required for the selection of the site of polarity initiation.

Overexpression of TeaC inhibits septum formation. We next tested whether overexpression of TeaC would also cause any morphological phenotype. We expressed *teaC* using the control of the *alcA* promoter under inducing conditions (threonine; see Materials and Methods). When the GFP-TeaC strain was grown on threonine MM colonies appeared smaller than the ones from wild type (Fig. 3A). The high expression level of TeaC was shown by Western blotting and an increase in GFP fluorescence (Fig. 3B and C; see also below). Under inducing conditions, we often observed lysis at the hyphal tips (Fig. 3D) and rarely branching of hyphae. Furthermore, the number of conidia that produced a second germ tube was reduced from 66% to 17% (*n* = 100) (Fig. 3E). Some conidia without a second germ tube grew continuously isotropic up to 20 μm in diameter after 2 days. Some hyphae appeared to be empty, probably because of leakage of the cytoplasm. This was visualized by calcofluor white staining of the cell wall and GFP staining of the cytoplasm. Whereas the spore on the right side in Fig. 3F showed fluorescence in both channels, the left spore showed only fluorescence of the cell wall, indicating an empty spore.

When we analyzed the number of septa, we found that *teaC* overexpression repressed almost completely septation (Fig. 4A). Because TeaC interacts with SepA and possibly regulates the localization and/or the activity (see below), we sought to determine which phenotype would be caused by overexpression of TeaC, together with the overexpression of SepA. The displayed phenotype was similar to the phenotype of *teaC* overexpression, namely, very few septa (Fig. 4B and C). In addition, conidia were swollen, hyphae had an irregular shape, and hyphal tips appeared very large. To quantify this effect, we counted the number of septa in germlings, which were between 100 and 300 μm in length (*n* = 50) (Fig. 4C). Overexpression of SepA alone did not cause a reduction of the number of septa, and the morphology was less severely affected (data not shown).

Localization of TeaC at the hyphal tip depends on microtubules (MTs) but not on the kinesin KipA. To investigate the subcellular localization of TeaC, we constructed an *A. nidulans* strain expressing a GFP-TeaC fusion protein under the control of the *alcA* promoter (see above and Materials and Methods). The construct was transformed into strain TN02A3, and a transformant was selected in which the construct was integrated into the *teaC* locus (SYH03). This leads to duplication of the 5′ end of the gene under the control of the endogenous promoter and the *GFP-teaC* fusion construct under the control of the *alcA* promoter. Under repressing conditions, the strain displayed the Δ*teaC* deletion phenotype (see above). Under derepressed conditions, wild-type hyphal morphology was obtained. This experiment showed that the observed phenotypes in the Δ*teaC* deletion strain were indeed caused by the deletion and not by another mutation, and it showed that the GFP-TeaC fusion protein was functional. GFP-TeaC localized to

FIG. 5. TeaC localization. (A) Hyphae of strain SYH03 [*alcA(p)-GFP-teaC*] grown on MM with glycerol as a carbon source. The upper row shows differential interference contrast (DIC) pictures; the lower row shows same hyphae in the GFP channel. GFP-TeaC localized to one point in the hyphal apex (enlarged in the inset), at the branching site, and at the septa. (B) Localization of TeaC (GFP) and the Spitzenkörper (visualized with FM4-64). (C) mRFP1-TeaC expressed under the control of the native promoter (SYH17). Fluorescence signals were observed at the hyphal tip and new branches and at the septa. Hyphae are 3 to 4 μm in diameter.

FIG. 4. Effect of overexpression of *teaC* on septation. (A) Strains SYH17 [*teaC(p)-mRFP1-teaC*] (WT) and SYH03 [*alcA(p)-GFP-teaC*] grown on threonine MM and stained with calcofluor white. The red arrows point to the stained septa. Hyphae are 3 to 4 μm in diameter. (B) Strain SYH26 [*alcA(p)-GFP-sepA* and *alcA(p)-mRFP1-teaC*] grown on MM with threonine as carbon source for 48 h and stained with calcofluor white. The ringlike structure is a small branch observed from the top. (C) Quantification of the number of septa in strains SYH17 (considered as the wild type), SYH03, SNT28 [*alcA(p)-GFP-sepA*], and SYH26 grown in threonine MM. A total of 50 germlings were counted for each strain. WT, wild type; CW, calcofluor white.

one bright point at all hyphal tips and at newly forming septa (Fig. 5A). In addition, some weaker points on the side of the tip were observed. The GFP-TeaC points always localized close to the plasma membrane or appeared attached to it. Furthermore, some spots appeared in the cytoplasm, which could represent the MT plus ends (see also Fig. 6A).

In growing tips, the Spitzenkörper has an important role as vesicle supply center. To compare the localization of TeaC with the Spitzenkörper, we stained hyphae with FM4-64, which has been used in several fungi to stain the Spitzenkörper (9, 23, 31). The Spitzenkörper appeared to colocalize with GFP-TeaC (Fig. 5B), although from these pictures it was not unambiguously clear whether TeaC is part of the Spitzenkörper or only attached to the membrane and therefore very close to the Spitzenkörper.

To confirm TeaC localization and to prove that the observed localization was not an artifact of the expression under *alcA*

promoter control, we constructed a strain (SYH17) producing mRFP1-TeaC under the control of the native promoter. SYH17, in which mRFP1-TeaC is the only source of TeaC, did not show the phenotype observed in the Δ*teaC* mutant, indicating that mRFP1-TeaC at this expression level was also biologically functional. Although signals of mRFP1 appeared much weaker, mRFP1-TeaC still localized to one point, and weaker signals were observed along the apex and at forming septa (Fig. 5C). The single spot of mRFP1-TeaC normally localized at the center of the hyphal apex (Table 3). At a small number of tips (13%, $n = 100$), mRFP1-TeaC localized along the tip membrane. For further experiments, we normally used strains producing mRFP1-TeaC under the native promoter, when we analyzed the localization of TeaC.

To test whether TeaC localization at the hyphal tip depends on MTs, we studied a strain with GFP-labeled α-tubulin and mRFP1-TeaC (SYH22) and found that TeaC localized to the plus end of the MTs, although the signal intensity was close to the detection limit (Fig. 6A). Next, we used the MT-destabilizing drug benomyl. After this treatment (2.5 μg of benomyl/ml), almost all fluorescence of GFP-MTs was diffused into the cytoplasm within 5 min (data not shown), and the mRFP1-TeaC point at the tips was sometimes divided into several points and disappeared after 30 to 40 min from >80% of the tips ($n = 100$) (Fig. 6B and Table 3). The delay between the disappearance of the TeaC spot and the disassembly of the MTs suggests that TeaC is rather stable at the cortex.
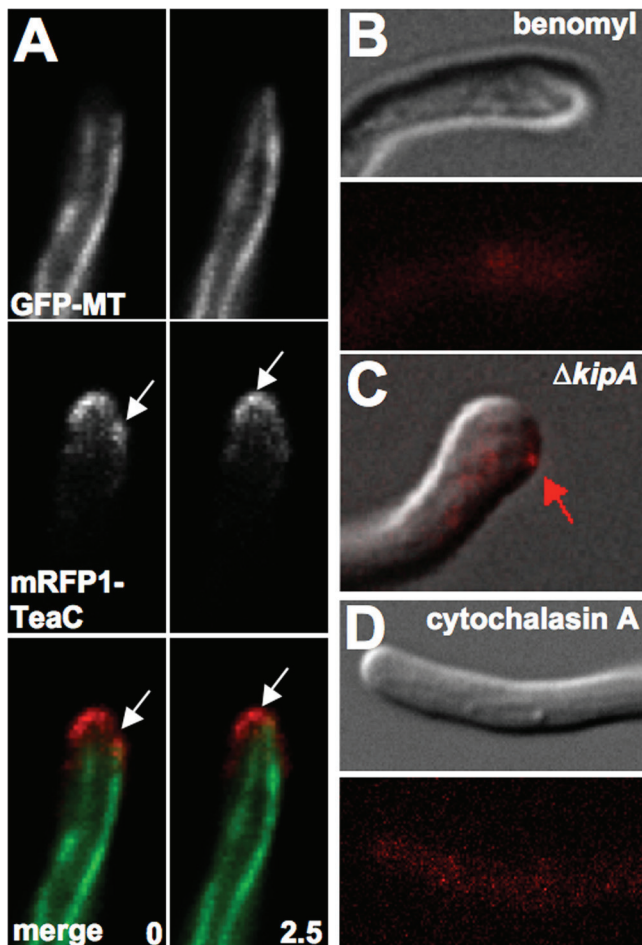
FIG. 6. Relationship between TeaC and MTs. (A) Observation of GFP-labeled MTs and mRFP1-labeled TeaC (SYH22). The arrows point to the MT plus ends. The same hyphae was observed at time zero and after 2.5 s, as indicated in the images. (B) Effect of benomyl on the localization of TeaC in strain SYH22 [*teaC(p)-mRFP1-teaC*]. *A. nidulans* was grown in MM with glycerol for 1 day and then shifted to medium containing 2.5 μg of benomyl/ml for 30 min. (C) In the Δ*kipA* mutant SYH25 TeaC moved away from the center of the apex to the side of the tip (arrow). (D) Effect of cytochalasin A on TeaC localization. SYH17 was grown in MM with glycerol for 1 day and shifted to medium containing 2 μg of cytochalasin A/ml for 2 min. Hyphae are 3 to 4 μm in diameter.

To analyze whether TeaC is transported in a kinesin-7-dependent way to the MT plus end, we studied TeaC localization in a Δ*kipA* mutant. mRFP1-TeaC still localized to one point at nearly 80% of the tips ($n = 100$), indicating KipA-independent polarization. However, the mRFP1-TeaC point did not localize to the center of the apex and moved away to the side of the hypha (Fig. 6C and Table 3). We further studied this effect by localization of TeaC in a KipA[rigor] mutant, in which KipA (fused to GFP) harbors a point mutation in the ATP-binding domain (16, 38). GFP-KipA[rigor] binds but does not move along MTs, and thus decorates them. In this strain (SYH23) mRFP1-TeaC still localized at 90% of the tips, but the mRFP1-TeaA point often moved away to the side of the apex and sometimes divided into two points (Table 3). These results indicate that TeaC can be transported independently of KipA to the tip and

that other KipA-transported proteins are probably required for exact positioning of TeaC. We are assuming that the key for further understanding of the cell end marker protein complex lies in the characterization of cargoes of the KipA motor protein.

We investigated also the effect of cytochalasin A (2 μg/ml), an inhibitor of actin polymerization, on TeaC localization. mRFP1-TeaC dispersed around the tips within 50% of the tips ($n = 100$) by 2 to 10 min after the treatment (Fig. 6D and Table 3) compared to the control strain only treated with 0.02% dimethyl sulfoxide. Taken together, our results suggest that TeaC localization depends on the MT and the actin cytoskeleton.

TeaC connects TeaA and SepA. To investigate whether *A. nidulans* TeaC colocalizes with TeaA, we constructed a strain (SYH13) expressing mRFP1-TeaA and GFP-TeaC and compared their localization patterns. The mRFP1-TeaA point at the apex colocalized with that of GFP-TeaC. If mRFP1-TeaA localized at two points (10%, $n = 100$) TeaC also colocalized to the same spots (Fig. 7A). Likewise, we tested colocalization of TeaC with SepA. We constructed a strain (SYH18) expressing GFP-SepA and *teaC(p)-mRFP1-teaC*. TeaC and SepA did not obviously colocalize at the hyphal apex. When SepA localized at the hyphal apex, TeaC appeared adjacent to the SepA signal (11%, $n = 100$). When TeaC localized at the hyphal apex at one point, SepA did not localize at the hyphal apex (89%, $n = 100$) (Fig. 7B).

We also found no obvious colocalization at septa (Fig. 7C). It appeared that TeaC surrounded SepA (Fig. 7C). While doing time course experiments, we found that SepA and TeaC follow a constricting ring but that TeaC constriction was slightly delayed in comparison to SepA (Fig. 7D and E).

Next, we sought to determine whether TeaA/TeaC and TeaC/SepA would interact. This was studied by BiFC. The N-terminal half of YFP (YFP[N]) was fused to SepA and TeaA, and the C-terminal half of YFP (YFP[C]) was tagged with TeaC. Strains expressing only YFP[N]-SepA, YFP[N]-TeaA, or YFP[C]-TeaC showed no YFP fluorescence. In contrast, in the strain expressing both YFP[N]-SepA and YFP[C]-TeaC produced YFP signals as a single point and along the apex and at hyphal septa

TABLE 3. Localization pattern of mRFP1-TeaC[a]

Category	mRFP1-TeaC localization pattern (%)				
Wild type	72	3	13	13	2
Wild type with benomyl	19	0	6	4	71
Δ*kipA* mutant	44	33	4	18	1
KipA[rigor] mutant	57	8	28	4	3
Wild type with cytochalasin A	25	5	7	13	50
Δ*teaA* mutant	0	4	0	2	94

[a] The localization pattern of mRFP1-TeaC of 100 to 200 hyphal tips was analyzed and grouped into six different categories. The construct was expressed from the *teaC* promoter. The numbers indicate the percentages of the hyphal tips of these groups. Hyphae were grown on minimal medium with glycerol as a carbon source for 1 day. For drug treatment, hyphae were incubated in the presence of 2.5 μg of benomyl/ml for 30 min or 2 μg of cytochalasin A/ml for 2 to 10 min.
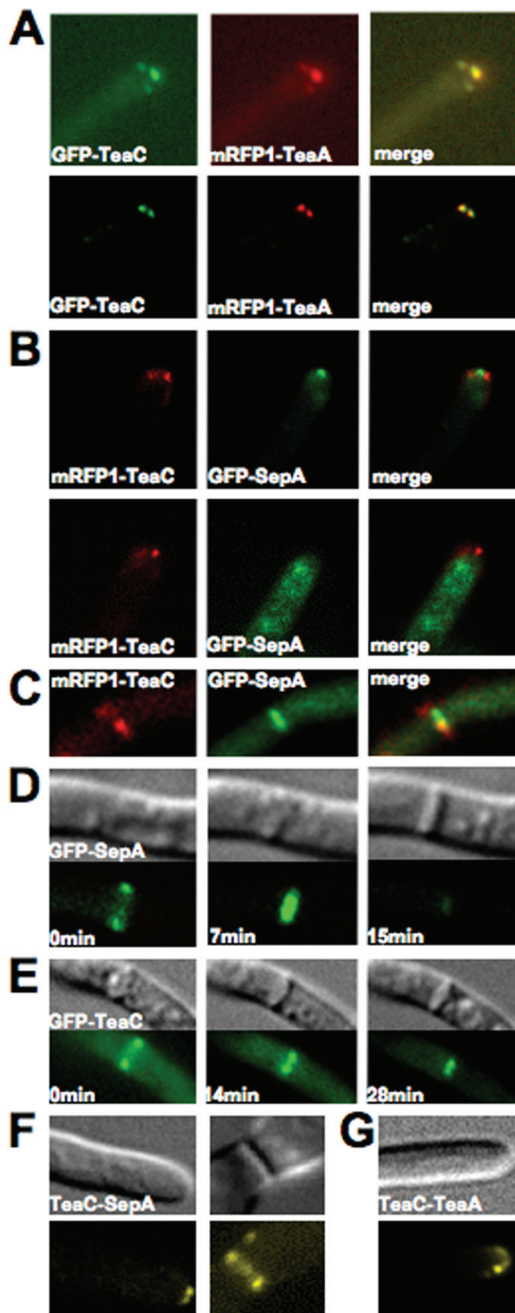
FIG. 7. Interaction of TeaC with TeaA and SepA. (A) Colocalization of TeaC and TeaA in strain SYH18; (B) visualization of TeaC and SepA in strain SYH13 at the hyphal tip; (C) partially colcalization of TeaC and SepA in strain SYH13 at the septa; (D) localization of SepA in strain SNT28; (E) localization of TeaC in strain SYH03; (F) interaction of TeaC with SepA (strain SYH05) shown in the bimolecular fluorescence complementation assay; (G) interaction of TeaC with TeaA (strain SYH06) shown in the bimolecular fluorescence complementation assay. Hyphae are 3 to 4 μm in diameter.

(Fig. 7F). In the case of the combination of YFP^N-TeaA and YFP^C-TeaC, YFP signals were detected only at the hyphal tip (Fig. 7G). We also tested YFP^N-TeaR (the membrane anchor protein) and YFP^C-TeaC interaction, but no YFP fluorescence was observed (data not shown). The observed interactions

were analyzed with the yeast-two hybrid system. TeaA showed self-interaction and interaction with TeaC. In both cases, the C termini of TeaA and TeaC were important for the interaction (Fig. 8). Interaction of TeaC and SepA could not be detected in this assay, because SepA alone already induced the expression of the yeast two hybrid reporters (data not shown).

Localization dependency of TeaC and TeaA. We analyzed TeaC localization in a Δ*teaA* mutant and found that the correct positioning of TeaC depends on TeaA (Fig. 9A and Table 3). In the absence of TeaA, TeaC appeared dispersed in the cytoplasm. We also analyzed TeaA localization in a Δ*teaC* mutant. mRFP1-tagged TeaA did not concentrate in one point in the apex but appeared as several points along the membrane (Fig. 9B).

DISCUSSION

Polarized growth of *A. nidulans* is achieved through a collaborative action of the MT and the actin cytoskeleton, in which cell end marker proteins regulate polarity maintenance through the putative conserved mechanism of *S. pombe* (8). In the present study, we analyzed another component of the *S. pombe* machinery, the SH3-domain protein Tea4, which is involved in the transmission of positional information through the interaction with both Tea1 and the formin For3 (18). We show here that in *A. nidulans* TeaC serves functions in polarized growth and in septation. The role of TeaC will be discussed in the light of recent findings for *S. pombe* Tea4 and the closest *S. cerevisiae* homologue Bud14 (4, 15).

Deletion of *teaC* caused a growth defect and zig-zag hyphal phenotype, similar to but not identical to the one of the *teaA* deletion mutant. Interaction studies revealed that TeaC interacted with TeaA and SepA at hyphal tips. These results suggest that the function of TeaC at the hyphal tips is comparable to the function of Tea4 in *S. pombe*, namely, the recruitment of SepA to the growth zone and hence the polarization of the actin cytoskeleton. However, TeaC and SepA did not obviously colocalize at the hyphal tips, although protein-protein interaction was found. This may be explained by the mechanism of actin polymerization by formin. In *S. pombe*, it was suggested that For3 is activated and promotes actin filament assembly at the cell cortex for only a few seconds, and then For3 is inactivated and released from the cortex by retrograde flow along actin filaments (17). In *S. cerevisiae* it was shown recently that Bud14 displaces the formin from growing barbed ends of actin cables (4). On the other hand, it can also be that SepA is very dynamic at the tip and the interaction with TeaC is only weak and transient.

The zig-zag hyphal phenotype in the *teaC*-deletion mutant was weaker than that in the *teaA* deletion mutant, suggesting that the contribution of TeaC to the function for polarity maintenance is lower than that of TeaA. TeaA probably serves additional functions. In fact, in *S. pombe*, Tea1 is necessary for the localization of Pom1, a DYRK-family protein kinase (33). Pom1 kinase interacts with Rga4, which plays a role as GAP for Cdc42, a regulator of F-actin (32).

Besides the action of TeaC at the hyphal tip, we discovered that the protein localized at the septa. Similar to the situation at the hyphal tip, BiFC analysis showed the interaction between TeaC and SepA at septa, but TeaC did not obviously
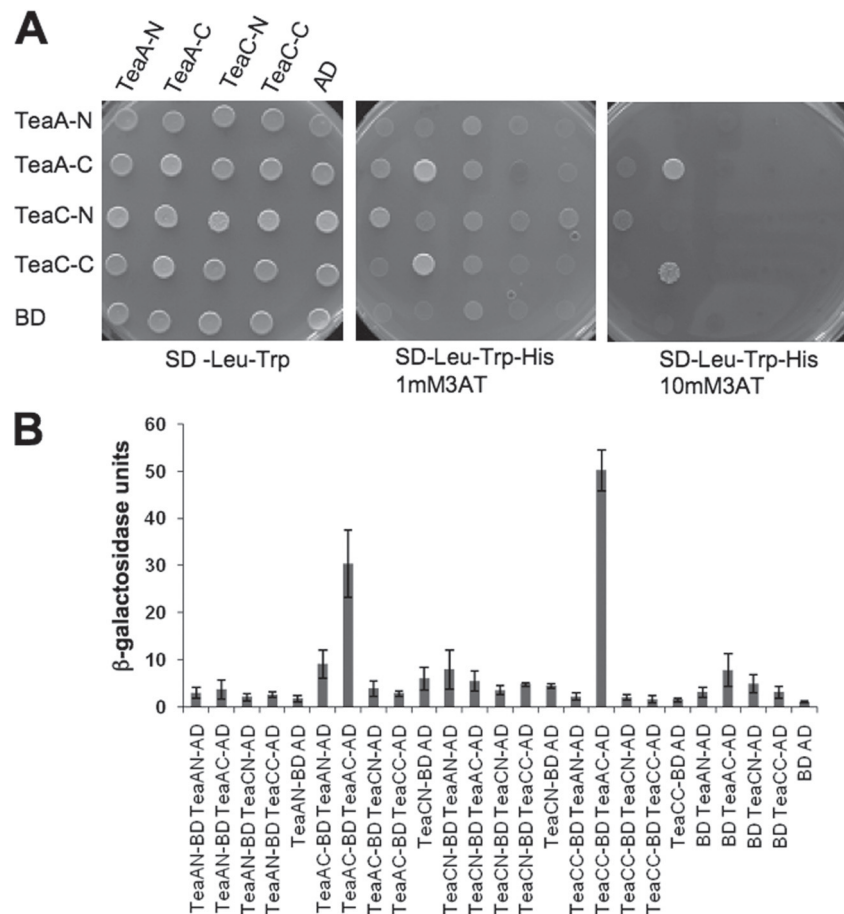
FIG. 8. Yeast two-hybrid assay to confirm the interactions described in Fig. 7. (A) Colonies of the yeast strains. The proteins indicated on the left side were fused to the binding domain (BD), and the proteins indicated above the picture were fused to the activation domain (AD). The mated yeasts were selected on SD−Leu−Trp plates and grown on SD medium (SD−Leu−Trp−His) supplemented with 1 mM or 10 mM 3AT (3-amino-1,2,4-triazole). (B) The β-galactosidase activity was analyzed from liquid cultures using ONPG as substrate and is expressed as Miller units. The data are expressed as the means of three independent experiments. The standard deviation is indicated.

colocalize with SepA. This may be explained again by the release of inactive formin from the plasma membrane at septation sites (17). The importance of TeaC at septa is also shown by our finding that overexpression of TeaC inhibits

FIG. 9. Localization dependency of TeaC and TeaA. (A) TeaC localization in the Δ*teaA* mutant (SYH19); (B) TeaA localization in the Δ*teaC* mutant (SYH24). Hyphae are 3 to 4 μm in diameter.

septation. However, in contrast to the role of SepA, TeaC appears not to be essential for septation, because deletion of *teaC* still allows normal septation (12a, 12b, 27a). There are several possibilities for how the inhibition effect can be explained. (i) Recently, it was shown that *S. cerevisiae* Bud14 negatively controls the activity of the formin Bni1 (4). If TeaC negatively controls SepA at septa, then overexpression would cause a reduction of the number of septa. Contradicting this idea is the finding that in *S. pombe* overexpression of Tea4 led to long actin cables (18). (ii) A large amount of TeaC protein in the cytoplasm could trap SepA in the cytoplasm and prevent specific localization at septation sites. In agreement with this hypothesis is the fact that we did not see any SepA-GFP rings when TeaC or TeaC and SepA were overexpressed and the germlings displayed in Fig. 4C observed in the GFP channel (data not shown). (iii) In *S. pombe*, the position of interphase nuclei determines the cleavage site through a protein called Mid1. Mid1 is a nuclear protein, which moves out of the nucleus upon phosphorylation and marks the cell cortex in the vicinity of the nucleus for septum formation (15, 21). Likewise, septation in *A. nidulans* depends on mitosis and the position of the nucleus (35, 36). However, as a difference to *S. pombe*,

septation does not follow every mitosis, with the result of multinucleate hyphal compartments (35). Given the importance of Mid1 for septum formation in *S. pombe*, we searched the *A. nidulans* genome for potential homologues but were unable to find one. Based on several examples, e.g., the cell end marker proteins are poorly conserved although they serve similar functions, we believe a Mid1 homologue could still exist in filamentous fungi. However, the activity of this postulated protein should be further regulated, because not all nuclear division planes are used for cytokinesis. TeaC might be involved in this selection by controlling the activity of a putative Mid1 homolgoue. Such a function for Tea4 has been shown recently as the mechanism for tip occlusion of septation in *S. pombe* (16). *teaC* deletion would thus impair site selection of septation. Indeed, we observed some short and empty compartments. Nevertheless, we did not find more septa close to the hyphal tip in *teaC* deletion strains, indicating that as-yet-unknown factors need to locally control the activity of a putative Mid1 homologue along the hyphae in addition to TeaC.

Another possibility to explain the role of TeaC in polarized growth and septation is the recruitment of other proteins involved in both processes. One candidate is the protein phosphatase 1 BimG, which is the *A. nidulans* homologue of *S. pombe* Dis2 and the *S. cerevisiae* homologue Glc7 (1, 10). This phosphatase localizes to different places in *A. nidulans*, among which is the membrane at growing tips and septa. The involvement in different processes, such as mitosis and hyphal growth, probably depends on several pathway-specific targets. Although there is evidence in *S. pombe* that Tea4 interacts with Dis2, and the localization pattern of TeaC at the septum resembles the pattern of BimG, the localization pattern of the two proteins at the tip looks different. Whereas BimG localizes along the membrane and excludes the very tip, TeaC appears to be restricted to the very tip. Therefore, a direct link to TeaC remains to be shown.

ACKNOWLEDGMENTS

REFERENCES

1. **Alvarez-Tabarés, I., A. Grallert, J. M. Ortiz, and I. M. Hagan.** 2007. *Schizosaccharomyces pombe* protein phosphatase 1 in mitosis, endocytosis and a partnership with Wsh3/Tea4 to control polarized growth. J. Cell Sci. **120:**3589–3601.
2. **Basu, R., and F. Chang.** 2007. Shaping the actin cytoskeleton using microtubule tips. Curr. Opin. Cell Biol. **19:**1–7.
3. **Browning, H., D. D. Hackney, and P. Nurse.** 2003. Targeted movement of cell end factors in fission yeast. Nat. Cell Biol. **5:**812–818.
4. **Chesarone, M., C. J. Gould, J. B. Moseley, and B. L. Goode.** 2009. Displacement of formins from growing barbed ends by Bud14 is critical for actin cable architecture and function. Dev. Cell **16:**202–302.
5. **Efimov, V., J. Zhang, and X. Xiang.** 2006. CLIP-170 homologue and NUDE play overlapping roles in NUDF localization in *Aspergillus nidulans*. Mol. Biol. Cell **17:**2021–2034.
6. **Enke, C., N. Zekert, D. Veith, C. Schaaf, S. Konzack, and R. Fischer.** 2007. *Aspergillus nidulans* Dis1/XMAP215 protein AlpA localizes to spindle pole bodies and microtubule plus ends and contributes to growth directionality. Eukaryot. Cell **6:**555–562.
7. **Feierbach, G., F. Verde, and F. Chang.** 2004. Regulation of a formin complex by the microtubule plus end protein tea1p. J. Cell Biol. **165:**697–707.
8. **Fischer, R., N. Zekert, and N. Takeshita.** 2008. Polarized growth in fungi: interplay between the cytoskeleton, positional markers, and membrane domains. Mol. Microbiol. **68:**813–826.
9. **Fischer-Parton, S., R. M. Parton, P. C. Hickey, J. Dijksterhuis, H. A. Atkin-son, and N. D. Read.** 2000. Confocal microscopy of FM4-64 as a tool for analyzing endocytosis and vesicle trafficking in living fungal hyphae. J. Microsc. **198:**246–259.
10. **Fox, H., P. C. Hickey, J. M. Fernández-Ábalos, P. Lunness, N. D. Read, and J. H. Doonan.** 2002. Dynamic distribution of BIMG[PP1] in living hyphae of *Aspergillus* indicates a novel role in septum formation. Mol. Microbiol. **45:**1219–1230.
11. **Galagan, J. E., S. E. Calvo, C. Cuomo, L.-J. Ma, J. R. Wortman, S. Batzoglou, S.-I. Lee, M. Bastürkmen, C. C. Spevak, J. Clutterbuck, V. Kapitonov, J. Jurka, C. Scazzocchio, M. Farman, J. Butler, S. Purcell, S. Harris, G. H. Braus, O. Draht, S. Busch, C. d'Enfert, C. Bouchier, G. H. Goldman, D. Bell-Pedersen, S. Griffiths-Jones, J. H. Doonan, J. Yu, K. Vienken, A. Pain, M. Freitag, E. U. Selker, D. B. Archer, M. A. Peñalva, B. R. Oakley, M. Momany, T. Tanaka, T. Kumagai, K. Asai, M. Machida, W. C. Nierman, D. W. Denning, M. Caddick, M. Hynes, M. Paoletti, R. Fischer, B. Miller, P. Dyer, M. S. Sachs, S. A. Osmani, and B. W. Birren.** 2005. Sequencing of *Aspergillus nidulans* and comparative analysis with *A. fumigatus* and *A. oryzae*. Nature **438:**1105–1115.
12. **Harris, S. D., N. D. Read, R. W. Roberson, B. Shaw, S. Seiler, M. Plamann, and M. Momany.** 2005. Polarisome meets Spitzenkörper: microscopy, genetics, and genomics converge. Eukaryot. Cell **4:**225–229.
12a. **Harris, S. D., L. Hamer, K. E. Sharpless, and J. E. Hamer.** 1997. The *Aspergillus nidulans sepA* gene encodes an FH1/2 protein involved in cytokinesis and the maintenance of cellular polarity. EMBO J. **16:**3474–3483.
12b. **Harris, S. D., J. L. Morrell, and J. E. Hamer.** 1994. Identification and characterization of *Aspergillus nidulans* mutants defective in cytokinesis. Genetics **136:**517–532.
13. **Hill, T. W., and E. Käfer.** 2001. Improved protocols for *Aspergillus* minimal medium: trace element and minimal medium salt stock solutions. Fungal Genet. Newsl. **48:**20–21.
14. **Horio, T., and B. R. Oakley.** 2005. The role of microtubules in rapid hyphal tip growth of *Aspergillus nidulans*. Mol. Biol. Cell **16:**918–926.
15. **Huang, Y., T. G. Chew, W. Ge, and M. K. Balasubramanian.** 2007. Polarity determinants Tea1p, Tea4p, and Pom1p inhibit division-septum assembly at cell end in fission yeast. Dev. Cell **12:**987–996.
16. **Konzack, S., P. Rischitor, C. Enke, and R. Fischer.** 2005. The role of the kinesin motor KipA in microtubule organization and polarized growth of *Aspergillus nidulans*. Mol. Biol. Cell **16:**497–506.
17. **Martin, S. G., and F. Chang.** 2006. Dynamics of the formin for3p in actin cable assembly. Curr. Biol. **16:**1161–1170.
18. **Martin, S. G., W. H. McDonald, J. R. r. Yates, and F. Chang.** 2005. Tea4p links microtubule plus ends with the formin for3p in the establishment of cell polarity. Dev. Cell **8:**479–491.
19. **Mata, J., and P. Nurse.** 1997. tea1 and the microtubular cytoskeleton are important for generating global spatial order within the fission yeast cell. Cell **89:**939–949.
20. **Miller, J. H.** 1972. Experiments in molecular genetics. Cold Spring Harbor Laboratory Press, Cold Spring Harbor, NY.
21. **Motegi, F., M. Mishra, M. K. Balasubramanian, and I. Mabuchi.** 2004. Myosin-II reorganization during mitosis is controlled temporally by its dephosphorylation and spatially by Mid1 in fission yeast. J. Cell Biol. **265:**685–695.
22. **Nayak, T., E. Szewczyk, C. E. Oakley, A. Osmani, L. Ukil, S. L. Murray, M. J. Hynes, S. A. Osmani, and B. R. Oakley.** 2006. A versatile and efficient gene targeting system for *Aspergillus nidulans*. Genetics **172:**1557–1566.
23. **Peñalva, M. A.** 2005. Tracing the endocytic pathway of *Aspergillus nidulans* with FM4-64. Fungal Genet. Biol. **42:**963–975.
24. **Riquelme, M., S. Bartnicki-Garcia, J. M. González-Prieto, E. Sánchez-León, J. A. Verdín-Ramos, A. Beltrán-Aguilar, and M. Freitag.** 2007. Spitzenkorper localization and intracellular traffic of green fluorescent protein-labeled CHS-3 and CHS-6 chitin synthases in living hyphae of *Neurospora crassa*. Eukaryot. Cell **6:**1853–1864.
25. **Riquelme, M., C. G. Reynaga-Peña, G. Gierz, and S. Bartnicki-García.** 1998. What determines growth direction in fungal hyphae? Fungal Genet. Biol. **24:**101–109.
26. **Sambrook, J., and D. W. Russell.** 1999. Molecular cloning: a laboratory manual. Cold Spring Harbor Laboratory Press, Cold Spring Harbor, NY.
27. **Sampson, K., and I. B. Heath.** 2005. The dynamic behavior of microtubules and their contributions to hyphal tip growth in *Aspergillus nidulans*. Microbiology **151:**1543–1555.
27a. **Sharpless, K. E., and S. D. Harris.** 2002. Functional characterization and localization of the *Aspergillus nidulans*. forming SEPA. Mol. Biol. Cell **13:**469–479.
28. **Snaith, H. A., and K. E. Sawin.** 2003. Fission yeast mod5p regulates polarized growth through anchoring of tea1p at cell tips. Nature **423:**647–651.
29. **Snell, V., and P. Nurse.** 1994. Genetic analysis of cell morphogenesis in fission yeast: a role for casein kinase II in the establishment of polarized growth. EMBO J. **13:**2066–2074.
30. **Stringer, M. A., R. A. Dean, T. C. Sewall, and W. E. Timberlake.** 1991. Rodletless, a new *Aspergillus* developmental mutant induced by directed gene inactivation. Genes Dev. **5:**1161–1171.
30a. **Taheri-Talesh, N., T. Horio, L. Araujo-Bazan, X. Dou, E. A. Espeso, M. A.**

Penalva, A. Osmani, and B. R. Oakley. 2008. The tip growth apparatus of *Aspergillus nidulans*. Mol. Biol. Cell **19:**1439–1449.

31. Takeshita, N., Y. Higashitsuji, S. Konzack, and R. Fischer. 2008. Apical sterol-rich membranes are essential for localizing cell end markers that determine growth directionality in the filamentous fungus *Aspergillus nidulans*. Mol. Biol. Cell **19:**339–351.

32. Tatebe, H., K. Nakano, R. Maximo, and K. Shiozaki. 2008. Pom1 DYRK regulates localization of the Rga4 GAP to ensure bipolar activation of Cdc42 in fission yeast. Curr. Biol. **18:**322–330.

33. Tatebe, H., K. Shimada, S. Uzawa, S. Morigasaki, and K. Shiozaki. 2005. Wsh3/Tea4 is a novel cell-end factor essential for bipolar distribution of Tea1 and protects cell polarity under environmental stress in *Schizosaccharomyces pombe*. Curr. Biol. **15:**1006–1015.

34. Veith, D., N. Scherr, V. P. Efimov, and R. Fischer. 2005. Role of the spindle-pole body protein ApsB and the cortex protein ApsA in microtubule organization and nuclear migration in *Aspergillus nidulans*. J. Cell Sci. **118:**3705–3716.

35. Wolkow, T. D., S. D. Harris, and J. E. Hamer. 1996. Cytokinesis in *Aspergillus nidulans* is controlled by cell size, nuclear positioning and mitosis. J. Cell Sci. **109:**2179–2188.

36. Xiang, X., S. M. Beckwith, and N. R. Morris. 1994. Cytoplasmic dynein is involved in nuclear migration in *Aspergillus nidulans*. Proc. Natl. Acad. Sci. USA **91:**2100–2104.

37. Yelton, M. M., J. E. Hamer, and W. E. Timberlake. 1984. Transformation of *Aspergillus nidulans* by using a trpC plasmid. Proc. Natl. Acad. Sci. USA **81:**1470–1474.

38. Zekert, N., and R. Fischer. 2009. The *Aspergillus nidulans* kinesin-3 UncA motor moves vesicles along a subpopulation of microtubules. Mol. Biol. Cell **20:**673–684.

Apical Sterol-rich Membranes Are Essential for Localizing Cell End Markers That Determine Growth Directionality in the Filamentous Fungus *Aspergillus nidulans*

Norio Takeshita, Yuhei Higashitsuji, Sven Konzack, and Reinhard Fischer

Applied Microbiology, University of Karlsruhe, D-76187 Karlsruhe, Germany

In filamentous fungi, hyphal extension depends on the continuous delivery of vesicles to the growing tip. Here, we describe the identification of two cell end marker proteins, TeaA and TeaR, in *Aspergillus nidulans*, corresponding to Tea1 and Mod5 in *Schizosaccharomyces pombe*. Deletion of *teaA* or *teaR* caused zig-zag-growing and meandering hyphae, respectively. The Kelch-repeat protein TeaA, the putatively prenylated TeaR protein, and the formin SepA were highly concentrated in the Spitzenkörper, a vesicle transit station at the tip, and localized along the tip membrane. TeaA localization at tips depended on microtubules, and TeaA was required for microtuble convergence in the hyphal apex. The CENP-E family kinesin KipA was necessary for proper localization of TeaA and TeaR, but not for their transportation. TeaA and TeaR localization were interdependent. TeaA interacted in vivo with TeaR, and TeaA colocalized with SepA. Sterol-rich membrane domains localized at the tip in *teaA* and *teaR* mutants like in wild type, and filipin treatment caused mislocalization of both proteins. This suggests that sterol-rich membrane domains determine cell end factor destinations and thereby polarized growth.

INTRODUCTION

The generation of asymmetry and polarization of cells is important in all kingdoms, and their molecular mechanisms are studied in different organisms. The diversity of cell shapes and functions suggests the development of different ways to generate and maintain polarity. However, it turns out that core mechanisms are conserved and that they may include the localized assembly of signaling complexes, the rearrangement of the cytoskeleton, the mobilization of proteins from intracellular pools, and the targeted vesicle delivery to sites of membrane growth (Nelson, 2003). One important early step for the generation of asymmetry is the local deposition of so-called landmark proteins at the surface of a cell, which serve as initiation sites for the localized assembly of additional proteins and thereby as a key for the reorientation of the cytoskeleton. In eukaryotes, polarity establishment is well studied at the molecular level in *Saccharomyces cerevisiae* and *Schizosaccharomyces pombe* (Chang and Peter, 2003).

In *S. pombe*, a visual mutant screening for strains with bent and T-shaped cells instead of cigar-like, straight cells led to the identification of one crucial component, the Kelch-repeat protein Tea1 (Snell and Nurse, 1994; Mata and Nurse, 1997). This protein is transported along microtubules (MTs) to their plus ends by the CENP-E family kinesin Tea2, and it is delivered to the cell ends by the growing MTs (Browning *et al.*, 2000, 2003. At the pole, Tea1 is anchored at the membrane by a second landmark protein, Mod5, which itself is

prenylated, and through this lipid moiety it is attached to the membrane (Snaith and Sawin, 2003). Because Tea1 and Mod5 accumulate at the growing cell end, they were named cell end markers. Along with a number of additional components, a large protein complex is formed, which recruits the formin For3 (Martin and Chang, 2003). For3 is required for actin cable formation; thus, it is crucial for the orientation of the actin cytoskeleton toward the growing cell end (Martin and Chang, 2006). Actin cables are required for polarized secretion of vesicles and hence membrane enlargement and secretion of cell wall-synthesizing enzymes (Montegi *et al.*, 2001).

In *S. cerevisiae*, several membrane-associated landmark proteins, such as Bud8 or Bud9, were described, which are absent from the *S. pombe* proteome (Pringle *et al.*, 1995; Zahner *et al.*, 1996; Kang *et al.*, 2001). Associated to the landmark proteins in *S. cerevisiae*, and localized at the emerging bud, is a large protein complex named polarisome that consists of a scaffold protein, Spa2; several other proteins; and characteristically the formin Bni1 (Sheu *et al.*, 1998). The kelch-domain protein Tea1 is conserved in *S. cerevisiae* (Kel1), where it is involved in mating projection formation (Philips and Herskowitz, 1998). In contrast, Mod5 is absent from the budding yeast proteome (Philips and Herskowitz, 1998; Snaith and Sawin, 2003).

If the polarized deposition of landmark proteins represents the crucial step in marking the zone of growth, the question arises which molecules or factors guide the proteins to their destination. There is increasing evidence that different membrane compositions or organizations may be important marks for the polarization of cells. It is known that eukaryotic membranes are differentiated into different functional areas, named lipid rafts (Rothberg *et al.*, 1990; Rajendra and Simons, 2005). They can vary in their lipid composition, and one type is characterized by a high content of sterols and is also found in fungi (Alvarez *et al.*, 2007). It

has been shown recently that the polarization of the membrane contributes to polar growth in *Candida albicans* (Martin and Konopka, 2004), but a link between the protein complexes described above and such membrane microdomains is missing.

Polarized growth is the dominant growth form of filamentous fungi. In these organisms, a structure localized in the apical dome of the hyphae and involved in polarized growth has been known for a long time, and it is named the Spitzenkörper (Girbardt, 1957). It represents an accumulation of vesicles and it determines growth direction of fungal hyphae (Grove and Bracker, 1970; Riquelme *et al.*, 1998). The exact structure and organization are still not completely understood. However, it could be an organelle-like structure rather than only an accumulation of vesicles (Wright *et al.*, 2007). Indeed, actin filaments have been observed in freeze-substituted samples (Howard, 1981). Molecular analyses in *Ashbya gossypii* and *Aspergillus nidulans* revealed that polarisome components may be components of the Spitzenkörper (Sharpless and Harris, 2002; Knechtle *et al.*, 2003; Harris *et al.*, 2005). Conversely, Crampin *et al.* (2005) described the Spitzenkörper as a structure distinct from the polarisome in *C. albicans*. They describe several components typical for the *S. cerevisiae* polarisome, such as Spa2 and Bud6, localized to a cap-like structure close to the cytoplasmic membrane, whereas the formin Bni1 was localized to the Spitzenkörper. Spa2 and Bud6 orthologues, SpaA and BudA, respectively, were also studied in *A. nidulans* (Virag and Harris, 2006). Deletion of either had an effect on polarized growth, but whereas SpaA could be localized at the tip, overlapping with the Spitzenkörper, BudA was only detectable at septa, indicating a role during cytokinesis. Several other *S. cerevisiae* landmark proteins are missing in filamentous fungal proteomes (Harris and Momany, 2004). Orthologues of the *S. pombe* cell end markers and the associated machinery have not yet been studied in filamentous fungi, but genome analyses revealed that one crucial component, the prenylated Mod5 protein, was not conserved in any filamentous fungus (Snaith and Sawin, 2003).

Previously, we showed that the deletion of the CENP-E family kinesin KipA, corresponding to Tea2 in *S. pombe* caused meandering hyphae (Konzack *et al.*, 2005). Here, we show that a protein with a similar function as Mod5, named TeaR, does exist in *A. nidulans*, and we show that TeaR together with a Tea1 orthologue, TeaA is involved in the initiation of polarized growth and the maintenance of straight-growing hyphae. We studied the relationship between KipA, the two cell end markers, and the formin SepA. Interestingly, the polarized localization of TeaA and TeaR depends on sterol-rich membrane domains.

MATERIALS AND METHODS

Strains, Plasmids and Culture Conditions

Supplemented minimal (MM) and complete media (CM) for *A. nidulans* were prepared as described, and standard strain construction procedures are described by Hill and Käfer (2001). A list of *A. nidulans* strains used in this study is given in Table 1. Standard laboratory *Escherichia coli* strains (XL-1 blue, Top 10 F') were used. Plasmids are listed in Table 2.

Molecular Techniques

Standard DNA transformation procedures were used for *A. nidulans* (Yelton *et al.*, 1984) and *Escherichia coli* (Sambrook and Russel, 1999). For polymerase chain reaction (PCR) experiments, standard protocols were applied using a capillary Rapid Cycler (Idaho Technology, Idaho Falls, ID) for the reaction cycles. DNA sequencing was done commercially (MWG Biotech, Ebersberg, Germany). Genomic DNA was extracted from *A. nidulans* with the DNeasy Plant Mini kit (QIAGEN, Hilden, Germany). DNA analyses (Southern hybridizations) were performed as described by Sambrook and Russel (1999).

Deletion of teaA and teaR

teaA flanking regions were amplified by PCR using genomic DNA and the primers teaA1-linke-Fla-for (5'-GAGAAACGTCCATACTTCTG-3') and teaA2-linke-Fla-rev-SfiI1 (5'-TGGTGGCCATCTAGGCCCAGAAACATTG-CTTTC-3') for the upstream region of *teaA* and teaA3-rechte-Fla-for-SfiI2 (5'-AATAGGCCTGAGTGGCCAACAGTGCAGTGTCAC-3') and teaA4-rechte-Fla-rev (5'-CCATCTCTGGTTCGGCTTAC-3') for the downstream region, and they were cloned into pCR2.1-TOPO to generate pSK74 and pSK75, respectively. The SfiI restriction sites are underlined. In a three-fragment-ligation, the *argB*-gene from plasmid pSK70 was ligated between the two *teaA*-flanking regions, resulting in vector pSK76. The deletion cassette was amplified with the primers teaA-for-n (5'-GAAGAACCAGCAGACTTCTG-3') and teaA-rev-n (5'-CTGGTCTGCTGCTGAAATG-3'), and the resulting PCR product was transformed into the arginin-auxotrophic *A. nidulans* strain SRF200.

teaR flanking regions were amplified by PCR using genomic DNA and the primers teaR1-KpnI (5'-GGTACCAGATGGCTGTTGAAGTTGTC-3') and teaR2-BamHI (5'-GGATCCAGCGTCCAACAGAAGAATGT-3') for the upstream region of *teaR* and teaR3-NotI (5'-GCGGCCGCTACCTCTGCTATTG-CAAGTAT-3') and teaR4-XbaI (5'-TCTAGATCTTGCTGGCCTTGCAGTA-3') for the downstream region and cloned into pCR2.1-TOPO, to generate pNT12 and pNT13, respectively. The restriction sites are underlined. The two *teaR*-flanking regions were ligated in upstream and downstream of the *pyr4* marker in pNRSTE1, generating pNT14. This plasmid was cut with KpnI and XbaI, generating a fragment containing *pyr4* flanked by *teaR* sequences. This fragment was transformed into the uracil-auxotrophic SRF200.

Transformants were screened by PCR for the homologous integration event. Single integration of the construct was confirmed by Southern blotting (data not shown). One *teaA*- and one *teaR*-deletion strain were selected from the transformants and named SSK91 and SNT33, respectively. The coupling of the observed phenotypes with the gene-deletion events was confirmed by crosses, recomplementation with *tea*- or *teaR*-derived clones, and by down-regulation of the genes through the inducible *alcA* promoter (see below).

Tagging of Proteins with Green Fluorescent Protein (GFP) and Monomeric Red Fluorescent Protein (mRFP) 1

To create an N-terminal GFP fusion construct of TeaA, a 0.7-kb N-terminal fragment of *teaA* (starting from ATG) was amplified from genomic DNA, with the primers tea_Efi_for (5'-GGGGCGCGCCCATGGCGTTCCTCTTTAAAT-CAAAG-3') and tea_Efi_rev (5'-GGTTAATTAATTGGTATCACCGCCAAA-GACGA-3') and cloned into pCR2.1-TOPO, yielding pNT1. The restriction sites are underlined. The AscI–PacI fragment from pNT1 was subcloned into the corresponding sites of pCMB17apx, yielding pNT5. To create an N-terminal mRFP1 fusion construct of TeaA, the AscI-PacI fragment from pNT1 was subcloned into the corresponding sites of pDM8, yielding pNT6. To produce TeaA N-terminally tagged with mRFP1 under the native promoter, a 1.5-kb fragment of the *teaA* promoter was amplified from genomic DNA with the primers teaA-proEcoRI (5'-GGGAATTCACAAAGGCCAACAGGTGA-TC-3') and teaA-proKpnI (5'-GGGTACCCGTGAAATCTTATATCGTATAC-3'), digested with EcoRI and KpnI, and ligated with EcoRI-KpnI–digested pNT6, yielding pNT28 (*alcA* promoter replaced with the *teaA* promoter in pNT6). Using the same approach as for TeaA, N-terminal GFP fusion constructs of TeaR and SepA were created. The primer set used for TeaR was tear_Efi_for (5'-GGGGCGCGCCCATGGCGGGTACAGCTAC-3') and tear_Efi_rev (5'-GGTTA-ATTAAATACTTGATGTACTAGAACC-3'). The PCR fragment was cloned into pCR2.1-TOPO and subsequently into pCMB17apx, yielding plasmid pNT7. A 1.5-kb fragment of the *teaR* promoter was amplified with the primers teaR-proEcoRI (5'-GAATTCGGCTTGGCTATATGGTCTGG-3') and teaR-proKpnI (5'-GGTACCCAGCGTCCAACAGAAGAATG-3') and ligated into EcoRI-KpnI–digested pNT7, yielding pNT30 (*alcA* promoter replaced with the *teaR* promoter in pNT7). The primer set used for SepA was sepA_Efi_for (5'-GGGGCGCGCCCATGCCGACATCCGATAAAT-3') and sepA_Efi_rev (5'-GGTTAATTAACTATCCATGCGTCTCTCGA-3'). The PCR fragment was cloned into pCR2.1-TOPO and subsequently into pCMB17apx, yielding pNT9. All plasmids were transformed into the uracil-auxotrophic TN02A3 (Δ*nkuA*). The integration events were confirmed by PCR and Southern blotting (data not shown).

To introduce a point mutation in the TeaR CAAX motif, the *teaR*-open reading frame (ORF) was amplified with primers, tear_Efi_for (5'-GGGGCGCGCCCATGGCGGGTACAGCTAC-3') and teaR-full-c-mut (5'-TTAATTAATCACATCACGATGCCGCATC-3'). The point mutation site is underlined and in bold. The PCR fragment was cloned into pCR2.1-TOPO and subsequently into pCMB17apx, yielding pNT32 (cysteine in the CAAX motif was replaced by glycine). As a control, the *teaR*-ORF was amplified with primers teaR_Efi_for (5'-GGGGCGCGCCCATGGCGGGTACAGCTAC-3') and teaR-full-c (5'-TTAATTAATCACATCACGATGCAGCATC-3'), and cloned into pCR2.1-TOPO and subsequently into pCMB17apx, yielding pNT31. To create TeaR tagged with GFP at the C terminus, the *teaR*-ORF was amplified with primers TeaR-pENTR-for (5'-CACCATGGCGGGTACAGC-TACG-3') and TeaR-pENTR-rev (5'-CATCACGATGCAGCATCC-3'), and cloned into the pENTR/TOPO vector (Invitrogen, NV Leek, The Nether-

Table 1. *A. nidulans* strains used in this study

Strain	Genotype	Source
SRF200	*pyrG89; ΔargB::trpCΔB; pyroA4; veA1*	Karos and Fischer (1999)
TN02A3	*pyrG89; argB2, nkuA::argB; pyroA4*	Nayak *et al.* (2005)
GR5	*pyrG89; wA3; pyroA4; veA1*	Waring *et al.* (1989)
RMS011	*pabaA1, yA2; ΔargB::trpCΔB; veA1*	Stringer *et al.* (1991)
SRL1	*ΔkipA::pyr4; pyrG89; pyroA4; veA1 (ΔkipA)*	Konzack *et al.* (2005)
SSK13	*pabaA1; wa3; ΔkipA::pyr4; veA1 (ΔkipA)*	Konzack *et al.* (2005)
SSK44	*wa3; ΔargB::trpCΔB; ΔkipA::pyr4; veA1 (ΔkipA)*	Konzack *et al.* (2005)
SJW02	*wA3; pyroA4; ΔargB::trpCΔB; alcA(p)::GFP::tubA; veA1 (GFP-MTs)*	J. Warmbold (Marburg, Germany)
SSK91	SRF200 transformed with pSK76, *ΔteaA::argB; pyrG89; ΔargB::trpCΔB; pyroA4; veA1 (ΔteaA)*	Konzack *et al.* (2005)
SSK92	*pyrG89; wA3; pyroA4;; alcA(p)::GFP::kipA; veA1 (GFP-KipA)*	(Konzack *et al.* (2005)
SSK114	*pyrG89; wA3; pyroA4;; alcA(p)::GFP::kipA-rigor; veA1 (GFP-KipA-rigor)*	Konzack *et al.* (2005)
SNR1	*ΔkinA::pyr4; pyrG89; yA2; ΔargB::trpCΔB; pyroA4; (ΔkinA)*	Requena *et al.* (2001)
SNT30	SSK91 transformed with pI4 (*ΔteaA*)	This study
SNT33	SRF200 transformed with pNT14, *ΔteaA::argB; pyrG89; ΔargB::trpCΔB; pyroA4; veA1 (ΔteaR)*	This study
SNT34	SNT33 transformed with pI4 (*ΔteaR*)	This study
SNT35	SNT33 transformed with pDC1 (*ΔteaR*)	This study
SNT14	SSK44 crossed to SSK91 (*ΔkipA, ΔteaA*)	This study
SNT40	SRL1 crossed to SNT34 (*ΔkipA, ΔteaR*)	This study
SNT39	SNT30 crossed to SNT33 (*ΔteaA, ΔteaR*)	This study
SNT4	TN02A3 transformed with pNT5, (GFP-TeaA)	This study
SNT13	SNT4 crossed to RSM011, (GFP-TeaA)	This study
SNT5	TN02A3 transformed with pNT6, (mRFP1-TeaA)	This study
SNT15	SNT5 crossed to RSM011, (mRFP1-TeaA)	This study
SNT49	TN02A3 transformed with pNT28, (*teaA*(p)-mRFP1-TeaA)	This study
SNT52	SNT49 crossed to RSM011, (*teaA*(p)-mRFP1-TeaA)	This study
SNT26	TN02A3 transformed with pNT7, (GFP-TeaR)	This study
SNT55	TN02A3 transformed with pNT30, (*teaR*(p)-GFP-TeaR)	This study
SNT61	SNT33 transformed with pNT32 and pDC1, (*ΔteaR*, GFP-TeaR-CAAX-mutant)	This study
SNT60	SNT33 transformed with pNT31 and pDC1, (*ΔteaR*, GFP-TeaR)	This study
SNT46	SNT33 transformed with pNT21 (*ΔteaR*, TeaR-GFP)	This study
SNT21	SJW02 transformed with pDC1, (GFP-MTs)	This study
SNT22	SNT21 crossed to SNT15, (GFP-MTs, mRFP1-TeaA)	This study
SNT31	SNT30 crossed to SJW02, (GFP-MTs, *ΔteaA*)	This study
SNT23	SSK92 crossed to SNT15, (GFP-KipA, mRFP1-TeaA)	This study
SNT41	SRL1 crossed to SNT15, (*ΔkipA*, mRFP1-TeaA)	This study
SNT50	SSK44 crossed to SNT49, (*ΔkipA, teaA*(p)-mRFP1-TeaA)	This study
SNT17	SSK114 transformed with pI4, (GFP-KipA-rigor)	This study
SNT51	SNT17 crossed to SNT49, (GFP-KipA-rigor, *teaA*(p)-mRFP1-TeaA)	This study
SNT28	TN02A3 transformed with pNT9, (GFP-SepA)	This study
SNT57	SNT28 crossed to SNT52, (GFP-SepA, *teaA*(p)-mRFP1-TeaA)	This study
SNT56	SNT26 crossed to SNT52, (GFP-TeaR, *teaA*(p)-mRFP1-TeaA)	This study
SNT27	SNT15 crossed to SNT26, (GFP-TeaR, mRFP1-TeaA)	This study
SNT58	TN02A3 transformed with pNT29 and pYH03, (YFP[N]-SepA and *teaA*(p)-YFP[C]-TeaA)	This study
SNT59	TN02A3 transformed with pNT29 and pYH04, (YFP[N]-TeaR and *teaA*(p)-YFP[C]-TeaA)	This study
SYH05	TN02A3 transformed with pYH01 and pYH05, (YFP[N]-TeaA and YFP[C]-KipA)	This study
SYH06	TN02A3 transformed with pYH03 and pYH05, (YFP[N]-SepA and YFP[C]-KipA)	This study
SYH07	TN02A3 transformed with pYH04 and pYH05, (YFP[N]-TeaR and YFP[C]-KipA)	This study
SYH08	TN02A3 transformed with pYH04 and pYH14, (YFP[N]-TeaR and YFP[C]-SepA)	This study
SNT43	SNT26 crossed to SSK13, (GFP-TeaR, *ΔkipA*)	This study
SNT42	SNT13 crossed to SNT35, (GFP-TeaA, *ΔteaR*)	This study
SNT53	SNT49 crossed to SNT34, (*teaA*(p)-mRFP1-TeaA, *ΔteaR*)	This study
SNT32	SNT30 crossed to SNT26, (GFP-TeaR, *ΔteaA*)	This study
SNT62	SNR3 crossed to SNT52, (*ΔkinA, teaA*(p)-mRFP1-TeaA)	This study

lands), yielding pNT16. The fusion of TeaR with GFP at the C terminus was done with the GATEway cloning system and vector pMT-sGFP (Toews *et al.*, 2004), yielding pNT21.

For bimolecular fluorescence complementation (BiFC) analyses, the N-terminal half of yellow fluorescent protein (YFP[N]) or the C-terminal half of YFP (YFP[C]) was fused to the N terminus of the protein of interest. YFP[N] (154 amino acids of YFP and 5-amino acid linker) was amplified with primers fwd_Kpn_YFP-N (5′-CGGTACCATGGTGAGCAAGGGCGAGGAGCTG-3′) and rev_YFP-N_Li_Asc (5′-CGGCGCGCCCGTGGCGATGGAGCGCAT-GATATAGACGTTGTGGCTGTTGTAG-3′). YFP[C] (86 amino acids of YFP and 17-amino acid linker) was amplified with primers fwd_Kpn_YFP-C (5′-CGGTACCATGGCCGACAAGCAGAAGAACGGCATCAAGG-3′) and rev_YFP-C_Li_Asc (5′-CGGCGCGCCGTGGTTCATGACCTTCTGTTTCAGG-TCGTTCGGGATCTTGCAGGCCGGGCGCTTGTACAGCTCGTCCATGCCG-AGAGTGATCCC-3′). The KpnI–AscI fragment of YFP[N] or YFP[C] was li-

gated into KpnI- and AscI-digested pCMB17apx, yielding pDV7 (GFP replaced with YFP[N] in pCMB17apx) and pDV8 (GFP replaced with YFP[C] in pCMB17apx). To create an N-terminal YFP[C] fusion construct of TeaA, the AscI–PacI fragment from pNT1 was subcloned into the corresponding sites of pDV8, yielding pYH02. To produce TeaA N-terminally tagged with YFP[C] under the *teaA* native promoter, a 1.5-kb fragment of the *teaA* promoter was amplified from genomic DNA with the primers teaA-pro-EcoRI and teaA-proKpnI, digested with EcoRI and KpnI, and ligated with EcoRI-KpnI–digested pYH02, yielding pNT29 (*alcA* promoter replaced with the *teaA* promoter in pYH02). Using the same approach, *kipA* and *sepA* fragments from pSK82 (Konzack *et al.*, 2005) and pNT9 were subcloned into the corresponding sites of pDV8, yielding pYH05 and pYH14. To create N-terminal YFP[N] fusion constructs, *teaA*, *sepA*, and *teaR* fragments from pNT1, pNT9, and pNT7 were subcloned into the corresponding sites of pDV7, yielding pYH01, pYH03, and pYH04.

Table 2. Plasmids used in this study

Plasmid	Construction	Source
pCR2.1-TOPO	Cloning vector	Invitrogen
pENTR/D-TOPO	GATEway TOPO cloning vector	Invitrogen
pCMB17apx	*alcA(p)::GFP*, for N-terminal fusion of GFP to proteins of interest; contains *N. crassa pyr4*	V. Efimov (Piscataway, NJ)
pDM8	GFP replaced mRFP1 in pCMB17apx	Veith *et al.* (2005)
pSK70	*argB* with SfiI sites	Vienken and Fischer (2006)
pI4	*pyroA* from *A. nidulans*	Osmani *et al.* (1999)
pDC1	*argB* from *A. nidulans*	Aramayo *et al.* (1989)
pSK74	1 0.5-kb 5′-flanking region of *teaA* with SfiI site in pCR2.1-TOPO	This study
pSK75	1.0-kb 3′-flanking region of *teaA* with SfiI site in pCR2.1-TOPO	This study
pSK76	*teaA*-deletion construct: flanking regions from pSK74 and pSK75 ligated with *argB* from pSK70	This study
pNRSTE1	1.9-kb *pyr4* with flanking BamHI and NotI sites in pCR2.1-TOPO	Requena *et al.* (2001)
pNT12	1 0.0-kb 5′-flanking region of *teaR* with KpnI and BamHI sites in pCR2.1-TOPO	This study
pNT13	1 0.0-kb 3′-flanking region of *teaR* with NotI and XbaI sites in pCR2.1-TOPO	This study
pNT14	*teaR*-deletion construct: flanking regions from pNT12 and pNT13 ligated with *pyr4* from pNRSTE1	This study
pNT1	0.7-kb *teaA* fragment in pCR2.1-TOPO	This study
pNT5	0.7-kb *teaA* fragment from pNT1 in pCMB17apx	This study
pNT6	0.7-kb *teaA* fragment from pNT1 in pDM8	This study
pNT28	1.5-kb *teaA*(p) fragment in pNT6	This study
pNT7	0.7-kb *teaR* fragment in pCMB17apx	This study
pNT30	1.5-kb *teaR*(p) fragment in pNT7	This study
pNT9	1.2-kb *sepA* fragment in pCMB17apx	This study
pNT16	*TeaR*-ORF without stop-codon in pENTR/D-TOPO	This study
pMT-sGFP	GATEway Vector, *alcA(p)::cccD*-box (incl. *attR*-sites)::*sGFP*, *argB*	Toews *et al.* (2004)
pNT21	*alcA(p)::teaR-sGFP*, *argB*; *teaR* from pNT16 via GATEway in pMT-sGFP	This study
pNT31	*TeaR*-ORF in pCMB17apx	This study
pNT32	*TeaR*-ORF with point mutation at Cys in CAAX motif in pCMB17apx	This study
pDV7	GFP replaced N-terminal half of YFP in pCMB17apx	This study
pDV8	GFP replaced C-terminal half of YFP in pCMB17apx	This study
pYH01	0.7-kb *teaA* fragment from pNT1 in pDV7	This study
pYH02	0.7-kb *teaA* fragment from pNT1 in pDV8	This study
pNT29	1.5-kb *teaA*(p) fragment in pYH02	This study
pYH03	1.2-kb *sepA* fragment from pNT9 in pDV7	This study
pYH04	0.7-kb *teaR* fragment from pNT7 in pDV7	This study
pYH05	1.0-kb *kipA* fragment from pSK82 in pDV8	This study
pYH14	1.2-kb *sepA* fragment from pNT9 in pDV8	This study
pNT33	N-terminal half of *teaA* cDNA in pGADT7	This study
pNT34	N-terminal half of *teaA* cDNA in pGABKT7	This study
pNT35	C-terminal half of *teaA* cDNA in pGADT7	This study
pSH19	C-terminal half of *teaA* cDNA in pGABKT7	This study
pSH10	Full-length of *teaR* cDNA in pGADT7	This study
pSH12	N-terminal half of *sepA* cDNA in pGADT7	This study
pSH14	C-terminal half of *sepA* cDNA in pGADT7	This study

Yeast Two-Hybrid Analysis

The yeast two-hybrid analysis was performed using the MatchMaker3 Gal4 two-hybrid system (Clontech, Mountain View, CA). For bait generation, fragments of *teaA* cDNA corresponding to the N-terminal half of TeaA (1-674 amino acids [aa]) with primers TeaA_EFF (5′-GGCCGAATTCATGGCGTTCCTCTTTA-AATC-3′) and TeaA_BMR (5′-GGCCGGATCCTTAACAAGGCCTCCTGGTGG-3′) or C-terminal half of TeaA (661-1474 aa) with primers TeaA_EMF (5′-GGC-CGAATTCCCTCGCTCACCACGGTT-3′) and TeaA_BRR (5′-GGCCGGATCC-TTAGATCATATTCGCTGCCG-3′) was amplified and cloned in the pGBK7 vector, which contains the GAL4 DNA-BD and the *TRP1* marker, yielding pNT34 and pSH19 (Clontech). The fragments of *teaA* cDNA corresponding to the N-terminal half and C-terminal half of TeaA from pNT34 and pNT19, full-length *teaR* cDNA with primers TeaRF (5′-AAGCAGTGGTATCAACGCA-GAGTGGATGGCGGGTACAGCTACG-3′) and TeaRR (5′-TCTAGAGGC-CGAGGCGGCCGACATGTCACATCACGATGCAGCAT-3′), and fragments of *sepA* cDNA corresponding to the N terminus of SepA (1–700 aa) with primers SepA,N,SMART (5′-AAGCAGTGGTATCAACGCAGAGTGGAT-GCCGACATCCGATAAATCG-3′) and SepA,N,CDS (5′-TCTAGAGGC-CGAGGCGGCCGACATGCTCCTATCCATAGCCACATA-3′) and fragments of *sepA* cDNA corresponding to the C terminus of SepA (715-1790 aa) with primers SepA,C,SMART (5′-AAGCAGTGGTATCAACGCAGAGTG-GCAGAGCTTGTTAGATCGACTA-3′) and SepA,C,CDS (5′-TCTAGAGGC-CGAGGCGGCCGACATGAGCACCATCATCGGTATTGTC-3′) were amplified and cloned in the pGADT7 vector, which contains the GAL4 DNA-AD and the *LEU2* marker (Clontech), yielding pNT33, pNT35, pSH10, pSH12, and pSH14. pGBK7 associated plasmids were transformed in yeast Y187 (mating type *MATα*) and pGADT7 associated plasmids were transformed in yeast AH109 (mating type *MAT*a). The system uses two reporter genes (*HIS3* and *LacZ*) under the control of the GAL4-responsive UAS. β-Galactosidase activity was analyzed by liquid culture assay using *o*-nitrophenyl β-D-galactopyrano-side (ONPG) (Sigma Chemie, Deisenhofen, Germany) as substrate.

Light and Fluorescence Microscopy

For live-cell imaging of germlings and young hyphae, cells were grown on coverslips in 0.5 ml of MM + 2% glycerol (induction of the *alcA* promoter) or MM + 2% glucose (repression of the *alcA* promoter). Cells were incubated at room temperature for 1–2 d. For pictures of young hyphae of each gene deletion strain, the spores were inoculated on microscope slides coated with MM + 2% glucose + 0.8% agarose and grown at 30°C for 1 d. Images were captured at room temperature using an Axiophot microscope (Carl Zeiss, Jena, Germany). Images were collected and analyzed with the AxioVision system (Carl Zeiss).

N-[3-Triethylammoniumpropyl]-4-
[p-diethylaminophenylhexatrienyl] pyridinium dibromide
(FM4-64), Benomyl, Cytochalasin A, and Filipin
Treatment

FM4-64 was used at a concentration of 10 μM in the medium. Coverslips were incubated for 5 min and washed. Filipin (Sigma Chemie) was used at a final concentration of 1, 3, 5 μg/ml in medium from a stock solution of 10 mg/ml in methanol. Benomyl, methyl 1-(butylcarbamoyl)-2-benzimidazole carbamate (Aldrich Chemical, Milwaukee, WI), was used at a final concentration of 2.5 μg/ml in medium from a stock solution of 1 mg/ml in ethanol. Cytochalasin A (Sigma Chemie) was used at a final concentration of 2 μg/ml in medium from a stock solution of 100 mg/ml in dimethyl sulfoxide (DMSO).

RESULTS

Isolation of TeaA and TeaR

We searched the *A. nidulans* database for proteins with similarity to the cell end marker protein Tea1 from *S. pombe*, and we identified an open reading frame (AN4564.3) with 27% identity per 1037 amino acids and an e-value of 3e-78 to Tea1. We named the gene *teaA* (Figure 1A). DNA and cDNA sequences were confirmed, and three introns of 88, 58, and 60 base pairs were determined. Although the overall sequence identity is rather low, the architecture of the two proteins is similar. They are 1474 (*A. nidulans*) and 1147 (*S. pombe*) amino acids, and they contain Kelch-repeats in their N-terminal halves and extended coiled-coil regions in their C-terminal halves (determined with http://www.ebi.ac.uk/InterProScan/, http://www.ch.embnet.org/software/COILS_form.html). Sequence identity to the *S. cerevisiae* Kel1 protein is 36% only in the Kelch-repeats. In comparison, orthologues of full-length TeaA are conserved in other filamentous fungi. Because in *S. pombe* a second Kelch-domain protein, Tea3, exists, which has similarity to Tea1 and is associated with the Tea1/Mod5 protein complex (Snaith *et al.*, 2005), we searched the *A. nidulans* database for Tea3 homologues. We found four Kelch-repeat domain-containing proteins, but only TeaA displayed sequence similarity outside the Kelch repeats. This was also the case in other filamentous fungi, besides *A. gossypii*, which contains homologues of Tea1 and of Tea3. However, as Mod5 (see below) demonstrates, it could well be that a functional homologue of Tea3 exists in filamentous fungi but that it displays only low sequence similarity.
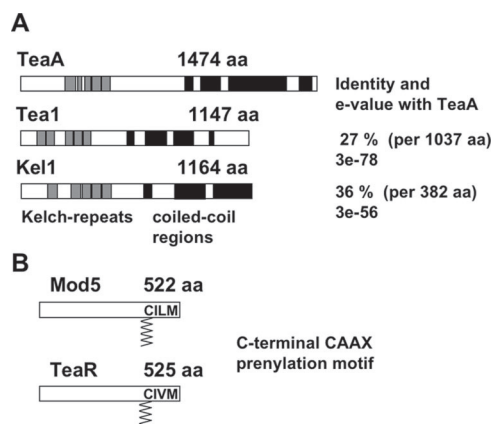
Figure 1. Characterization of TeaA and TeaR. (A) Scheme of *A. nidulans* TeaA, *S. pombe* Tea1, and *S. cerevisiae* Kel1. All three proteins share Kelch-repeats (gray boxes) at the N terminus and extended coiled-coil regions (black boxes) in the C-terminal half of the proteins. (B) Scheme of *A. nidulans* TeaR and *S. pombe* Mod5. The proteins are characterized by a C-terminal CAAX prenylation motif.

Besides Tea1, another crucial cell end marker protein in *S. pombe* is Mod5, which interacts with Tea1 at cell tips and thereby anchors Tea1 along with the formin For3 (Snaith and Sawin, 2003; Martin *et al.*, 2005; Snaith *et al.*, 2005). Despite the important role of Mod5 for polarized growth in *S. pombe*, no sequence homologue was identified in any filamentous fungus. Mod5 is anchored at the membrane through the prenyl residue, which itself is attached to Mod5 via a conserved C-terminal CAAX motif (cysteine, two aliphatic amino acids, any amino acid). Therefore, we anticipated that a functional homologue in *A. nidulans* could also harbor a CAAX motif at the C terminus. We searched the *A. nidulans* database for proteins with such a motif, and we identified 22 candidates. Their sequence identities with Mod5 were below 16%. We selected one (AN4214.3) that showed second highest identity to Mod5 (15.4%), was conserved only in filamentous fungi, and all of those fungal proteins harbored CAAX motifs at their C termini. Because we considered this protein as a putative receptor for TeaA, we named the gene *teaR* (TeaA receptor). DNA and cDNA sequences were confirmed and one intron of 105 base pairs was determined. The TeaR protein consists of 525 amino acids, and it is similar in size to the 522 amino acids of Mod5 (Figure 1B).

Deletion of teaA and teaR

To analyze the function of *teaA* in *A. nidulans*, we constructed a *teaA*-deletion strain (see *Materials and Methods*). The size of the colonies of the Δ*teaA* strain was ~75% compared with that of a wild-type strain (Figure 2A). In the Δ*teaA* strain, the maintenance of growth directionality was altered. Whereas wild-type hyphae normally grow straight, the Δ*teaA* mutant showed zigzag morphology (Figure 2B). A similar effect was shown for the kinesin motor mutant Δ*kipA* (Konzack *et al.*, 2005). The Δ*kipA* mutant displayed curved hyphae, which are similar but not identical to the Δ*teaA*-mutant hyphae (Figure 2B). It has been revealed that the Spitzenkörper, whose position is associated with growth direction, often moved away from the center of the hyphal apex in the Δ*kipA* mutant, and the hyphae grew in the direction of the Spitzenkörper. In the Δ*teaA* hyphae, the Spitzenkörper often mislocalized and moved away from the center to one side in the hyphal apex (data not shown). The curved hyphae in the Δ*kipA* mutant and the zigzag hyphae in the Δ*teaA* mutant were most prominent in younger hyphae. In particular, most hyphae at the edge of a larger colony of the Δ*kipA* mutant looked normal, and the Δ*kipA* mutant did not show growth delay. Conversely, mature hyphae in the Δ*teaA* mutant showed hyperbranching, and colonies grew slower than wild type or the Δ*kipA* strain.

In the Δ*kipA* mutant, another polarity defect has been detected in the way the second germ tube emerges from a conidiospore. In wild type, the second hypha emerges from the side of the spore opposite to the germ tube (bipolar) in 73% of the spores (Figure 2C; n = 200). In contrast, the second hyphae emerged in random positions in 80% of the spores in the Δ*kipA* mutant. A similar defect was observed in 58% of the spores in the Δ*teaA* mutant. This shows that TeaA also determines the initiation of polarity.

To explore the function of *teaR*, we constructed a *teaR*-deletion strain (see *Materials and Methods*). The Δ*teaR* mutant also showed the defect in the maintenance of growth directionality, and it displayed curved hyphae, which was identical to the Δ*kipA* mutant (Figure 2B), suggesting that TeaR functions in the same pathway as KipA. Likewise, the curved hyphae in the Δ*teaR* mutant were prominent in young hyphae, but they were not observed at the edge of a mature colony. Hence, the Δ*teaR* mutant did not show a
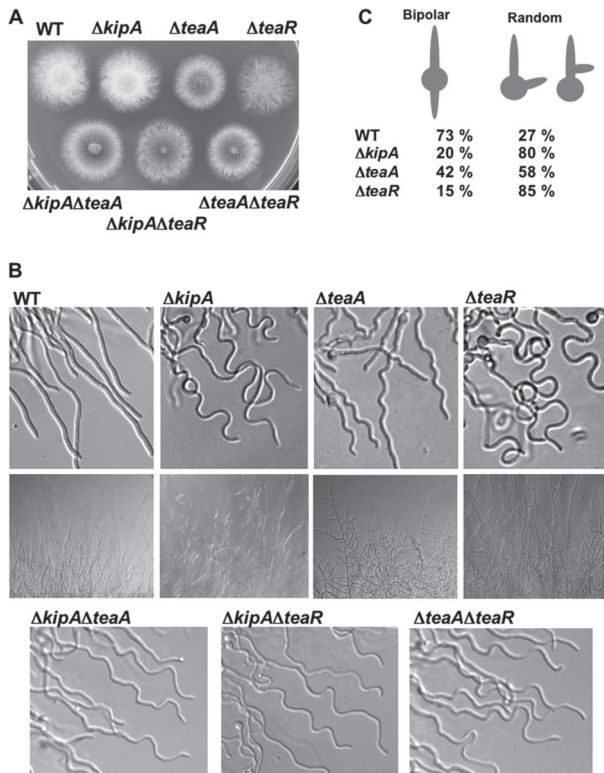
Figure 2. Phenotypic comparison of Δ*kipA*, Δ*teaA*, Δ*teaR*, and corresponding double mutants. (A) Colonies of wild type (GR5), Δ*kipA* (SRL1), Δ*teaA* (SSK91), Δ*teaR* (SNT33), Δ*kipA*/Δ*teaA* (SNT14), Δ*kipA*/Δ*teaR* (SNT40), and Δ*teaA*/Δ*teaR* (SNT39) strains. Strains were grown on minimal medium glucose agar plates for 2 d. (B) Differential interference contrast images of wild type, Δ*kipA*, Δ*teaA*, Δ*teaR*, Δ*kipA*/Δ*teaA*, Δ*kipA*/Δ*teaR*, and Δ*teaA*/Δ*teaR* strains as indicated. Strains were grown on microscope slides coated with minimal medium, with glucose and 0.8% agarose for 1 d (top and bottom). Strains were grown on minimal medium glucose agar plates for 2 d (middle). Hyphae are 3–4 μm in diameter. (C) Quantification of the effect of the gene deletions on second germ tube formation. Conidia of each strain were germinated in minimal medium with glucose, and then they were analyzed for the emergence of the second germ tube. For each strain, 200 germlings were counted.

growth delay when colony diameters were compared (Figure 2A). When we determined the site of the second hypha formation from a spore, we found random emergence in 85% of the spores in the Δ*teaR* mutant (Figure 2C).

To analyze the genetic interaction of *kipA*, *teaA*, and *teaR*, corresponding double-deletion strains were constructed by crossing. All three strains showed a curved hyphal phenotype (Figure 2B), which were identical to those in the Δ*kipA* and the Δ*teaR* mutant. The Δ*kipA*/Δ*teaA* mutant and Δ*teaA*/Δ*teaR* mutant showed a slight growth defect, although their colonies were bigger than that of the Δ*teaA* single mutant (Figure 2A), and they did not show a significant increase in branching. The Δ*kipA*/Δ*teaA* mutant showed no additional phenotype in comparison to the single mutants. All single mutants showed defects in growth directionality and only the Δ*teaA* mutant showed a growth defect. Genetic analysis indicated that deletion of *kipA* or *teaR* could partially suppress the growth defect of the Δ*teaA* mutant but not the maintenance of growth directionality.

Localization of TeaA and TeaR

To investigate TeaA localization, we constructed an *A. nidulans* strain expressing a GFP-TeaA fusion protein under the control of the regulatable *alcA* promoter (see *Materials and Methods*). Under repressing conditions, the strain, in which GFP-TeaA is the only source of TeaA, showed the zigzag hyphal phenotype observed in the Δ*teaA* mutant (data not shown), whereas the phenotype was restored under derepressed conditions, proving that GFP-TeaA is biologically functional. Using the same approach, we confirmed that mRFP1-TeaA was also biologically functional, and thus GFP or mRFP1 tagging did not show any difference. Under derepressed conditions, GFP-TeaA localized to one point at all hyphal tips (Figure 3A). The GFP-TeaA points always attached or localized quite close to the plasma membrane. GFP-TeaA detached from the cortex was not observed. A single GFP-TeaA spot was also observed in conidiospores before germination (bottom left). Some GFP signal spots,
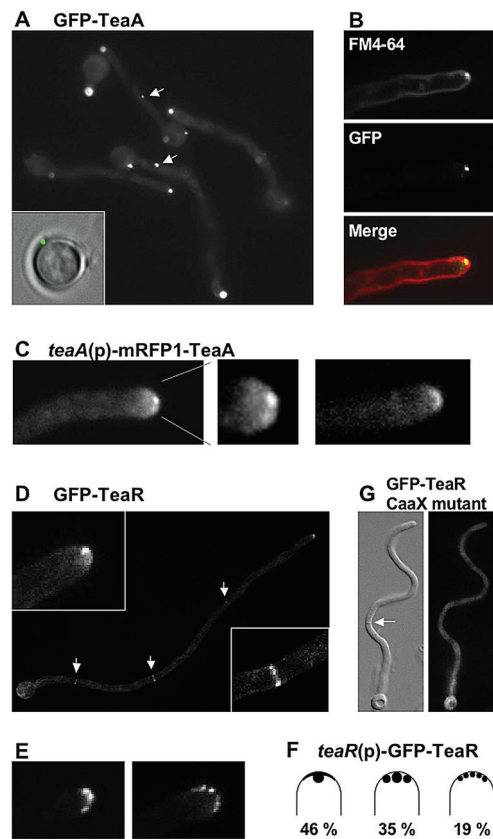

Figure 3. TeaA and TeaR localization. Strains SNT4 (A and B), SNT49 (C), SNT26 (D, E), SNT55 (F), and SNT61 (G) were grown on minimal medium with glycerol as carbon source. (A) GFP-TeaA localized to one point in the apex of all hyphal tips and some points in the cell body (arrows). The TeaA spot showed up in conidia before germination (left bottom). (B) The membrane was stained with FM4-64 (top, red in merged image). The Spitzenkörper labeled by FM4-64 colocalized with GFP-TeaA point (middle, green in merged image) at the tip. (C) mRFP1-TeaA produced under native promoter control localized to one point at most of tips and weaker signals were observed along the tip membrane. (D) GFP-TeaR localized to one point at hyphal tips and along the apex (left inset) and septa (arrows, right inset). (E) GFP-TeaR localized to one main point and two smaller points next to the main point at hyphal tips (left). GFP-TeaR spots aligned along the apex (right). (F) The percentage of GFP-TeaR localization pattern; 100 hyphal tips were analyzed. Hyphae are 3–4 μm in diameter.

Table 3. Localization pattern of mRFP1-TeaA

teaA(p)-mRFP1-TeaA					
WT[a]	80	7	0	13	0
WT with benomyl[b]	2	3	10	2	83
ΔkipA[c]	43	35	8	14	0
KipA-rigor[d]	30	34	15	9	10
cytochalasin A[e]	56	6	6	9	23

The localization pattern of 100–200 hyphal tips was analyzed and grouped into five different categories. The numbers indicate the percentage of hyphal tips of these groups.

SNT49 (a), SNT50 (c), and SNT51 (d) were grown on minimal medium with glycerol for 1 day. SNT49 (b) and SNT57 (e) were grown under the same conditions as above and treated with 2.5 μg/ml benomyl (b) or 2 μg/ml cytochalasin A (e) for 30 min. mRFP1-TeaA localization was analyzed within 10 min.

which were weaker compared with the point at the hyphal apex, were observed in the hyphal body (arrows). To compare the localization of TeaA and the Spitzenkörper, we stained hyphae with FM4-64. This compound has been used in several fungi to stain the Spitzenkörper (Fischer-Parton *et al.*, 2000; Peñalva, 2005). The Spitzenkörper labeled by FM4-64 colocalized with GFP-TeaA at the hyphal apex (Figure 3B), although the Spitzenkörper was labeled only in a small number of tips under our experimental conditions. To confirm the TeaA localization, we constructed strains producing mRFP1-TeaA under the control of the native promoter. A strain, in which mRFP1-TeaA is the only source of TeaA, did not show the phenotype observed in the Δ*teaA* mutant, indicating that mRFP1-TeaA also was biologically functional. Although signals of mRFP1 seemed weaker, mRFP1-TeaA still localized to one point at most of the tips, and weaker signals were observed along the apex (Figure 3C, left). The single spot of mRFP1-TeaA normally localized at the center of the hyphal apex (Table 3). At a small number of tips, mRFP1-TeaA localized along the tip membrane but not to one point (Figure 3C, right, and Table 3). Hereafter, we normally used strains producing mRFP1-TeaA under the native promoter, when we analyzed the localization of TeaA.

Using the same approach as for TeaA, we constructed a strain producing GFP-TeaR under *alcA* promoter control (see *Materials and Methods*). Under repressing conditions, the strain showed curved hyphae as observed in the Δ*teaR* mutant (data not shown). In contrast, under derepressing conditions, the curved hyphal phenotype was restored, indicating that GFP-TeaR is functional. GFP-TeaR localized to hyphal tips and all septa (Figure 3D). GFP-TeaR localized to one point at most of the tips, and weaker signals were observed along the apex, similar to the localization of TeaA. The GFP-TeaR point also colocalized with the Spitzenkörper labeled by FM4-64 (data not shown). Sometimes, one or two smaller GFP-TeaR spots localized close to a larger point (Figure 3E). At <20% of the tips, GFP-TeaR spots aligned along the apex, but they did not localize uniform along the cortex. To study the localization of TeaR under native conditions, we constructed strains producing GFP-TeaR under *teaR* promoter control. The strains did not show the phenotype of a Δ*teaR* mutant, indicating the functionality of the GFP-TeaR fusion protein. The localization of GFP-TeaR was identical to that in of the *alcA* promoter (Figure 3F). There-

fore, we used strains producing GFP-TeaR under *alcA* promoter control, when we analyzed the localization of TeaR. In addition, it seems that TeaR localizes to septa; however, we did not observe any alteration in septation in *teaR*-deletion strains (data not shown).

TeaR is assumed to localize to the plasma membrane through its prenyl residue. The nonuniform spot-like localization of TeaR at the apex may reflect sterol-rich membrane microdomains (see below). To prove the importance of the C-terminal CAAX motif in TeaR, we constructed a strain, producing TeaR (GFP tag at the N terminus) where the cysteine residue in the CAAX motif was changed to glycine by point mutation. The mutated GFP-TeaR could not rescue the phenotype of the Δ*teaR* mutant, and only weak GFP fluorescence was observed throughout the hyphae (Figure 3G), whereas GFP-tagged wild-type TeaR could rescue the phenotype of the Δ*teaR* mutant, and it localized to tips and septa (data not shown). Likewise, TeaR tagged with GFP at the C terminus, and thus masking the CAAX motif, failed to rescue the phenotype of the Δ*teaR* mutant, and it did not localize to tips and septa (data not shown). These results demonstrate that the C-terminal CAAX motif is necessary for TeaR localization and function.

Role of TeaA in Microtubule Organization at Hyphal Tips

To analyze the role of TeaA at hyphal tips, we investigated the relationship of TeaA and MTs. In wild type, MTs elongate toward the apex, reach the tip cortex, and normally converge in one point at the center of the tip. To compare the localization of TeaA and the convergence point of MTs, we constructed a strain expressing GFP-labeled α-tubulin and mRFP1-TeaA. We found that the point where GFP-MTs converged colocalized with the mRFP1-TeaA spot (Figure 4A and Supplemental Movie 1).

In *S. pombe*, Tea1 is delivered by growing MTs to the cell tip, and its localization at the cell tips depends on MTs. Whereas in *A. nidulans* KipA showed the same behavior as Tea1 in *S. pombe*, we have no evidence that TeaA accumulates at the MT plus ends. To test whether TeaA localization at tips nevertheless depends on MTs, we used the MT-destabilizing drug benomyl. After this treatment (2.5 μg benomyl/ml), almost all fluorescence of GFP-MTs was diffused into the cytoplasm within 5 min (data not shown), and the mRFP1-TeaA point at the tips was sometimes divided into several points and disappeared from >80% of the tips after 30–40 min (Figure 4B and Table 3; n = 100). Control treatment with 0.25% ethanol did not show the effect on the localization of mRFP1-TeaA. These results indicated that TeaA localization at tips depends on MTs.

To study the behavior of MTs in a Δ*teaA* mutant, we compared wild type and Δ*teaA* strains expressing GFP-labeled α-tubulin. These strains did not show apparent differences in the number of MTs in the cytoplasm. In the tip of wild type, MTs elongated toward the apex and normally converge in one point at the center of the tip (>80% of tips during 1-min observation), and they paused there without elongating until a catastrophe event caused depolymerization. In the Δ*teaA* mutant, MTs reached the tip cortex, but sometimes they did not converge to one, but attached to several points. The phenomenon was observed at 45 tips (n = 100) during 1-min observation (Figure 4, C and E, and Supplemental Movie 2). Moreover, MTs in the Δ*teaA* mutant seemed more curved than those of wild type, and a few MTs bent around the tips. The bending of MTs could be due to continuous elongation after they reached the cortex. Bending of MTs was observed in 22 tips (n = 100) during 1-min observation in the Δ*teaA* mutant, whereas it was observed in
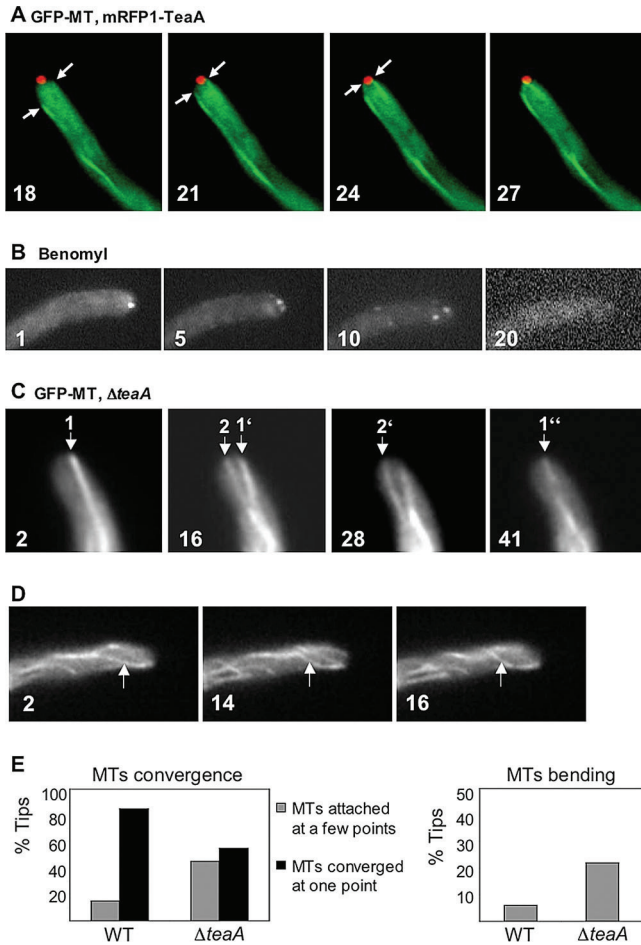
Figure 4. Relationship between TeaA and microtubules (MT). (A) In strain SNT22 (GFP-MT, mRFP1-TeaA), GFP-MTs elongated toward the hyphal tip (arrow) and merged at one point at the apex. The point colocalized with mRFP1-TeaA point at the apex (see Supplemental Movie 1). Times are indicated in seconds. (B) SNT49 [*teaA*(p)-mRFP1-TeaA] was grown in minimal medium with glycerol for 1 d and treated with the medium containing 2.5 µg/ml benomyl. mRFP1-TeaA point at tips was sometimes divided into a few points and disappeared from >80% of tips after 30 min (see Table 3). Elapsed time is given in minutes. (C) In strain SNT 31 (Δ*teaA*, GFP-MT), GFP-MTs did not merge in one point at the apex but instead attached to a few points (arrows indicate points where MT attached; see Supplemental Movie 2). Elapsed time is given in seconds. (D) In the strain SNT 31, GFP-MTs became more curved than those in wild type. GFP-MTs bent, probably because they kept growing after they reached the cortex (arrows; see Supplemental Movie 3). Elapsed time is given in seconds. Hyphae are 3–4 µm in diameter. (E) Quantification of MTs behavior in SNT22 (GFP-MT, mRFP1-TeaA) and SNT31 (Δ*teaA*, GFP-MT). The percentage of tips where GFP-MTs merged in one point (black bar) or attached to a few points (gray bar) (left), and the percentage of tips where GFP-MTs bent after they attached to the cortex (right). Data from 100 tips of strain SNT22 and SNT31 during 1-min observation.

six tips (n = 100) during 1-min observation in wild type (Figure 4, D and E, and Supplemental Movie 3).

Relationship between KipA and TeaA

In *S. pombe*, Tea1 is transported by the kinesin Tea2 along MT to the plus end, where both proteins accumulate. This leads to comet-like structures in time-lapse observations (Busch *et al.*, 2004). To test whether *A. nidulans* TeaA is
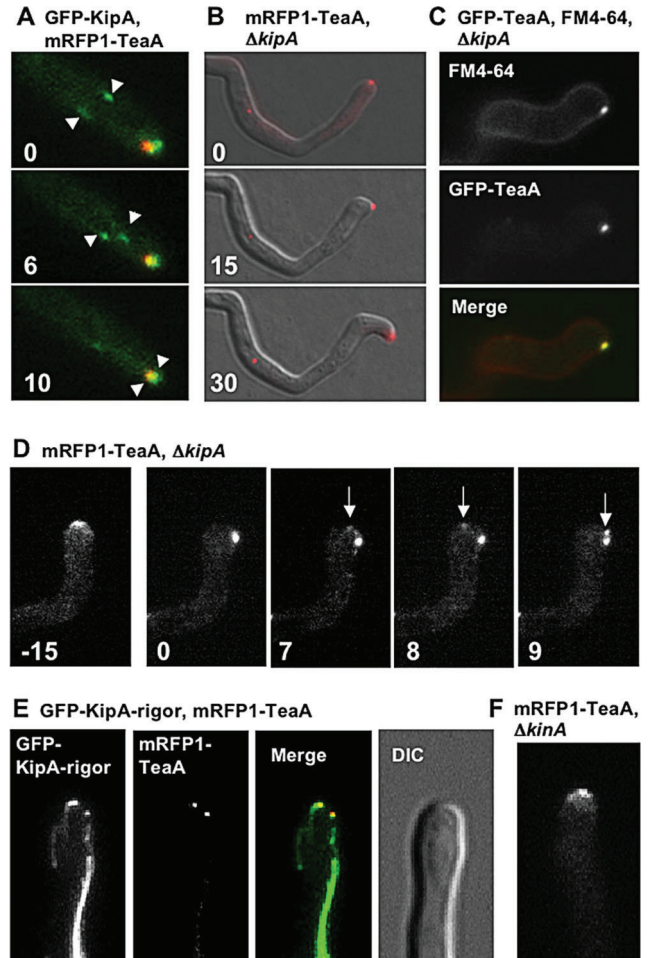
Figure 5. Relationship between TeaA and KipA. (A) In strain SNT23 (GFP-KipA, mRFP1-TeaA), GFP-KipA spots, which label MT plus ends, moved toward the hyphal tip (arrows), and they merged at one point at the apex with mRFP1-TeaA (see Supplemental Movie 4). Elapsed time is given in seconds. (B and C) In the Δ*kipA* mutant (SNT41), mRFP1-TeaA still localized to one point at the hyphal tip but often moved away from the center of the apex (see Table 3). Elapsed time is given in minutes. (C) In the Δ*kipA* mutant (SNT9), the Spitzenkörper labeled by FM4-64 (top, red in merged image) also often moved away from the center of the apex and colocalized with the GFP-TeaA point at the tips (middle, green in merged image). (D) In the Δ*kipA* mutant (SNT50), mRFP1-TeaA moved away from the center of the apex to the side of the tip, and it divided into two points (arrows; see Supplemental Movie 5). Elapsed time is given in minutes. (E) In the *kipA*-rigor mutant (SNT51), mRFP1-TeaA sometimes localized to two points at the tip (see Table 3), whereas GFP-KipA[G223E] decorated MTs and MTs attached to the two points. (F) Deletion of *kinA* did not affect mRFP1-TeaA tip localization (strain SNT62). Hyphae are 3–4 µm in diameter.

transported by KipA, the Tea2 orthologue, we compared TeaA and KipA localization. The GFP-KipA signal accumulated at MT plus ends, moved toward the tip, and converged to the mRFP1-TeaA point at the apex (Figure 5A and Supplemental Movie 4). In contrast, TeaA was not detected at MT plus ends. This could be explained if TeaA uses a different mechanism to reach the cell tip or if TeaA accumulates at the MT plus end only to very low concentrations, below the detection level of mRFP1. To test the second possibility, we analyzed TeaA localization in a Δ*kipA* mutant. GFP- or mRFP1-tagged TeaA still localized to one point
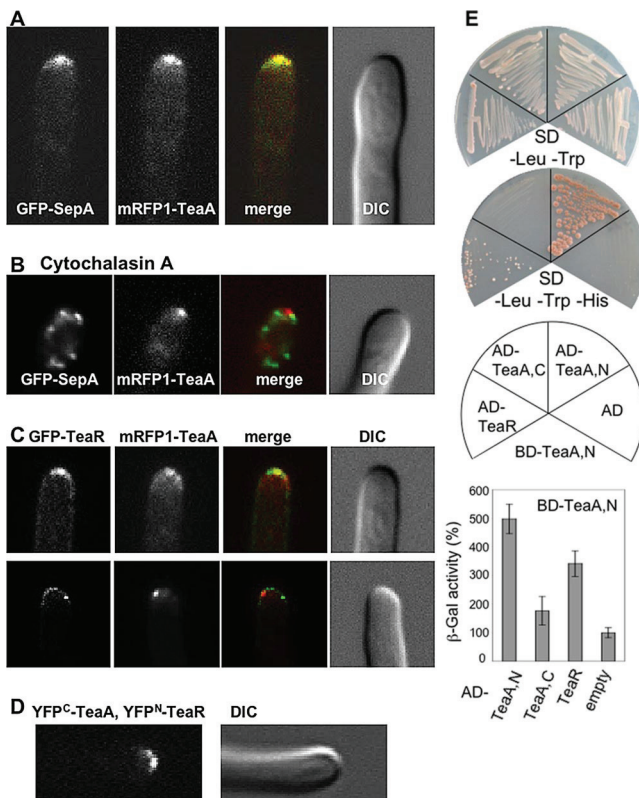
Figure 6. Interaction of TeaA, SepA and TeaA, TeaR. (A) GFP-SepA and mRFP1-TeaA colocalized to one point at the apex and along the apex in strain SNT57. (B) Strain SNT57 grown in minimal medium with glycerol for 1 d was treated with the medium containing 2 μg/ml cytochalasin A for 30 min. (C) In strain SNT56, the mRFP1-TeaA point at the apex colocalized with that of GFP-TeaR, although their localization was not identical. (D) BiFC analysis of TeaA and TeaR. In SNT59 expressing TeaR tagged with the N-terminal half of YFP and TeaA tagged with the C-terminal half of YFP, the YFP signal was detected at the tip. (E) Yeast two-hybrid interaction between the DNA binding domain fused to the TeaA N-terminal half (BD-TeaA,N) and the activation domain fused to the TeaA N- or C-terminal half (AD-TeaA,N, AD-TeaA,C), TeaR full length (AD-TeaR), or as control the empty vector (AD). The mated yeasts were selected on SD/−Leu/−Trp plate (top) and grown on nutritionally selective plate SD/−Leu/−Trp/-His (bottom). β-Galactosidase activity was analyzed by liquid culture assay using ONPG as substrate. The value of BD-TeaA,N and AD was used as a standard (100%). The data are expressed as the mean ± SD (n = 4).

at ~80% of tips, but often it did not localize to the center of the apex (Figures 5B and 7A and Supplemental Table 3). When the mRFP1-TeaA point moved away from the center of the apex to right or left side of the apex, hyphae grew in the direction of the TeaA location (Figure 5B). This result suggests that TeaA localization is involved in the determination of growth direction and that the ΔkipA mutant displays meandering hyphae possibly partly due to mislocalization of TeaA at tips. The Spitzenkörper labeled by FM4-64 also often mislocalized and colocalized with TeaA at the tips (Figure 5C). Besides mislocalization of TeaA to a side of the cortex at the tips, TeaA occurred as two points at <10% of the tips (Figure 5D and Table 3). The TeaA point moved along the tip cortex and divided into two points (Figure 5D and Supplemental Movie 5). To analyze further the role of KipA for TeaA localization, we checked TeaA localization in a kipA-rigor mutant, in which KipA harbors a point muta-

tion in the ATP-binding domain (P-loop, G223E). The mutated GFP-KipA-rigor binds but does not move along MTs; thus, it decorates them (Konzack et al., 2005). In the kipA-rigor mutant, mRFP1-TeaA still localized at 90% of the tips, but the mRFP1-TeaA point often moved away to the side of the apex and sometimes divided into two points (Table 3). These results indicate that TeaA accumulation at tips is independent of KipA, but KipA is necessary for proper TeaA anchorage at the tips. MTs visualized by GFP-KipA-rigor elongated to tips and attached to mRFP1-TeaA even if it localized to a point at the side of the apex or if mRFP1-TeaA was split into two points (Figure 5E). This supported the idea that TeaA is necessary for proper MT organization in the tip.

Because conventional kinesin has been reported to transport dynein toward the MT plus end (Zhang et al., 2003), we analyzed TeaA localization in a conventional kinesin kinA-deletion strain, but we found no difference to TeaA localization in wild type (Figure 5F).

Interaction of TeaA and SepA

One of the important functions of Tea1 in S. pombe is the contribution to cell polarity and actin cable organization through interaction with the formin For3 (Feierbach et al., 2004). Tea4, which was identified as Tea1-interacting protein, binds Tea1 and For3 directly and links Tea1 with For3 (Martin et al., 2004). Therefore, we investigated whether A. nidulans TeaA colocalized with the formin SepA. We constructed a strain expressing GFP-SepA and mRFP1-TeaA, and we found colocalization in one point and along the apex (Figure 6A). Direct interaction of TeaA and SepA was tested with the yeast two-hybrid system, but no interaction was detected (data not shown).

It has been shown that SepA localization at hyphal tips depends on the actin cytoskeleton (Sharpless and Harris, 2002). After treatment with 2 μg/ml cytochalasin A, an inhibitor of actin polymerization, GFP-SepA points dispersed around the tips within 10 min (Figure 6B). In contrast, mRFP1-TeaA localization was partially affected by the drug but remained concentrated at >70% of the tips after the 30- to 40-min treatment (Figure 6B and Table 3). We confirmed that the control treatment with 0.02% DMSO did not show the effect on the localization of TeaA and SepA. These observations suggest that TeaA can localize to the tips independently of SepA and independently of an intact actin cytoskeleton.

Interaction of TeaA and TeaR

To investigate whether TeaR functions as a TeaA receptor, we constructed a strain expressing mRFP1-TeaA and GFP-TeaR, and we compared their localization. The mRFP1-TeaA point at the apex colocalized with that of GFP-TeaR at >80% of the tips, although their localization was not identical. GFP-TeaR was restricted to the tip membrane, whereas mRFP1-TeaA was observed at the membrane, and as a gradient away from the membrane (Figures 3C and 6C, top). When GFP-TeaR was observed as some spots along the membrane (Figure 3E, left), the mRFP1-TeaA point colocalized with one of the GFP-TeaR spots, but it did not accumulate at additional points (data not shown). At a few tips, several GFP-TeaR spots aligned along the apex, whereas only one mRFP1-TeaA point was visible (Figure 6C, bottom).

Colocalization of TeaA and TeaR was confirmed by BiFC analysis. The YFP[N] was fused to TeaR, and the YFP[C] was tagged with TeaA. In the strain expressing only YFP[N]-TeaR or YFP[C]-TeaA, no YFP fluorescence was detected. In con-
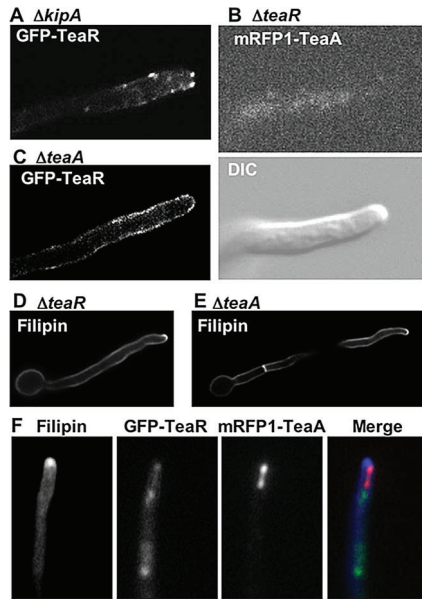
Figure 7. Localization dependency of KipA, TeaA, TeaR, and sterol-rich regions. (A) In the Δ*kipA* mutant (SNT43), some GFP-TeaR signal localized at the membrane of the apex, and other signal dispersed along the membrane away from the tip. (B) In the Δ*teaR* mutant (SNT53), mRFP1-TeaA was not observed at the tip. (C) In the Δ*teaA* mutant (SNT32), GFP-TeaR lost the preference for the hyphal tip and diffused all along the membrane. (D and E) The Δ*teaR* (SNT33) and Δ*teaA* (SSK91) mutants were stained with 10 μg/ml filipin for 5 min. (F) Strain SNT27 was treated with 10 μg/ml filipin for 5 min. Filipin accumulated at the tip (blue in merged image), GFP-TeaR lost the membrane association (green in merged image), and mRFP1-TeaA dispersed at the tip (red in merged image). Hyphae are 3–4 μm in diameter.

trast, in the strain expressing both YFP^N-TeaR and YFP^C-TeaA, YFP signals were detected as a single point and along the apex (Figure 6D). The localization pattern of the YFP signal was similar to that of GFP-TeaR. Together, the results suggest that some TeaA colocalizes with TeaR at the apex but that additional TeaA localizes to the tips independently of TeaR.

The protein-protein interaction between TeaA and TeaR was analyzed with the yeast two-hybrid system. Direct interaction between the TeaA N-terminal half and TeaR was detected, although it was weak (Figure 6E). Moreover, self-interaction of the N-terminal halves of TeaA was discovered.

We also checked possible interactions of KipA and TeaA, KipA and TeaR, KipA and SepA, and TeaR and SepA by the BiFC system, but none of these combinations resulted in YFP fluorescence (data not shown). The combination of TeaA with SepA gave a positive YFP signal, but an interaction could not be verified with the yeast two-hybrid assay.

Localization Dependency of KipA, TeaA, and TeaR
As mentioned above, in the Δ*kipA* mutant GFP-TeaA still localized to hyphal tips but often moved away from the center of the apex (Figure 5, B–D, and Table 3). Next, we studied the effect of *kipA*-deletion on TeaR localization. In wild type, TeaR were concentrated in the Spitzenkörper or some spots of TeaR aligned along the membrane at the apex (Figure 3, D and E), whereas in the Δ*kipA* mutant, some GFP-TeaR dots remained at the apex, but in addition, other dots moved to the subapical membrane (Figure 7A, within

10 μm from the tip). These results indicated that KipA is required for TeaR anchorage and proper TeaA positioning.

To determine whether TeaR is involved in TeaA localization, we investigated TeaA localization in a Δ*teaR* mutant. Fluorescence of mRFP1-TeaA was not observed at hyphal tips (Figure 7B). These results indicate that TeaR is required for TeaA anchorage. In contrast, we analyzed the localization of TeaR in a Δ*teaA* mutant and found that GFP-TeaR spread away from hyphal tips (Figure 7C), indicating that TeaA is also required for TeaR anchorage. These results show that TeaA and TeaR localizations are interdependent.

Localization Dependency of TeaA, TeaR, and Sterol-rich Membrane Domains
TeaR is assumed to localize to the membrane through its prenyl residue; therefore, it could be that the membrane environment is important for TeaR localization. In other eukaryotes such membrane microdomains are important for cell signaling, polarity, and protein sorting (Rajendran and Simons, 2005). In fungi, sterol-rich plasma membrane domains were observed by sterol-binding fluorescent dye filipin staining at tips of mating projections in *S. cerevisiae* (Bagnat and Simons, 2002) and *Cryptococcus neoformans* (Nichols *et al.*, 2004), at cell ends and septa in *S. pombe* (Wachtler *et al.*, 2003), and at hyphal tips and septa in *C. albicans* hyphae (Martin and Konopka, 2004). In *A. nidulans*, filipin stained the hyphal tip membrane and septa (Pearson *et al.*, 2004). In Δ*kipA*, Δ*teaA*, and Δ*teaR* strain, filipin stained the hyphal tip and septa identical to wild type (Figure 7, D and E; data not shown). Incubation of cells in high filipin concentrations, for longer times, or both has been demonstrated to alter the sterol-containing membranes and disrupt their functions (Rothberg *et al.*, 1990; Wachtler *et al.*, 2003). Therefore, we analyzed the localization of mRFP1-TeaA and GFP-TeaR under high concentrations of filipin (10 μg/ml; 5 min), and we found that GFP-TeaR was shifted from the membrane at the apex to the cytoplasm or internal membranes (Figure 7F). Filipin treatment changed also slightly the mRFP1-TeaA localization, which resembled the one in the absence of TeaR. The YFP signal from YFP^N-TeaR and YFP^C-TeaA also disappeared from the apex after filipin treatment (data not shown).

To investigate the effect of filipin on hyphal growth and on the localization of TeaA and TeaR in more detail, we observed the hyphal morphology under conditions with different filipin concentrations. With <1 μg/ml filipin, hyphae grew normally. Increasing filipin concentrations abolished hyphal growth, and with 5 μg/ml filipin germination was completely inhibited (Figure 8A). The control treatment with 0.05% of methanol did not show the effect. In the presence of 3–4 μg/ml filipin, abnormal hyphal morphologies were often observed (Figure 8B). Next, we investigated the effect of different filipin concentrations on the localization of TeaA and TeaR. To compare the sensitivity of TeaA and TeaR toward filipin treatment, we studied the localization of the proteins at 1, 3, or 5 μg/ml filipin (Figure 8C). Treatment with 1 μg/ml filipin for 1 h had little effect on the localization, whereas 3 μg/ml filipin caused mRFP1-TeaA and GFP-TeaR disappearance at 80% of the hyphal tips. Immediately after the treatment of 3 μg/ml filipin, filipin stained almost all the apex and the signal intensity became gradually stronger (Figure 8D). Although GFP-TeaR often moved away from the apex to subapical membrane regions immediately, mRFP1-TeaA could stay at tips for several minutes and then start to disperse around tips and finally disappear. These results suggest that filipin treatment disrupts TeaR localization and indirectly affects TeaA localization. However, the hyphae treated with filipin did not show the
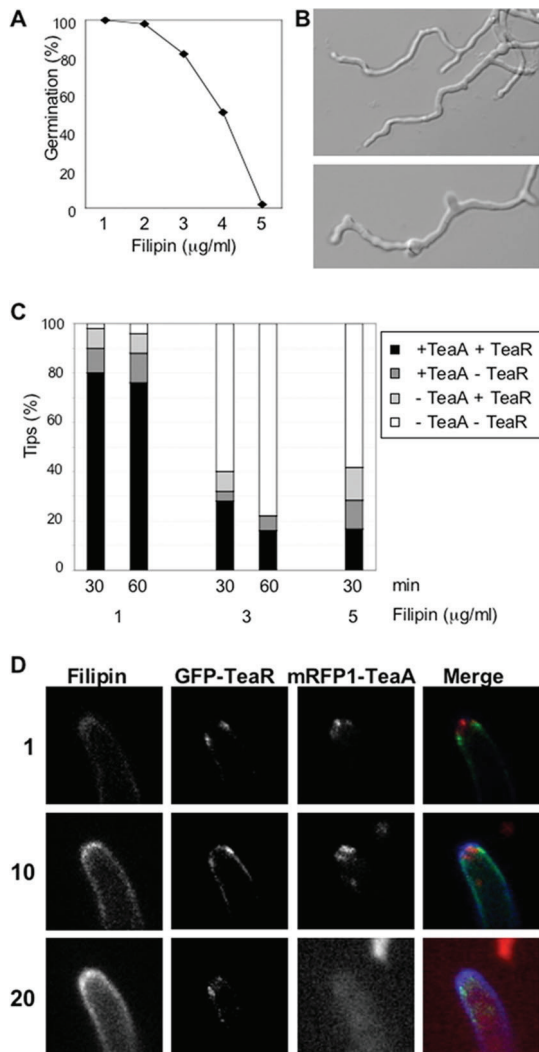
Figure 8. Effect of filipin treatment on hyphal growth and localization of TeaA and TeaR. (A) Germination efficiency. Conidia of wild type (GR5) were inoculated in minimal medium with glycerol in the presence of 1–5 μg/ml filipin, incubated for 36 h, and analyzed for germ tube emergence. Two hundred germlings or conidia were counted. (B) Differential interference contrast images of wild type grown in minimal medium with glycerol and 3 μg/ml filipin for 36 h. (C) Quantification of the number of tips where mRFP1-TeaA and GFP-TeaR localized correctly or not at the tip membrane. Strain SNT56 grown in minimal medium with glycerol for 24 h was treated with the medium containing 1, 3, or 5 μg/ml filipin for 30 or 60 min. Percentage of the tips with the correct localization of mRFP1-TeaA and GFP-TeaR (black bar), with only mRFP1-TeaA (dark gray bar), with only GFP-TeaR (bright gray bar), and without both (white bar); 100 tips were counted. (D) Time course illustration of the localization patterns after the treatment with 3 μg/ml filipin quantified in C. Elapsed time is given in minutes. Hyphae are 3–4 μm in diameter.

same hyphal morphology as Δ*teaA* or Δ*teaR* mutants. This suggests that filipin treatment disrupts not only TeaA and TeaR localization and function but also other polarity factors.

DISCUSSION

Polarized growth is essential in many elongated cells, such as neurites, pollen tubes, or filamentous fungi (Nelson,

2003). Three main structures have been described in fungi to be important for the establishment and maintenance of polarity: the polarisome, cell end factors or landmark proteins, and the Spitzenkörper. Whereas landmark proteins of *S. cerevisiae* seem largely not to be conserved in filamentous fungi (Harris and Momany, 2004; Wendland and Walther, 2006), we show here that the functions of *S. pombe* cell end markers seem to be conserved. However, it has to be noted that also *S. cerevisiae* polarity factors—besides the components of the polarisome—can be used for filamentous growth, for example, in *A. gossypii* (Wendland, 2003; Philippsen *et al.*, 2005). Although the genomes of the two fungi are very similar and reflect a common history, the growth modes are very different, budding in the one and obligatory filamentously in the other species (Dietrich *et al.*, 2004).

The detailed study of TeaA and TeaR in this article revealed that main players of polarity establishment of *S. pombe* are conserved in *A. nidulans* but also that significant differences exist. For example, in *S. pombe* Tea1 is transported by Tea2 toward the MT plus end, with which it hitchhikes through the cell to arrive at the growing tip, whereas in *A. nidulans* we do not have any evidence for such a transport mechanisms. TeaA tip localization was independent of the Tea2 homologue KipA, although it was affected by an MT-depolymerizing drug. Likewise, lack of KipA only slightly affected MT plus-end localization of ClipA, the Clip-170 homologue in *A. nidulans*, at elevated temperature (Efimov *et al.*, 2006), whereas MT plus-end localization of Tip1, the Clip-170 homologue in *S. pombe*, strictly depended on Tea2 (Busch *et al.*, 2004). Nevertheless, we found that KipA is important for proper localization of TeaA and also TeaR in *A. nidulans*. Deletion of *teaR* prevents the formation of a discrete, spot-like structure of TeaA in the tip, and *kipA* deletion allows the formation of the spot but affects its proper localization in the tip, and finally deletion of *kipA* leads to spreading of TeaR along the tip membrane. These results suggest that TeaA mislocalization in the *kipA* mutant cannot be explained solely by the mislocalization or absence of TeaR but rather they suggest that KipA is transporting another protein, which is required for proper localization of TeaR. This is supported also by the different hyphal phenotypes of the mutants. Whereas *kipA* and *teaR* deletion produce meandering hyphae, *teaA* deletion caused zig-zag growth. The identification of proteins transported by KipA should help to further unravel this puzzle.

In *A. nidulans*, a formin, SepA, characteristic for the *S. cerevisiae* polarisome, was detected at the tip membrane and in the Spitzenkörper. This suggested, that the Spitzenkörper represents an organelle consisting of vesicles but also proteins, in addition to actin, required for the organization of the actin cytoskeleton (Sharpless and Harris, 2002; Harris *et al.*, 2005). Here, we identified that TeaA and TeaR localized to tips and accumulated at one point at the apex, which colocalized with the Spitzenkörper stained with FM4-64, whereas the accumulation at one point is not observed in Tea1 and Mod5 of *S. pombe*. However, the resolution of the localization of the proteins and the Spitzenkörper may not be sufficient to really determine whether the proteins are components of the Spitzenkörper. There is evidence that TeaA and TeaR are not closely associated with this organelle. We found that the TeaA point at the tip was resistant to cytochalasin A treatment, whereas the Spitzenkörper dissolved. In contrast, SepA localization was affected by cytochalasin A. In *C. albicans*, it was suggested that the Spitzenkörper and the polarisome protein complex are distinct structures in the tip of growing hyphae (Crampin *et al.*, 2005). Thus, it could be that TeaA and TeaR define a protein

complex in *A. nidulans* overlapping with but being distinct from the Spitzenkörper.

Our yeast two-hybrid and BiFC experiments demonstrated interaction between TeaA and TeaR. TeaA and TeaR often colocalized at the tips, but the localization was not always the same, and the TeaA point could temporarily localize to tips independently of TeaR. One explanation could be that only a fraction of TeaR interacts with TeaA. Furthermore, it has to be considered that TeaR localization was also dependent on TeaA, suggesting that TeaA could be anchored independently of TeaR at the membrane. Likewise, we found that filipin treatment first affects TeaR localization without changing obviously the localization of TeaA. Another possibility is that upon filipin treatment the interaction of TeaA and TeaR is disrupted, and TeaA just remains close to the membrane.

Although TeaA localization at tips depends on MTs, TeaA at the tips also plays a role in the regulation of MT dynamics. In the *teaA*-deletion mutant, some MTs did not converge at tips and other MTs failed to stop growing after reaching the tips and bent. Several proteins have been identified to regulate the MT plus-end dynamics referred to +TIPs in eukaryotic cells. In *S. pombe*, one of the +TIPs, CLIP-170 homologue Tip1 is revealed to interact with Tea1 at MT plus ends (Feierbach *et al.*, 2004). Interactions of TeaA with +TIPs in *A. nidulans*, such as ClipA and AlpA corresponding to CLIP-170 and Dis1/XMAP215 (Efimov *et al.*, 2006; Enke *et al.*, 2007), have to be analyzed. In the *kipA* mutant, the TeaA point at tips sometimes divided into a few points and MTs attached to the TeaA points (Figure 5E), suggesting TeaA accumulation at one point is associated with the convergence of MTs at the tips. The convergence of MTs at tips is possibly involved in the formation of the Spitzenkörper, because it is thought that MTs are necessary for long-distance vesicle transport toward the Spitzenkörper (Schuchardt *et al.*, 2005).

The effect of filipin on the distribution of the two cell-end markers, TeaA and TeaR, suggests an important role of sterol-rich microdomains in the membrane for localized insertion of the cell end factors (Alvarez *et al.*, 2007). Filipin has a specific affinity for sterols; thus, it integrates into regions with high sterol contents. Thereby, it possibly disturbs the structure of the membrane and, in our case, causes the mislocalization of TeaA and TeaR. There have been reports that sterol-rich lipid microdomains may play important roles in polarized growth in fungi, because they were detected in *C. neoformans* at bud tips and at protrusions that elongate to conjugation tubes during mating and at the tips of mating projections in *S. cerevisiae* and *S. pombe* (Bagnat and Simons, 2002; Nichols *et al.*, 2004; Wachtler and Balasubramanian, 2006). However, a link between the cell end markers and the membrane domains was missing. Recently, another tip-localized membrane protein was described in *A. nidulans*, MesA (Pearson *et al.*, 2004). This protein contains predicted transmembrane domains, and it is necessary for the stable recruitment of SepA. Whether the sterol-rich microdomains are also necessary for localization of this protein and whether it interacts with the TeaA–protein complex, remains to be uncovered.

ACKNOWLEDGMENTS

REFERENCES

Alvarez, F. J., Douglas, L. M., and Konopka, J. B. (2007). Sterol-rich plasma membrane domains in fungi. Eukaryot. Cell *6*, 755–763.

Bagnat, M., and Simons, K. (2002). Cell surface polarization during yeast mating. Proc. Natl. Acad. Sci. USA *99*, 14183–14188.

Browning, H., Hackney, D. D., and Nurse, P. (2003). Targeted movement of cell end factors in fission yeast. Nat. Cell Biol. *5*, 812–818.

Browning, H., Hayles, J., Mata, J., Aveline, L., Nurse, P., and McIntosh, J. R. (2000). Tea2p is a kinesin-like protein required to generate polarized growth in fission yeast. J. Cell Biol. *151*, 15–27.

Busch, K. E., Hayles, J., Nurse, P., and Brunner, D. (2004). Tea2p kinesin is involved in spatial microtubule organization by transporting tip1p on microtubules. Dev. Cell *16*, 831–843.

Chang, F., and Peter, M. (2003). Yeasts make their mark. Nat. Cell Biol. *5*, 294–299.

Crampin, H., Finley, K., Gerami-Nejad, M., Court, H., Gale, C., Berman, J., and Sudbery, P. (2005). *Candida albicans* hyphae have a Spitzenkörper that is distinct from the polarisome found in yeast and pseudohyphae. J. Cell Sci. *118*, 2935–2947.

Dietrich, F. S. *et al*. (2004). The *Ashbya gossypii* genome as a tool for mapping the ancient *Saccharomyces cerevisiae* genome. Science *304*, 304–307.

Efimov, V., Zhang, J., and Xiang, X. (2006). CLIP-170 homologue and NUDE play overlapping roles in NUDF localization in *Aspergillus nidulans*. Mol. Biol. Cell *17*, 2021–2034.

Enke, C., Zekert, N., Veith, D., Schaaf, C., Konzack, S., and Fischer, R. (2007). *Aspergillus nidulans* Dis1/XMAP215 protein AlpA localizes to spindle pole bodies and microtubule plus ends and contributes to growth directionality. Eukaryot. Cell *6*, 555–562.

Feierbach, G., Verde, F., and Chang, F. (2004). Regulation of a formin complex by the microtubule plus end protein tea1p. J. Cell Biol. *165*, 697–707.

Fischer-Parton, S., Parton, R. M., Hickey, P. C., Dijksterhuis, J., Atkinson, H. A., and Read, N. D. (2000). Confocal microscopy of FM4-64 as a tool for analysing endocytosis and vesicle trafficking in living fungal hyphae. J. Microsc. *198*, 246–259.

Girbardt, M. (1957). Der Spitzenkörper von *Polystictus versicolor*. Planta *50*, 47–59.

Grove, S. N., and Bracker, C. E. (1970). Protoplasmic organization of hyphal tips among fungi: vesicles and Spitzenkörper. J. Bacteriol. *104*, 989–1009.

Harris, S. D., and Momany, M. (2004). Polarity in filamentous fungi: moving beyond the yeast paradigm. Fungal Genet. Biol. *41*, 391–400.

Harris, S. D., Read, N. D., Roberson, R. W., Shaw, B., Seiler, S., Plamann, M., and Momany, M. (2005). Polarisome meets Spitzenkörper: microscopy, genetics, and genomics converge. Eukaryot. Cell *4*, 225–229.

Hill, T. W., and Käfer, E. (2001). Improved protocols for *Aspergillus* minimal medium: trace element and minimal medium salt stock solutions. Fungal Genet. Newsl. *48*, 20–21.

Howard, R. J. (1981). Ultrastructural analysis of hyphal tip cell growth in fungi: Spitzenkörper, cytoskeleton and endomembranes after freeze-substitution. J. Cell Sci. *48*, 89–103.

Kang, P. J., Sanson, A., Lee, B.-Y., and Park, H. O. (2001). A GDP/GTP exchange factor involved in linking a spatial landmark to cell polarity. Science *292*, 1376–1378.

Karos, M., and Fischer, R. (1999). Molecular characterization of HymA, an evolutionarily highly conserved and highly expressed protein of *Aspergillus nidulans*. Mol. Genet. Genomics *260*, 510–521.

Knechtle, P., Dietrich, F., and Philippsen, P. (2003). Maximal polar growth potential depends on the polarisome component AgSpa2 in the filamentous fungus *Ashbya gossypii*. Mol. Biol. Cell *14*, 4140–4154.

Konzack, S., Rischitor, P., Enke, C., and Fischer, R. (2005). The role of the kinesin motor KipA in microtubule organization and polarized growth of *Aspergillus nidulans*. Mol. Biol. Cell *16*, 497–506.

Martin, S. G., and Chang, F. (2003). Cell polarity: a new mod(e) of anchoring. Curr. Biol. *13*, R711–R730.

Martin, S. G., and Chang, F. (2006). Dynamics of the formin for3p in actin cable assembly. Curr. Biol. *16*, 1161–1170.

Martin, S. G., McDonald, W. H., Yates, J. R., and Chang, F. (2005). Tea4p links microtubule plus ends with the formin for3p in the establishment of cell polarity. Dev. Cell *8*, 479–491.

Martin, S. W., and Konopka, J. B. (2004). Lipid raft polarization contributes to hyphal growth in *Candida albicans*. Eukaryot. Cell *3*, 675–684.

Mata, J., and Nurse, P. (1997). Tea1 and the microtubular cytoskeleton are important for generating global spatial order within the fission yeast cell. Cell *89*, 939–949.

Montegi, F., Arai, R., and Mabuchi, I. (2001). Identification of two type V myosins in fission yeast, one of which functions in polarized cell growth and moves rapidly in the cell. Mol. Biol. Cell *12*, 1367–1380.

Nelson, W. J. (2003). Adaptation of core mechanisms to generate cell polarity. Nature *422*, 766–774.

Nichols, C. B., Fraser, J. A., and Heitman, J. (2004). PAK kinases Ste20 and Pak1 govern cell polarity at different stages of mating in *Cryptococcus neoformans*. Mol. Biol. Cell *15*, 4476–4489.

Pearson, C. L., Xu, K., Sharpless, K. E., and Harris, S. D. (2004). MesA, a novel fungal protein required for the stabilization of polarity axes in *Aspergillus nidulans*. Mol. Biol. Cell *15*, 3658–3672.

Peñalva, M. A. (2005). Tracing the endocytic pathway of *Aspergillus nidulans* with FM4-64. Fungal Genet. Biol. *42*, 963–975.

Philippsen, P., Kaufmann, A., and Schmitz, H.-P. (2005). Homologues of yeast polarity genes control the development of multinucleated hyphae in *Ashbya gossypii*. Curr. Opin. Microbiol. *8*, 370–377.

Philips, J., and Herskowitz, I. (1998). Identification of Kel1p, a kelch-domain-containing protein involved in cell fusion and morphology in *Saccharomyces cerevisiae*. J. Cell Biol. *143*, 375–389.

Pringle, J. R., Bi, E., Harkins, H. A., Zahner, J. E., DeVirglio, C., Chant, J., Corrado, K., and Fares, H. (1995). Establishment of cell polarity in yeast. Cold Spring Harb. Symp. Quant. Biol. 729–744.

Rajendra, L., and Simons, K. (2005). Lipid rafts and membrane dynamics. J. Cell Sci. *118*, 1099–1102.

Riquelme, M., Reynaga-Peña, C. G., Gierz, G., and Bartnicki-García, S. (1998). What determines growth direction in fungal hyphae? Fungal Genet. Biol. *24*, 101–109.

Rothberg, K. G., Ying, Y.-S., Kamen, B. A., and Anderson, R.G.W. (1990). Cholesterol controls the clustering of the glycophospholipid-anchored membrane receptor for 5-methoyltetrahydrofolate. J. Cell Biol. *111*, 2931–2938.

Sambrook, J., and Russel, D. W. (1999). Molecular Cloning: A Laboratory Manual, Cold Spring Harbor, NY: Cold Spring Harbor Laboratory Press.

Schuchardt, I., Assmann, D., Thines, E., Schuberth, C., and Steinberg, G. (2005). Myosin-V, Kinesin-1, and Kinesin-3 cooperate in hyphal growth of the fungus Ustilago maydis. Mol. Biol. Cell *16*, 5191–5201.

Sharpless, K. E., and Harris, S. D. (2002). Functional characterization and localization of the *Aspergillus nidulans* formin SEPA. Mol. Biol. Cell *13*, 469–479.

Sheu, Y. J., Santos, B., Fortin, N., Costigan, C., and Snyder, M. (1998). Spa2p interacts with cell polarity proteins and signaling components involved in yeast cell morphogenesis. Mol. Cell. Biol. *18*, 4053–4069.

Snaith, H. A., Samejima, I., and Sawin, K. E. (2005). Multistep and multimode cortical anchoring of tea1p at cell tips in fission yeast. EMBO J. *24*, 3690–3699.

Snaith, H. A., and Sawin, K. E. (2003). Fission yeast mod5p regulates polarized growth through anchoring of tea1p at cell tips. Nature *423*, 647–651.

Snell, V., and Nurse, P. (1994). Genetic analysis of cell morphogenesis in fission yeast–a role for casein kinase II in the establishment of polarized growth. EMBO J. *13*, 2066–2074.

Toews, M. W., Warmbold, J., Konzack, S., Rischitor, P. E., Veith, D., Vienken, K., Vinuesa, C., Wei, H., and Fischer, R. (2004). Establishment of mRFP1 as fluorescent marker in *Aspergillus nidulans* and construction of expression vectors for high-throughput protein tagging using recombination in *Escherichia coli* (GATEWAY). Curr. Genet. *45*, 383–389.

Vienken, K., and Fischer, R. (2006). The Zn(II)$_2$Cys$_6$ putative transcription factor NosA controls fruiting body formation in *Aspergillus nidulans*. Mol. Microbiol. *61*, 544–554.

Virag, A., and Harris, S. D. (2006). Functional characterization of Aspergillus nidulans homologues of *Saccharomyces cerevisiae* Spa2 and Bud6. Eukaryot. Cell *5*, 881–895.

Wachtler, V., and Balasubramanian, M. K. (2006). Yeast lipid rafts? An emerging view. Trends Cell Biol. *16*, 1–4.

Wachtler, V., Rajagopalan, S., and Balasubramanian, M. K. (2003). Sterol-rich plasma membrane domains in the fission yeast Schizosaccharomyces pombe. J. Cell Sci. *116*, 867–874.

Wendland, J. (2003). Analysis of the landmark protein Bud3 of *Asbya gossypii* reveals a novel role in septum construction. EMBO Rep. *4*, 200–204.

Wendland, J., and Walther, A. (2006). Septation and cytokinesis in fungi. In: The Mycota, Growth Differentiation and Sexuality, Vol. I, ed. U. Kües and R. Fischer, Heidelberg, Germany: Springer, 105–121.

Wright, G. D., Arlt, J., Poon, W. C., and Read, N. D. (2007). Optical tweezer micromanipulation of filamentous fungi. Fungal Genet. Biol. *44*, 1–13.

Yelton, M. M., Hamer, J. E., and Timberlake, W. E. (1984). Transformation of *Aspergillus nidulans* by using a *trpC* plasmid. Proc. Natl. Acad. Sci. USA *81*, 1470–1474.

Zahner, J. E., Harkins, H. A., and Pringle, J. R. (1996). Genetic analysis of the bipolar pattern of bud site selection in the yeast *Saccharomyces cerevisiae*. Mol. Cell Biol. *16*, 1857–1870.

Zhang, J., Li, S., Fischer, R., and Xiang, X. (2003). Accumualtion of cytoplasmic dynein and dynactin at microtubule plus ends in Aspergillus nidulans is kinesin dependent. Mol. Biol. Cell *14* 1479–1488.